VOLUME 87 NO. SM5
OCTOBER 1961
PART 1

JOURNAL of the

Soil Mechanics and Foundations Division

PROCEEDINGS OF THE

AMERICAN SOCIETY
OF CIVIL ENGINEERS

BASIC REQUIREMENTS FOR MANUSCRIPTS

Original papers and discussions of current papers should be submitted to the Manager of Technical Publications, ASCE. Authors should indicate the technical division to which the paper is referred. The final date on which a discussion should reach the Society is given as a footnote with each paper. Those who are planning to submit material will expedite the review and publication procedures by complying with the following basic requirements:

1. Titles must have a length not exceeding 50 characters and spaces.

2. A summary of approximately 50 words must accompany the paper, a 300-word synopsis must precede it, and a set of conclusions must end it.

3. The manuscript (an original ribbon copy and two duplicate copies) should be double-spaced on one side of 8½-inch by 11-inch paper. Three copies of all illustrations, tables, etc., must be included.

4. The author's full name, Society membership grade, and footnote reference stating present employment must appear on the first page of the paper.

5. Mathematics are recomposed from the copy that is submitted. Because of this, it is necessary that letters be drawn carefully, and that special symbols be properly identified. The letter symbols used should be defined where they first appear, in the illustrations or in the text, and arranged alphabetically in an Appendix.

6. Tables should be typed (an original ribbon copy and two duplicate copies) on one side of 8½-inch by 11-inch paper. Specific illustrations and explanation must be made in the text for each table.

7. Illustrations must be drawn in black ink on one side of 8½-inch by 11-inch paper. Because illustrations will be reproduced with a width of between 3-inches and 4½-inches, the lettering must be large enough to be legible at this width. Photographs should be submitted as glossy prints. Explanations and descriptions must be made within the text for each illustration.

8. The desirable average length of a paper is about 12,000 words and the absolute maximum is 18,000 words. As an approximation, each full page of typed text, table, or illustration is the equivalent of 300 words.

9. Technical papers intended for publication must be written in the third person.

10. The author should distinguish between a list of "Reading References" and a "Bibliography," which would encompass the subject of his paper.

Reprints from this Journal may be made on condition that the full title, name of author, name of publication, page reference, and date of publication by the Society are given. The Society is not responsible for any statement made or opinion expressed in its publications.

This Journal is published bi-monthly by the American Society of Civil Engineers. Publication office is at 2500 South State Street, Ann Arbor, Michigan. Editorial and General Offices are at United Engineering Center, 345 East 47th Street, New York 17, N. Y. $4.00 of a member's dues are applied as a subscription to this Journal. Second-class postage paid at Ann Arbor, Michigan.

The index for 1960 was published as ASCE Publication 1961-15 (list price $2.00); indexes for previous years are also available.

Vol. 87, No. SM 5

Journal of the

SOIL MECHANICS AND FOUNDATIONS DIVISION

Proceedings of the American Society of Civil Engineers

SOIL MECHANICS AND FOUNDATIONS DIVISION
EXECUTIVE COMMITTEE
Thomas M. Leps, Chairman; Reginald A. Barron, Vice Chairman;
John Lowe, III; Jorg O. Osterberg; H. Bolton Seed, Secretary
Charles W. Britzius, Board Contact Member

COMMITTEE ON PUBLICATIONS
Robert V. Whitman; Chairman; John A. Focht, Jr.; Harold J. Gibbs;
James P. Gould; Dennis S. Lane; Frank E. Richart, Jr.; H. Bolton Seed;
Woodland G. Shockley; Thomas H. Thornburn

CONTENTS

October, 1961

Papers

Page

Slope Stability Analysis by a New Graphical Method
by M. Arnold 1

Simplified Design of Combined Footings
by Fritz Kramrisch and Paul Rogers 19

Displacement of Long Footings by Dynamic Loads
by William L. Wallace 45

Tank Foundations in Eastern Venezuela
by Emery D. Carlson and Stephen P. Fricano 69

(over)

Copyright 1961 by the American Society of Civil Engineers.

Note.--Part 2 of this Journal is the 1961-36 Newsletter of the Soil Mechanics and Foundations Division.

The three preceding issues of this Journal are dated April 1961, June 1961, and August 1961.

Page

Analysis of Seepage Problems
by Milton E. Harr and Robert C. Deen 91

DISCUSSION

Pile Driving Analysis by Wave Equation, by E. A. L. Smith. (August, 1960. Prior discussion: February, 1961. Discussion closed.)
by E. A. L. Smith (closure) 111

Grouting of Granular Materials, by John C. King and E. G. W. Bush. (March, 1961. Prior discussion: August, 1961. Discussion closed.)
by R. H. Grice 117

Grouting to Prevent Vibration of Machinery Foundations, by J. P. Gnaedinger. (April, 1961. Prior discussion: July, 1961. Discussion closed.)
by Richard R. Schindler. 119

Uncertainties in Earth Dam Design, by John M. Bird. (June, 1961. Prior discussion: None. Discussion closes November 1, 1961.)
by B. V. Rangantham 123

Journal of the
SOIL MECHANICS AND FOUNDATIONS DIVISION
Proceedings of the American Society of Civil Engineers

SLOPE STABILITY ANALYSIS BY A NEW GRAPHICAL METHOD

By M. Arnold,[1] M. ASCE

SYNOPSIS

The stability of slopes is commonly analyzed by the "method of slices," which involves certain simplifying assumptions and, as normally applied, leads to conservative values of the factor of safety. A method of analysis developed by A. W. Bishop leads to more realistic values of the factor of safety but involves a tedious tabular form of computation.

The derivation of Bishop's equation for the factor of safety of a slope is outlined briefly, and a graphical solution, similar to that introduced by D. R. May for the "method of slices," is developed in detail. This graphical method is then applied to the stability analysis of two hypothetical slopes.

INTRODUCTION

Notation.—The letter symbols used in this paper are defined where they first appear, in the illustrations or in the text, and are arranged alphabetically, for convenience of reference, in the Appendix.

General.—The determination of the stability of a slope is affected both by inaccurate field data and by the inaccuracies inherent in the common methods of stability analysis. Where the importance of the structure demands greater reliability from the field data, particularly pore-pressure measurements, the use of greater refinements in calculation may be justified.

Note.—Discussion open until March 1, 1962. To extend the closing date one month, a written request must be filed with the Executive Secretary, ASCE. This paper is part of the copyrighted Journal of the Soil Mechanics Division, Proceedings of the American Society of Civil Engineers, Vol. 87, No. SM 5, October, 1961.

[1] Senior Lecturer in Civ. Engr., Univ. of Adelaide, Adelaide, South Australia.

It has been shown[2] that in a typical earth dam, even assuming idealized elastic properties for the soil, local overstress will occur when the factor of safety (by the slip-circle method) lies below a value of about 1.8. As the majority of stability problems involve factors of safety lower than this, a state of plastic equilibrium must be considered to exist throughout some of the slope. For these conditions the factor of safety (F) can be defined as the ratio of the available shear strength of the soil to that required to maintain equilibrium when incipient failure is postulated.[3]

If the shear strength mobilized is denoted as s, then

$$F = \frac{1}{s}\left\{c' + \left(p - u_w\right) \tan \phi'\right\} \quad \ldots\ldots\ldots\ldots (1)$$

in which c' is the cohesion (in terms of the effective stress), ϕ' denotes the angle of shearing resistance (in terms of effective stress), p is the total normal stress, and u_w represents the pore pressure.

Failure is assumed along a continuous rupture surface, the shape of which is influenced by the distribution of pore pressures and the variations of the shear parameters within the slope. For practical analysis a circular arc is usually assumed for the surface of rupture and the problem is assumed to be one of plane strain.

DERIVATION OF BISHOP'S EQUATION

A complete graphical analysis of the equilibrium of the mass of soil above the slip surface is most laborious; several simplified procedures have been developed using the "friction circle" method which is, however, limited to cases in which ϕ' is constant over the whole failure surface. More generally the "method of slices" is used with a simplifying assumption about the effect of the forces between the slices.

The significance of this assumption may be examined by considering the equilibrium of the mass of soil (of unit thickness) bounded by the circular arc, ABCD, of radius R and with center at 0 [Fig. 1 (a)].

In the case in which no external forces act on the surface of the slope, equilibrium must exist between the weight of the soil above ABCD and the resultant of the total forces acting on ABCD.

Let:

E_n and E_{n+1} = the resultants of the total horizontal forces on the sections n and n + 1, respectively;

X_n and X_{n+1} = the vertical shear forces;

W = the total weight of the slice of soil;

P = the total normal force acting on its base = pl;

S = the shear force acting on its base = sl;

---

2 "The Stability of Earth Dams," by A. W. Bishop, thesis presented to the Univ. of London in London, England, in 1952, in partial fulfilment of the requirements for the degree of Doctor of Philosophy.

3 "The Use of the Slip Circle in the Stability Analysis of Slopes," by A.W. Bishop, Geotechnique, Vol. 5, No. 1, 1955, p. 7.

h = the height of the element;

db = the breadth of the element;

l = the length BC;

α = the angle between BC and the horizontal; and

x = the horizontal distance of the slice from the center of rotation.

Hence, from Eq. 1

$$F = \frac{1}{s}\left\{c' + \left(\frac{P}{l} - u_w\right)\tan\phi'\right\} \quad \ldots\ldots\ldots\ldots\ldots (2)$$

Equating the moment about 0 of the weight of the soil within ABCD with the moment of the external forces acting on the sliding surface we obtain

$$\sum W\,x = \sum S\,R = \sum s\,l\,R \quad \ldots\ldots\ldots\ldots\ldots (3)$$

and Eq. 2 becomes

$$F = \frac{R}{\sum W\,x}\sum\left[c'\,l + \left(P - u_w\,l\right)\tan\phi'\right] \quad \ldots\ldots\ldots (4)$$

Considering the equilibrium of the soil in the slice above BC and resolving in a direction normal to the slip surface [Fig. 1 (b)] it follows that

$$P = \left(W + X_n - X_{n+1}\right)\cos\alpha - \left(E_n - E_{n+1}\right)\sin\alpha \quad \ldots\ldots (5)$$

Eq. 4 thus becomes

$$F = \frac{R}{\sum W\,x}\sum\left[c'\,l + \tan\phi'\left(W\cos\alpha - u_w\,l\right) + \tan\phi'\left\{\left(X_n - X_{n+1}\right)\cos\alpha - \left(E_n - E_{n+1}\right)\sin\alpha\right\}\right] \quad \ldots\ldots\ldots (6)$$

D. R. May's graphical method of analysis[4] implies that the sum of the terms representing the effect of the forces between the slices may be neglected without serious loss of accuracy, that is,

$$\sum\tan\phi'\left\{\left(X_n - X_{n+1}\right)\cos\alpha - \left(E_n - E_{n+1}\right)\sin\alpha\right\} = 0 \quad \ldots (7)$$

Thus, writing $x = R\sin\alpha$, Eq. 6 becomes

$$F = \frac{1}{\sum W\sin\alpha}\sum\left[c'\,l + \left(W\cos\alpha - u_w\,l\right)\tan\phi'\right] \quad \ldots\ldots (8)$$

---

4 "Proposed Methods of Calculating the Stability of Earth Dams," by D.R. May and J.H.A. Brahtz, Transactions, 2nd Congress on Large Dams, Vol. 4, 1936, p. 539.

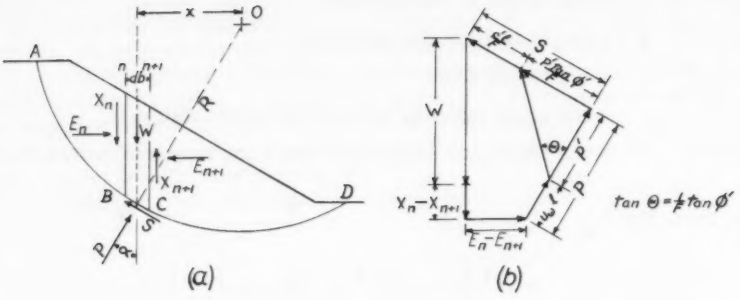

FIG. 1.–FORCES IN THE SLICES METHOD

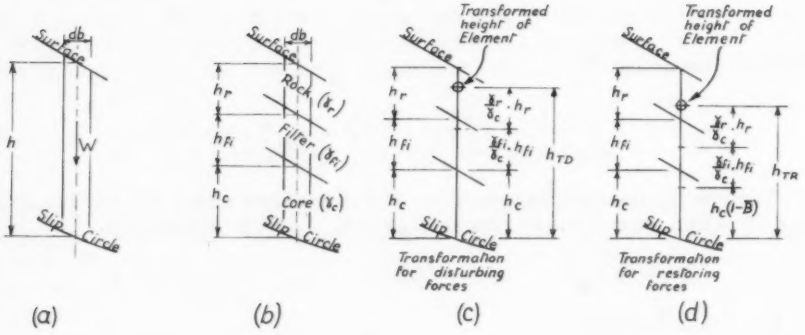

FIG. 2.–DERIVATION OF TRANSFORMED HEIGHTS

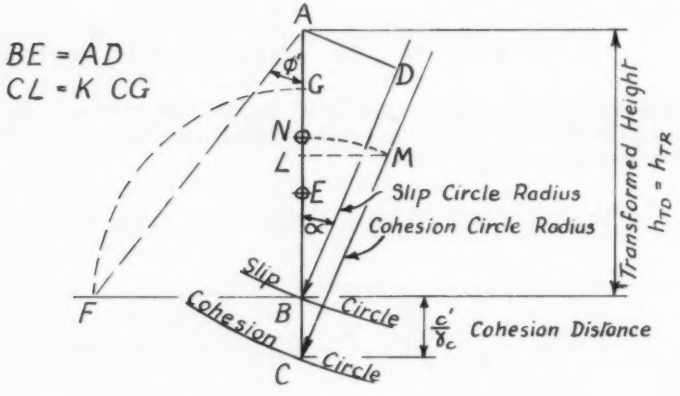

FIG. 3.–DERIVATION OF STRESS AREA ORDINATES

In earth-dam design the construction pore pressures are often expressed as a function of the total weight of the column of soil above the point considered, that is,

$$u_w = \overline{B}\,\frac{W}{(db)} \qquad \ldots\ldots\ldots\ldots\ldots\ldots (9)$$

in which $\overline{B}$ is a soil parameter based on either field data or laboratory tests and is assumed, for most design purposes, to have a constant value throughout the impervious zone.

Thus, putting $l = db \sec \alpha$ the expression for the factor of safety (Eq. 8) becomes

$$F = \frac{1}{\sum W \sin \alpha} \sum \left[c' \, l + \tan \phi' \, W (\cos \alpha - \overline{B} \sec \alpha) \right] \ldots\ldots (10)$$

Eqs. 8 and 10 are implicit in the commonly accepted methods of analyzing slope stability. However, values of F obtained from these expressions are, in general, found to be conservative, especially where conditions permit deep slip circles around which the variation in α is large.

To derive a method of analysis that largely avoids this error, the effective normal force $\left(P - u_w l\right)$ of Eqs. 4 is replaced by P' [Fig. 1 (b)] and, after the forces on the slice have been resolved vertically, the following expression is obtained:

$$P' = \frac{W + X_n - X_{n+1} - l\left(u_w \cos \alpha + \frac{c'}{F} \sin \alpha\right)}{\cos \alpha + \frac{\tan \phi' \sin \alpha}{F}} \qquad \ldots\ldots\ldots (11)$$

Substituting Eq. 11 into Eq. 4 and putting

$$l = db \sec \alpha \qquad \ldots\ldots\ldots\ldots\ldots\ldots (12a)$$

and

$$x = R \sin \alpha \qquad \ldots\ldots\ldots\ldots\ldots\ldots (12b)$$

there results

$$F = \frac{1}{\sum W \sin \alpha} \sum \left[\left\{ c' \, db + \tan \phi' \left[W \, (1 - \overline{B}) + \left(X_n - X_{n+1} \right) \right] \right\} \frac{\sec \alpha}{1 + \frac{\tan \phi' \tan \alpha}{F}} \right] \qquad \ldots\ldots\ldots\ldots (13)$$

As before, the term $(X_n - X_{n+1})$ may be neglected for practical purposes without appreciable error and Eq. 13 then becomes

$$F = \frac{1}{\sum W \sin \alpha} \sum \left[\left\{ c' \, db + W (1 - \overline{B}) \tan \phi' \right\} \frac{\sec \alpha}{1 + \frac{\tan \phi' \tan \alpha}{F}} \right] \quad . . (14)$$

which is the form of Bishop's equation normally used in the analysis of unsubmerged slopes.

Eq. 11 indicates the fundamental difference between Bishop's method and the original "method of slices." Whereas the commonly accepted method specifically implies that the resultant effect of the vertical and horizontal forces between slices is negligible, by resolving forces vertically to obtain P', Bishop eliminates the need for any assumption about the horizontal forces and, for practical purposes, only the resultant effect of the vertical forces between slices is assumed to be negligible.

The expression for F includes the value of the factor of safety on both sides of the equality, necessitating a solution by trial and error and requiring a time-consuming tabular form of computation in the same way as for the original method of slices. A purely graphical solution similar to that introduced by May for the method of slices considerably reduces the tediousness of the operation and is outlined herewith.

DEVELOPMENT OF GRAPHICAL SOLUTION

It is convenient to write

$$1 + \frac{\tan \phi' \tan \alpha}{F} = \frac{1}{K} \quad . . . . . (15)$$

in which form K can be plotted for all generally used values of α, ϕ', and F (Fig. 5).

Referring to Fig. 2, let

γ = the unit weight of material, [Fig. 2 (a)];

γ_c = the unit weight of core material;

γ_{fi} = the unit weight of filter material;

γ_r = the unit weight of rockfill material;

h = the height of an elementary slice;

h_c = the height of the core material in an elementary slice;

h_{fi} = the height of the filter material in an elementary slice;

h_r = the height of the rockfill material in an elementary slice;

h_{TD} = the transformed height of the elementary slice for distrubing forces;

h_{TR} = the transformed height of the elementary slice for restoring forces; and

db = the width of the elementary slice.

For unsubmerged, homogeneous slopes, considering an elementary slice [Fig. 2 (a)], the expression for the factor of safety, Eq. 14, can be written

$$F = \frac{1}{\sum \gamma\ h\ db\ \sin\ \alpha} \sum \left[\left\{ \gamma\ \frac{c'}{\gamma}\ db + \gamma\ h\ db\ (1 - \overline{B})\ \tan\ \phi' \right\} K\ \sec\ \alpha \right]$$

$$= \frac{1}{\sum h\ db\ \sin\ \alpha} \sum \left[\left\{ \frac{c'}{\gamma}\ db + h\ (1 - \overline{B})\ db\ \tan\ \phi' \right\} K\ \sec\ \alpha \right] \quad \ldots\ldots (16)$$

For zoned slopes [Fig. 2 (b)] it is convenient to handle the computation by referring all unit weights to one basis, such as the unit weight of the core material (γ_c). The total weight of the slice can, thus, be written as follows:

For Disturbing Forces.—

$$W = \gamma_c\ h_c\ db + \gamma_{fi}\ h_{fi}\ db + \gamma_r\ h_r\ db$$

$$= \gamma_c\ db \left(h_c + \frac{\gamma_{fi}}{\gamma_c}\ h_{fi} + \frac{\gamma_r}{\gamma_c}\ h_r \right)$$

$$= \gamma_c\ db\ h_{TD} \quad \ldots\ldots\ldots\ldots\ldots\ldots\ldots\ldots (17)$$

in which h_{TD} is the transformed height of an element for disturbing forces [Fig. 2 (c)].

For Restoring Forces.—Where pore pressures are involved in the restoring forces, the expression W (1 - $\overline{B}$) becomes

$$W\ (1 - \overline{B}) = \gamma_c\ db \left(h_c + \frac{\gamma_{fi}}{\gamma_c}\ h_{fi} + \frac{\gamma_r}{\gamma_c}\ h_r \right) (1 - \overline{B})$$

$$= \gamma_c\ db\ h_{TD}\ (1 - \overline{B})$$

$$= \gamma_c\ db\ h_{TR} \quad \ldots\ldots\ldots\ldots\ldots\ldots\ldots\ldots (18)$$

in which h_{TR} is the transformed height of an element for restoring forces [Fig. 2 (d)].

Thus, repeating the process for various elements, the full section can be transformed into equivalent sections for the purpose of plotting the disturbing and restoring forces.

Eq. 16 then becomes

$$F = \frac{1}{\sum db\ h_{TD}\ \sin\ \alpha} \sum \left[\left\{ \frac{c'}{\gamma_c}\ db + db\ h_{TR}\ \tan\ \phi' \right\} K\ \sec\ \alpha \right] \ldots (19)$$

The values of c' and ϕ' are those applicable on the slip circle at the particular element.

By assuming an initial value of F (conveniently F = 1.0), and, hence, establishing an initial value of K, a simple graphical solution of the expression for the factor of safety can be developed. To do this, a cohesion circle is plotted

with radius equal to that of the slip circle and with center a distance $\frac{c'}{\gamma_c}$ (cohesion distance) vertically below the center of the slip circle (Figs. 3, 7, and 9). The cohesion distance will vary for the different materials through which the slip circle passes and will, of course, be zero where the slip circle passes through cohesionless material. The cohesion circle will then coincide with the slip circle.

The basic graphical construction is shown in Fig. 3, to which the following explanation refers:

Let BA denote the transformed height of an element for the case $h_{TD} = h_{TR}$ (that is, $\overline{B} = 0$).

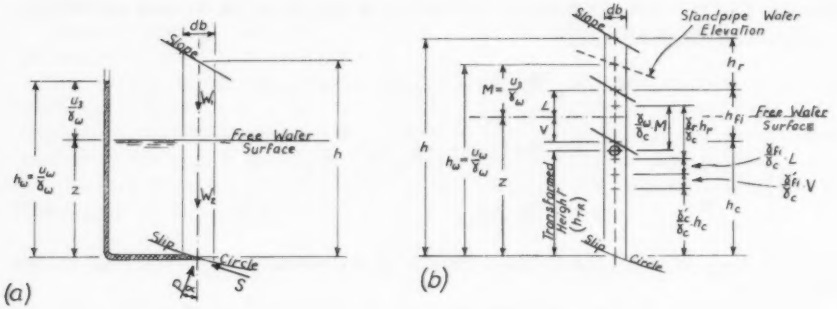

FIG. 4.–PARTIALLY SUBMERGED SLOPES

From A a perpendicular AD is drawn to the slip circle radius BD and then BE is plotted equal to AD.

Thus,

$$BE = AD = h_{TD} \sin \alpha \quad \ldots\ldots\ldots\ldots\ldots\ldots (20)$$

Joining successive points E on the whole section will give an area of stress between this line and the slip circle, representing, to scale, the disturbing forces on the slip circle (Figs. 6 and 8); that is

$$\text{Area of stress} = \sum db\ h_{TD} \sin \alpha \quad \ldots\ldots\ldots\ldots (21)$$

Next, considering restoring forces, AF is drawn at an angle ϕ' to BA to meet the horizontal through B at F; BF is then rotated to the vertical BG.

Thus,

$$BG = BF = h_{TR} \tan \phi' \quad \ldots\ldots\ldots\ldots\ldots\ldots (22)$$

and

$$CG = \frac{c'}{\gamma_c} + h_{TR} \tan \phi' \quad \ldots\ldots\ldots\ldots\ldots\ldots (23)$$

From Fig. 5 the value of K, corresponding to the relevant values of α, ϕ' and $F = 1.0$, is found and the height CG is reduced or increased in proportion (with

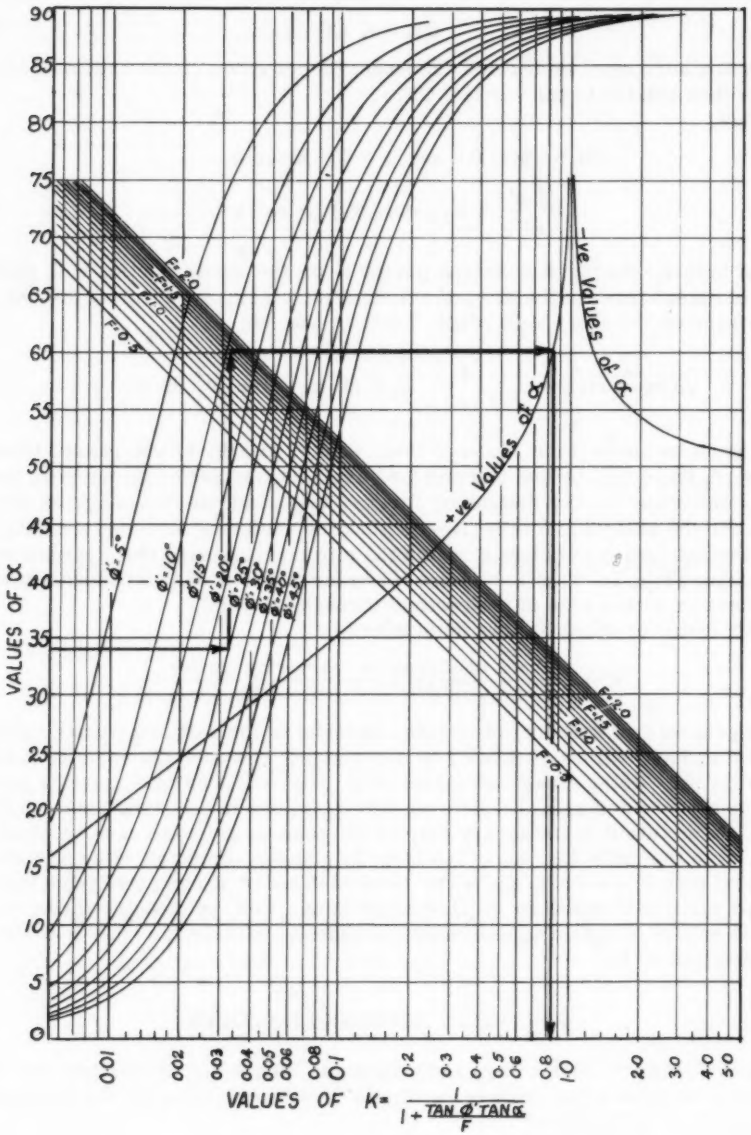

FIG. 5.–CHART FOR THE DETERMINATION OF K. To determine the value of K for $\alpha = 34°$, $\phi' = 25°$, and F = 1.5: Enter the chart on the left hand side at $\alpha = 34°$, proceed horizontally to intersect the curve for $\phi' = 25°$, rise vertically to intersect the line for F = 1.5 then continue horizontally to intersect the curve for positive values of α and read off the value of K = 0.83 on the scale below. For values of $\alpha < 45°$ the factor K can be determined directly with equal facility on certain types of slide rule.

the use of proportional dividers or by a simple geometrical construction) giving

$$CL = K\ CG \quad \ldots\ldots\ldots\ldots\ldots\ldots \quad (24)$$

From L a horizontal is drawn to intersect the cohesion circle radius at M and CM is then rotated to the vertical CN.

Thus,

$$CN = CM = CL \sec \alpha = CG\ K \sec \alpha$$

$$= \left(\frac{c'}{\gamma_c} + h_{TR} \tan \phi' \right) K \sec \alpha \quad \ldots\ldots\ldots\ldots \quad (25)$$

As before, joining successive points N on the whole section will give an area of stress between the line and the cohesion circle representing the restoring forces on the slip circle (Figs. 7 and 9), that is

$$\text{Area of stress} = \sum \left[\left\{ \frac{c'}{\gamma_c} db + db\ h_{TR} \tan \phi' \right\} K \sec \alpha \right] \ldots\ldots (26)$$

It must be noted (Figs. 6 and 7) that, where the slip circle passes through the core, there will be two transformed sections, one excluding the pore pressure coefficient for the distrubing forces (h_{TD}) and one including the coefficient for the restoring forces (h_{TR}). Also, the restoring force stress diagram has discontinuities at points at which the slip circle passes from one material to another (Fig. 7). This is because the value of tan ϕ' and, consequently also, K differs on either side of the vertical through the point.

The factor of safety is then determined by

$$F = \frac{\text{Area of stress for restoring forces}}{\text{Nett area of stress for disturbing forces}} \quad \ldots\ldots\ldots \quad (27)$$

In general this will not, of course, be equal to the initially chosen value of F = 1.0 and new values of K must be determined, based on the value of F found from Eq. 27. Using these new values of K, new positions of N must be plotted to give a corrected area of restoring forces for use in a further determination of F. To do this it is necessary only to increase or decrease each vertical CN (Fig. 3) in the ratio $K_F / K_{1.0}$ in which $K_{1.0}$ is the computed value of K at the vertical with F = 1.0 and K_F is the revised value of K computed from the assumed value of F based on the first trial value. Two, or possibly three, trials should suffice to obtain approximate coincidence between the chosen and computed values of F.

PARTIALLY SUBMERGED SLOPES

Considering the elementary slice shown in Fig. 4 (a) divided into two sections by the free water surface, a similar treatment leads to the expression for the factor of safety as

$$F = \frac{1}{\sum (W_1 + W_2) \sin \alpha} \sum \left[\left\{ c'\ db + \tan \phi' \left(W_1 + W_2 - db\ u_3 \right) \right\} \frac{\sec \alpha}{1 + \frac{\tan \phi' \tan \alpha}{F}} \right] \quad \ldots\ldots\ldots\ldots \quad (28)$$

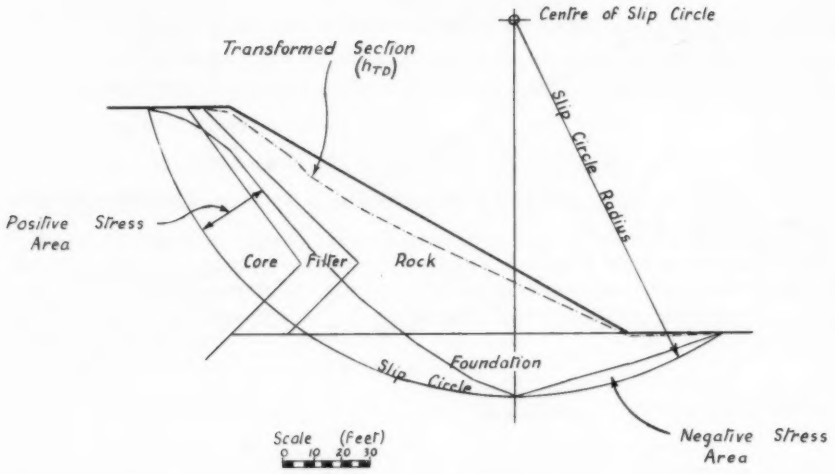

FIG. 6.–DISTURBING FORCES FOR A ZONED SLOPE (EXAMPLE 1)

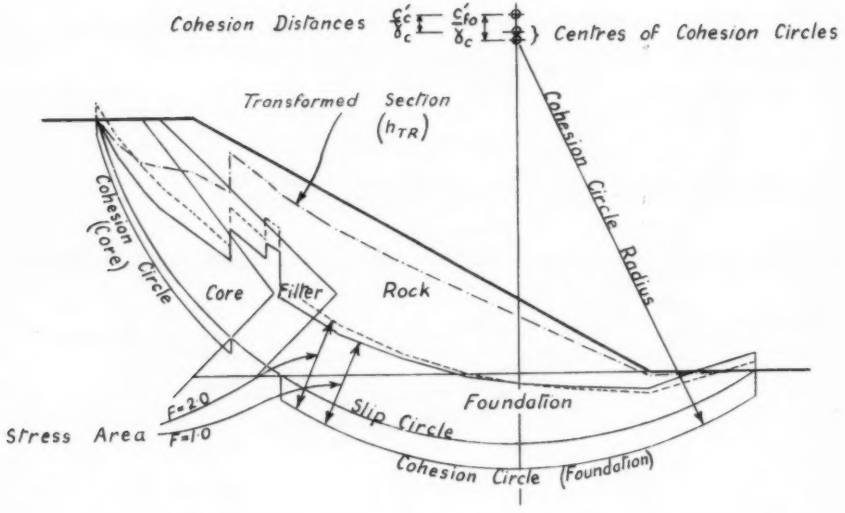

FIG. 7.–RESTORING FORCES FOR A ZONED SLOPE (EXAMPLE 1)

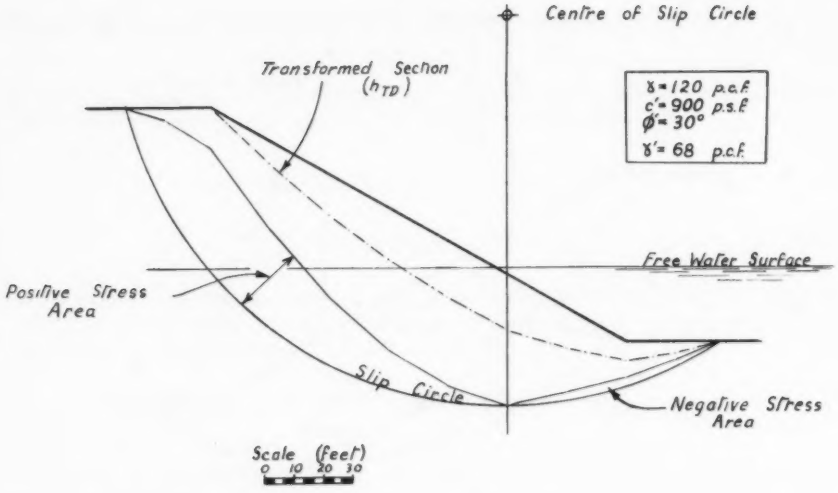

FIG. 8.–DISTURBING FORCES FOR A PARTIALLY SUBMERGED HOMOGENEOUS SLOPE (EXAMPLE 2)

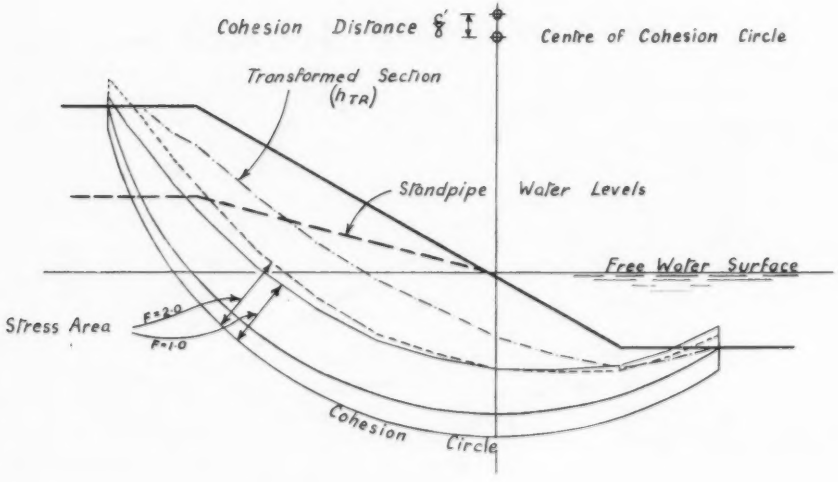

FIG. 9.–RESTORING FORCES FOR A PARTIALLY SUBMERGED HOMOGENEOUS SLOPE (EXAMPLE 2)

in which

W_1 = the full weight of soil in the slice above the free water surface;

W_2 = the submerged weight of soil in the slice below the free water surface;

u_3 = the pore pressure expressed as an excess over the hydrostatic pressure corresponding to the water level outside the slope = $\gamma_w (h_w - Z)$;

γ_w = the unit weight of water;

h_w = the standpipe water elevation at the element; and

Z = the depth of the slice below the free water surface.

It should be noted that the free water surface implies nothing about the magnitude of the pore pressure inside the slope and is only used to obtain the statically equivalent disturbing moment. The pore pressure at the base of the element is still represented by the standpipe water height h_w as shown in Fig. 4 (a).

Referring to Figs. 4 (a) and 4 (b), let

γ' = the submerged unit weight of material below the free water surface;

γ'_c = the sumberged unit weight of the core material; and

γ'_{fi} = the sumberged unit weight of the filter material.

Then

$$W_1 = \gamma \; db \; (h - Z)$$

$$= \gamma_r \; h_r \; db + \gamma_{fi} \; L \; db$$

$$= \gamma_r \; h_r \; db + \gamma_{fi} \left(h_c + h_{fi} - Z\right) db \quad \ldots\ldots\ldots (29)$$

$$W_2 = \gamma' \; db \; Z$$

$$= \gamma'_c \; h_c \; db + \gamma'_{fi} \; V \; db$$

$$= \gamma'_c \; h_c \; db + \gamma'_{fi} \left(Z - h_c\right) db \quad \ldots\ldots\ldots\ldots (30)$$

$$W_1 + W_2 = \gamma_r \; h_r \; db + \gamma_{fi} \left(h_c + h_{fi} - Z\right) db + \gamma'_c \; h_c \; db + \gamma'_{fi} \left(Z - h_c\right) db$$

$$= \gamma_c \; db \left[\frac{\gamma_r}{\gamma_c} \; h_r + \frac{\gamma_{fi}}{\gamma_c} \left(h_c + h_{fi} - Z\right) + \frac{\gamma'_c}{\gamma_c} \; h_c + \frac{\gamma'_{fi}}{\gamma_c} \left(Z - h_c\right)\right]$$

$$= \gamma_c \; db \left[\frac{\gamma'_c}{\gamma_c} \; h_c + \frac{\gamma'_{fi}}{\gamma_c} \; V + \frac{\gamma_{fi}}{\gamma_c} \; L + \frac{\gamma_r}{\gamma_c} \; h_r\right]$$

$$= \gamma_c \; db \; h_{TD} \quad \ldots\ldots\ldots\ldots\ldots\ldots\ldots\ldots\ldots\ldots (31)$$

$$W_1 + W_2 - db\ u_3 = \gamma_c\ db\left(\frac{\gamma'_c}{\gamma_c}\ h_c + \frac{\gamma'_{fi}}{\gamma_c}\ V + \frac{\gamma_{fi}}{\gamma_c}\ L + \frac{\gamma_r}{\gamma_c}\ h_r\right)$$

$$- \gamma_w\ db\ (h_w - Z)$$

$$= \gamma_c\ db\left(\frac{\gamma'_c}{\gamma_c}\ h_c + \frac{\gamma'_{fi}}{\gamma_c}\ V + \frac{\gamma'_{fi}}{\gamma_c}\ L + \frac{\gamma_r}{\gamma_c}\ h_r - \frac{\gamma_w}{\gamma_c}\ M\right)$$

$$= \gamma_c\ db\ h_{TR} \quad \ldots\ldots\ldots\ldots\ldots\ldots\ldots\ldots\ldots\ldots (32)$$

and

$$h_{TR} = h_{TD} - \frac{\gamma_w}{\gamma_c}\ M \quad \ldots\ldots\ldots\ldots\ldots\ldots (33)$$

in which h_{TD} and h_{TR} are the transformed heights of the element as before. From Fig. 4 and the expressions derived previously, the method of determining the transformed heights h_{TD} and h_{TR} is self-evident. (For clarity, only h_{TR} is shown in Fig. 4.)

TABLE 1.—PHYSICAL DATA FOR EXAMPLE 1 (FIGS. 6 AND 7)

Zone	γ, in pcf	$\frac{\gamma}{\gamma_c}$	ϕ', in degrees	c', in psf
(1)	(2)	(3)	(4)	(5)
Rockfill	100	0.833	40	———
Filter	110	0.917	35	———
Core	120	1.000	30	600 (c'_c)
Foundation	110	0.917	25	900 (c'_{fo})

TABLE 2.—RESULTS OF ANALYSES

Example 1 (Figs. 6 and 7)		Factor of Safety
Graphical Method	F = 1.0	1.83
	F = 2.0	1.97
Tabular Computation	F = 1.0	1.85
	F = 2.0	1.99
May's Graphical Analysis		1.63
Example 2 (Figs. 8 and 9)		
Graphical Method	F = 1.0	1.81
	F = 2.0	1.99
Tabular Computation	F = 1.0	1.80
	F = 2.0	1.97

Eq. 28 thus reduces to

$$F = \frac{1}{\sum db\ h_{TD} \sin \alpha} \sum \left[\left\{ \frac{c'}{\gamma_c} db + db\ h_{TR} \tan \phi' \right\} K \sec \alpha \right] \quad . . (29)$$

which is identical to Eq. 19 and can be solved in the same way.

EXAMPLE

For comparison between this method and the tabular computation, two arbitrary slopes were selected and the factor of safety of each was calculated for the following conditions:

1) Zoned fill with no tailwater and $\overline{B} = 0.4$ for the core material (Figs. 6 and 7)

2) Homogeneous slope with 25 ft tailwater and with standpipe water elevations represented by the broken line shown (Figs. 8 and 9)

Assumed physical data for example (1) are shown in Table 1 and for example (2) are shown in Fig. 8. Results of analyses are shown in Table 2.

CONCLUSIONS

The graphical method outlined is less tedious than the tabular computation method and the procedure at each section is a logical expression of the individual terms of the equation for the factor of safety. Once the transformed section has been plotted the sequence of operations is almost as straghtforward as in May's graphical method but only requires the measurement of one area each for the disturbing and restoring forces.

APPENDIX.—NOTATION

The following symbols, adopted for use in the paper, conform essentially with "Glossary of Terms and Definitions in Soil Mechanics," prepared by the Committee on Glossary of Terms and Definitions in Soil Mechanics of the Soil Mechanics and Foundations Division, Proceedings Paper 1826, October 1958:

$\overline{B}$ = pore pressure coefficient;

c' = cohesion per unit area;

db = width of an elementary slice;

E_n = resultant of horizontal forces on an elementary slice;

F = factor of safety;

h = height of an elementary slice:

- h_c = height of core material in an elementary slice;
- h_{fi} = height of filter material in an elementary slice;
- h_r = height of rockfill material in an elementary slice;
- h_w = height of standpipe water elevation above slip circle;
- h_{TD} = transformed height of an elementary slice for disturbing forces;
- h_{TR} = transformed height of an elementary slice for restoring forces;

K = a function of F, ϕ' and α;

L = height of filter material above free water surface;

l = slope length of the base of an elementary slice;

M = standpipe water elevation above free water surface;

P = total normal force acting on the base of an elementary slice;

p = total normal stress;

R = radius of the slip circle;

S = shear force acting on the base of an elementary slice;

s = shear strength mobilized;

u_w = pore pressure;

u_3 = pore pressure expressed as an excess over the hydrostatic pressure corresponding to the water level outside the slope;

V = height of free water surface above base of filter material;

W = total weight of an elementary slice of soil:

- W_1 = weight of the portion of an elementary slice below the free water surface;
- W_2 = weight of the portion of an elementary slice above the free water surface;

X_n = vertical shear force on an elementary slice;

x = horizontal distance from the center of an elementary slice to the center of rotation;

Z = height of free water surface above base of an elementary section;

α = angle between the tangent to the slip circle and the horizontal;

γ = unit weight of material:

- γ_c = unit weight of core material;
- γ_{fi} = unit weight of filter material;
- γ_r = unit weight of rockfill material;
- γ_w = unit weight of water;

γ' = submerged unit weight of material;

γ'_c = submerged unit weight of core material;

γ'_{fi} = submerged unit weight of filter material;

ϕ' = angle of shearing resistance; and

θ = function of F and ϕ' [Fig. 1 (b)].

Journal of the
SOIL MECHANICS AND FOUNDATIONS DIVISION
Proceedings of the American Society of Civil Engineers

SIMPLIFIED DESIGN OF COMBINED FOOTINGS

By Fritz Kramrisch,[1] F. ASCE, and Paul Rogers,[2] F. ASCE

SYNOPSIS

An empirical method for the evaluation of moments and contact pressures due to subgrade reactions is presented for combined footings conforming to certain stipulated limitations regarding continuity, rigidity, and variations in loading or column spacing. The values, although developed for continuous beam footings, can also be applied to grid or mat foundations. The results obtained by the empirical method are compared with those obtained by elastic analysis and are found sufficiently accurate for practical purposes.

An expression for the rigidity of the foundation with consideration of the subgrade reaction of the soil is also developed. This expression can be used, within the stipulated limitations, as a characteristic for all foundations responsive to a contact pressure distribution governed by subgrade reactions.

INTRODUCTION

The design of combined footings by means of subgrade reactions has been restricted from general application to singular cases for two principal reasons.

One reason was due to the uncertainties in selection of the correct subgrade reaction; the other reason stemmed from the difficulties of the theory and its application to practical cases.

A considerable amount of research work was undertaken to explore the problems in connection with the subgrade reaction produced by various soils. A

Note.–Discussion open until March 1, 1962. To extend the closing date one month, a written request must be filed with the Ececutive Secretary, ASCE. This paper is part of the copyrighted Journal of the Soil Mechanics Division, Proceedings of the American Society of Civil Engineers, Vol. 87, No. SM 5, October, 1961.

[1] Assoc., Albert Kahn Associated Architects and Engrs., Inc., Detroit, Mich.
[2] Pres., Paul Rogers & Assocs., Inc., Cons. Engrs., Chicago, Ill.

paper presented in 1956 provides[3] sufficient information to determine, at least for design purposes, the magnitude of the subgrade reaction from the data obtained from a standard soil exploration (see Appendix I). Because the computations of moments, contact pressures, and so on, by means of the exact theory are not sensitive to the selection of the k-value, such an estimate is usually sufficient. If necessary, it can be checked later by actual testing.

Much work was done also to develop the basic idea theoretically. Since its original concept (Winkler, 1867), engineers were always intrigued by the mathematical potentialities of this method. Realizing its difficulties, tables have been worked out (Hayashi, Hetenyi, and so forth) and methods have been developed (Malter, Gazis, Ray, Popov, and so on, to mention only a few) to facilitate the computations. Most of the papers produced quite ingenious new methods of approach to the exact solution, but none appeared to be simple enough to be used for general application. Consequently, most of the economical advantage of the theory remained untapped.

Practical engineers realize that the uncertainty of their assumptions often does not warrant the extreme exactness of the result. It is known for example, that soil in general does not satisfy the basic assumption of elastic support; that the k-factor is by no means a constant; that the homogeneity of the soil is certainly questionable, and that the rigidity of the super-structure is difficult to evaluate. These are only a few of the deficiencies that can be enumerated.

It must be borne in mind, therefore, that the importance of this method lies primarily in its value as a "tool," but not in the extreme exactness of its results.

The following derivations will show that, if certain requirements are fulfilled, a simplified approximate method can be developed for the computation of moments, shears, and contact pressures for a combined footing which will furnish sufficiently accurate results. Other designs that cannot be fitted into the limitations and requirements of this simplified method must be solved by one of the exact methods. This approach is similar to that of the American Concrete Institute (ACI) Building Code for flat slabs, which stipulates the requirements of an empirical method for typical conditions alongside an exact elastic analysis for special cases.

Although the method described is for a continuous beam foundation, other combined footings, such as grid foundations and mat foundations, can be analyzed on the same basis by dividing them into strips. Each strip, then, must be considered as an independent unit and must be analyzed by using the full column loads in each direction. In the case of a mat foundation, each strip will have a width extending from center to center of adjacent bays and will consist of a column-strip bordered by two half middle-strips. The moments, shears, and contact pressures obtained by this method are for the entire strip. They will have to be subdivided and apportioned to the column-strip and to the middle-strip.

Basic Requirements.—The basic requirements for the applicability of this simplified method are as follows:

1. Each footing strip shall have not less than three bays or four columns in a row in order to ascertain the characteristics of a continuous beam.

---

[3] "Evaluation of Coefficients of Subgrade Reactions," which was published by the Institution of Civil Engineers, London S.W.I.

2. The ratio between adjacent spans and adjacent column loads may differ by a maximum of 20% of the greater value. It will be shown that even such liberal deviations from the basic case of equal loads and equal spacings can be tolerated without excessive loss in the accuracy of the end results.

3. The average column spacing $\bar{l}$ shall be greater than $\frac{1.75}{\lambda}$ and smaller than $\frac{3.50}{\lambda}$ in which λ is the "characteristic" in the classical theory of a beam supported by subgrade reactions. The meaning of this requirement will be explained subsequently.

In a continuous beam footing, the column spacings must stay between certain limits to keep the footing responsive to the reactions of the subgrade. Column spacings that are too small will make the foundation act as infinitely stiff, whereas column spacings that are too big will dissolve the continuous footing into single units with wasted interconnecting pieces. The selection of these

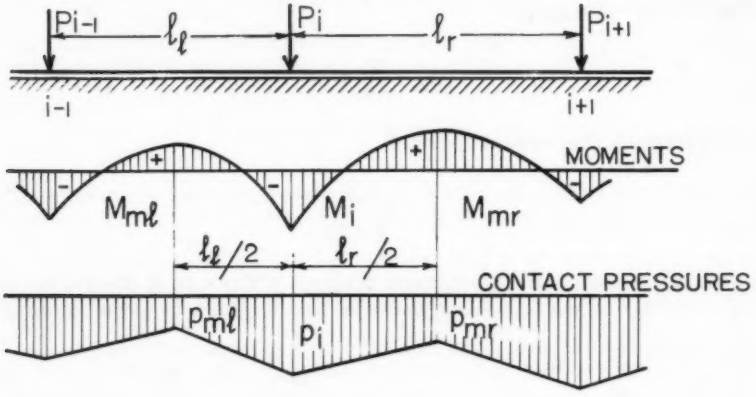

FIG. 1

limitations permitted the computation of the maximum negative moment under the columns by means of an approximate formula using a simple straight-line expression instead of the trigonometric function of the exact theory.

The evaluation of the contact pressures, positive moments, and shears was simplified by the assumption of a straight-line distribution of the contact pressure with a maximum value under the columns and a minimum value at the center of each bay.

All formulae and derivations are based on the assumption that the continuous beam footings or strips are of prismatic cross section. Small variations in the width of the footing, making the narrowest part not less than three-fourths of the widest part, will be tolerated without difficulty.

Fig. 1 shows, schematically, the moments and the simplified distribution of the contact pressures on a continuous beam footing. But it should be kept in mind that the moments shown in Fig. 1 are produced by the column loads only

and must be superposed, if necessary, with moments caused by the settlement deformation (dishing) of the combined footing as a whole.

This paper deals only with the moments and contact pressures produced by the column loads.

In order not to expand the scope of this paper unnecessarily, it will be presumed that the classical theory of a beam supported by subgrade reactions (or, as previously called "beam or elastic foundation") is known. Standard articles and text books on this subject are available.[4,5,6]

Notation.—The letter symbols adopted for use in this paper are defined where they first appear, in the illustrations or in the text, and are listed alphabetically, for convenience of reference, in Appendix II.

MOMENT UNDER INTERIOR COLUMNS

For an infinite long beam of prismatic cross-section, supported by subgrade reaction, the exact theory furnishes the following formula for the bending moment M_x due to the load P:

$$M_x = \frac{P}{4\lambda} C_{\lambda x} \quad \ldots\ldots\ldots\ldots\ldots \quad (1)$$

In this formula the "characteristic"

$$\lambda = \sqrt[4]{\frac{k}{4EI}} \quad \ldots\ldots\ldots\ldots\ldots \quad (2)$$

in which k is the coefficient of subgrade reaction of the soil, E denotes the modulus of elasticity of the foundation material and $\bar{I}$ refers to the moment of in-

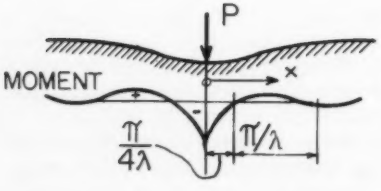

FIG. 2

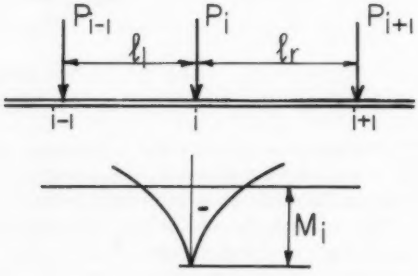

FIG. 3

4 "Theorie des Traegers auf Elastischer Unterlage," by K. Hayashi, Springer, Berlin, 1921.

5 "Beams on Elastic Foundation," by M. Hetenyi, Univ. of Michigan Press, Ann Arbor, Mich., 1946.

6 "Die Lehre von Elastizitaet und Festikeit," by E. Winkler, Prag., 1867.

ertia of the footing strip based on its average width $\bar{b}$. For the evaluation of k and λ for various soil conditions and footing size ratios, see Appendix I.

$$C_{\lambda x} = e^{-\lambda x} (\cos \lambda x - \sin \lambda x) \quad \ldots\ldots\ldots\ldots \quad (3)$$

is a trigonometric function for which tables have been prepared for various values of λx. If several loads are acting on the beam, the total moment at point c will be the sum of all moment influences produced by the loads acting on the beam.

$$M_c = \frac{P_1}{4\lambda} C_{\lambda x_1} + \frac{P_2}{4\lambda} C_{\lambda x_2} + \ldots \frac{P_n}{4\lambda} C_{\lambda x_n} = \sum \frac{P_{1,2,..n}}{4\lambda} C_{\lambda x_{1,2,..n}} \quad \ldots \quad (4)$$

$x_1, x_2, \ldots x_n$ are distances of loads $P_1, P_2 \ldots P_n$ from point c.

If the spacing of the loads is arbitrarily restricted, for now, to values between $\frac{1.75}{\lambda}$ and $\frac{3.50}{\lambda}$, the trigonometric function for $C_{\lambda x}$ can be approximated by a straight-line relation. The total moment under an interior column load at point i can then be written as

$$M_i = -\frac{P_i}{4\lambda} (0.24 \lambda \bar{l} + 0.16) \quad \ldots\ldots\ldots\ldots \quad (5)$$

This moment is the sum of the moment due to the column load P_i at point i and the influence of one adjacent column load at each side, P_{i-1} and P_{i+1}, located at an average distance $\bar{l} = \frac{l_l + l_r}{2}$ from point i, as shown in Fig. 3.

The following will explain the selection of the limiting values for the average spacing of the column loads.

If concentrated loads are placed very close together, the foundation will act like an infinitely stiff beam, and the distribution of the contact pressure will follow a straight line. In this case, the maximum negative moment at the column will approach the value of the negative moment of an inverted continuous beam carrying an equal distributed load (contact pressure).

$$-\frac{P_i}{4\lambda} (0.24 \lambda \bar{l}_{min} + 0.16) = -\frac{P_i \bar{l}_{min}}{12} \quad \ldots\ldots\ldots \quad (6)$$

From Eq. 6 the lower limit l_{min} can be evaluated as $\frac{1.78}{\lambda}$. For reasons of simplicity it was assumed to be $\frac{1.75}{\lambda}$. For column spacings closer than this value, Eq. 5 will furnish moments that are greater than those produced by a straight-line distribution of the contact pressure. Such moments are statically produced only by loadings or contact pressures which are greater at the center of the span than at the support. However, such a condition is not feasible in actual practice. In addition to the selection of the minimum column spacing with $\frac{1.75}{\lambda}$, the maximum negative moment shall be checked so as not to exceed $\frac{Pl}{12}$. If this value is exceeded the foundation must be assumed infinitely stiff and the distribution of the contact pressure will follow a straight line.

From the evaluation of the function for $C_{\lambda x}$ (see also Fig. 2), it can be seen that the moment influence from column loads located at a distance greater than $\approx \frac{\pi}{\lambda}$ can be disregarded. The upper limit was selected with $\frac{3.50}{\lambda}$ to satisfy this requirement. At the same time, its magnitude eliminates the need for adding the influence of the second adjacent column in either direction, even for the smallest admissible column spacing (3.5 = 2 x 1.75).

Eq. 5 is an approximate formula, however, within the stipulated limitations it furnishes quite accurate results, even if the permissible variations of column loads and column spacings up to 20% of the greater value are considered. The following equations give the relationship between the approximate Eq. 5

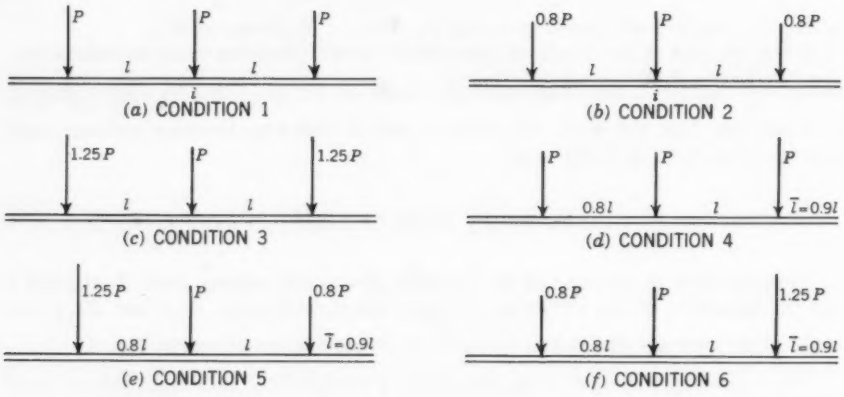

FIG. 4

and the exact results for the most unfavorable combinations of variations in loadings and spacings (as shown in Fig. 4):

From Eq. 6

$$M_i = -\frac{P}{4\lambda}(0.24\,\lambda\,\bar{l} + 0.16) = -\frac{P}{4\lambda}F_o$$

for condition 1 (Fig. 4a)

$$M_{i(1)} = -\frac{P}{4\lambda}\left(C_{\lambda 1} + C_{\lambda o} + C_{\lambda 1}\right) = -\frac{P}{4\lambda}F_1 \quad \ldots\ldots \quad (7a)$$

For condition 2 (Fig. 4b)

$$M_{i(2)} = -\frac{P}{4\lambda}\left(0.8\,C_{\lambda 1} + C_{\lambda o} + 0.8\,C_{\lambda 1}\right) = -\frac{P}{4\lambda}F_2 \quad \ldots. \quad (7b)$$

For condition 3 (Fig. 4c)

$$M_{i(3)} = -\frac{P}{4\lambda}\left(1.25\,C_{\lambda 1} + C_{\lambda o} + 1.25\,C_{\lambda 1}\right) = -\frac{P}{4\lambda}F_3 \quad \ldots \quad (7c)$$

For condition 4 (Fig. 4d)

$$M_{i(4)} = -\frac{P}{4\lambda}\left(C_{\lambda\,0.89\bar{l}} + C_{\lambda\,0} + C_{\lambda\,1.11\bar{l}}\right) = -\frac{P}{4\lambda}F_4 \quad \ldots \quad (7d)$$

For condition 5 (Fig. 4e)

$$M_{i(5)} = -\frac{P}{4\lambda}\left(1.25\,C_{\lambda\,0.89\bar{l}} + C_{\lambda\,0} + 0.8\,C_{\lambda\,1.11\bar{l}}\right) = -\frac{P}{4\lambda}F_5 \quad \ldots\ldots \quad (7e)$$

For condition 6 (Fig. 4f)

$$M_{i(6)} = -\frac{P}{4\lambda}\left(0.8\,C_{\lambda\,0.89\bar{l}} + C_{\lambda\,0} + 1.25\,C_{\lambda\,1.11\bar{l}}\right) = -\frac{P}{4\lambda}F_6 \quad \ldots\ldots \quad (7f)$$

The evaluation of loading conditions 1 to 6 for stiffness ratios varying from 1.75 to 3.50 is recorded in Table 1 and diagrammatically shown in Fig. 5. For

TABLE 1.—TABLE OF MOMENT FACTORS F_0 TO F_6

$\bar{l}\,\lambda$	F_0	F_1	F_2	F_3	F_4	F_5	F_6
1.75	0.5800	0.5960	0.6768	0.4950	0.6062	0.5914	0.6013
2.00	0.6400	0.6414	0.7131	0.5517	0.6478	0.6282	0.6497
2.25	0.7000	0.7036	0.7629	0.6295	0.7058	0.6840	0.7130
2.50	0.7600	0.7702	0.8162	0.7127	0.7679	0.7458	0.7783
2.75	0.8200	0.8330	0.8664	0.7912	0.8257	0.8053	0.8374
3.00	0.8800	0.8874	0.9099	0.8587	0.8783	0.8607	0.8898
3.25	0.9400	0.9314	0.9451	0.9142	0.9205	0.9060	0.9310
3.50	1.0000	0.9646	0.9717	0.9557	0.9529	0.9416	0.9618

equal column loads and equal column spacings, the greatest deviation of the values found by means of the approximate Eq. 5 is about 3.5% of the exact value. The most unfavorable combination of loading, spacing, and stiffness ratio shows a deviation of 16%, but the average deviations are considerably smaller. At any rate, the deviations affect only the magnitudes of the negative moments, that is the distribution of positive and negative moments, but not the total amount.

CONTACT PRESSURE UNDER INTERIOR COLUMNS

The magnitude and distribution of the contact pressure under an interior column load is not determined directly from the exact theory, but from the moment obtained by Eq. 5.

In order to simplify the procedure, the following two assumptions were made:

Assumption 1.—The resultant of all subgrade reactions acting on each interior foundation part shall be equal, concentric, and of opposite direction to the column load acting on this part.

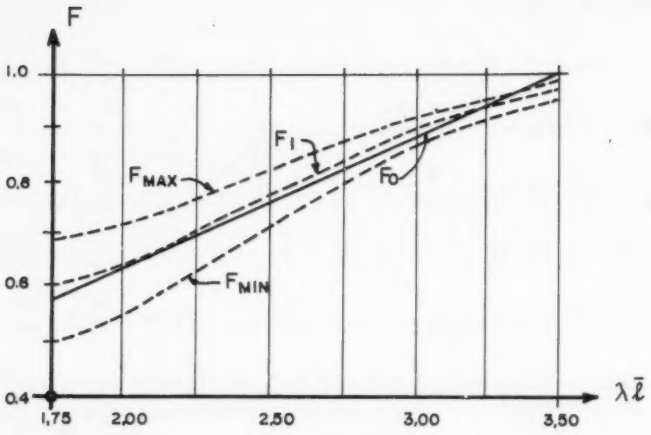

DEVIATIONS OF MOMENT FACTORS F_1 TO F_6.

FIG. 5

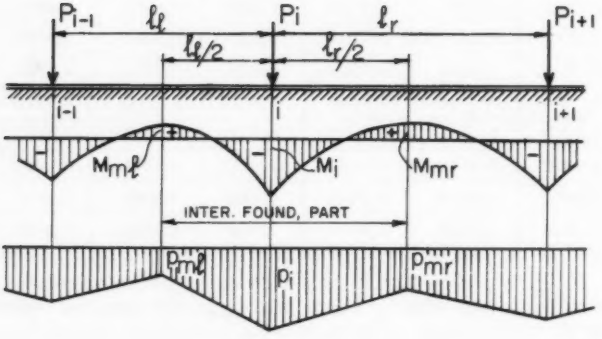

FIG. 6

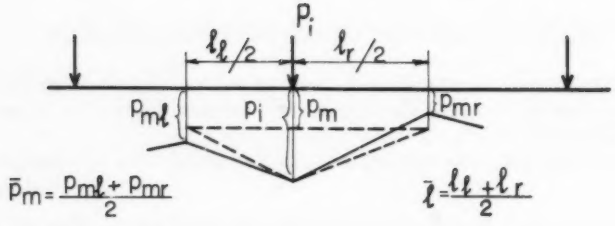

FIG. 7

(An interior foundation part is that portion of a combined footing which primarily supports one interior column load. It is assumed to extend from center to center of adjacent bays.)

Assumption No. 1 satisfies the fundamental requirement that the resultant of all subgrade reactions acting on a combined footing shall be equal, concentric, and of opposite direction to the resultant of all column loads acting on the combined footing; but, due to its restricted form, it simplifies the analysis and facilitates the computation.

Assumption 2.—The contact pressures under an interior foundation part are assumed to have a maximum value under the column, a minimum value at the center of the bay, and shall follow a straight-line distribution between the column and center of the bay. (See Fig. 6.)

Because the negative moment at a column is affected but little by variations in the loads of adjacent columns, the maximum contact pressure under a column can be approximated from a symmetrical loading condition over the average span l as shown in Fig. 7. From this distribution of the contact pressure the negative moment $-M_i$ can be determined as

$$-M_i = -\frac{\bar{p}_m \bar{l}^2}{12} - (p_i - \bar{p}_m)\frac{\bar{l}^2}{32} = -\frac{\bar{l}^2}{96}(3\,p_i + 5\,\bar{p}_m) \quad \ldots\ldots \quad (8)$$

in which

$$P_i = \frac{(\bar{p}_m + p_i)}{2}\bar{l} \quad \ldots\ldots\ldots\ldots\ldots \quad (9a)$$

and

$$\bar{p}_m = \frac{2\,P_i}{\bar{l}} - p_i \quad \ldots\ldots\ldots\ldots\ldots \quad (9b)$$

By introducing $\bar{p}_m$ into Eq. 8 p_i, the approximate maximum contact pressure for the entire width of the beam is obtained, as

$$p_i = \frac{5\,P_i}{\bar{l}} + \frac{48\,M_i}{\bar{l}^2} \quad \ldots\ldots\ldots\ldots\ldots \quad (10)$$

The minimum contact pressures at the middle of the adjacent spans can then be determined as follows:

$$P_i = \frac{(p_{ml} + p_i)}{2}\frac{l_e}{2} + \frac{(p_i + p_{mn})}{2}\frac{l_n}{2} \quad \ldots\ldots\ldots \quad (11)$$

and

$$\frac{(p_{ml} + p_i)}{2}\frac{l_e}{2}\frac{l_e}{6}\frac{(2\,p_{me} + p_i)}{(p_{ml} + p_i)} = \frac{(p_i + p_{mn})}{2}\frac{l_n}{2}\frac{l_n}{6}\frac{(p_i + 2\,p_{mn})}{(p_i + p_{mn})} \quad \ldots \quad (12)$$

from which

$$p_{ml} = 2\,P_i\frac{l_n}{l_e\,\bar{l}} - p_i\frac{\bar{l}}{l_e} \quad \ldots\ldots\ldots\ldots\ldots (13a)$$

and

$$p_{mn} = 2\,P_i \frac{l_e}{l_n \bar{l}} - p_i \frac{\bar{l}}{l_n} \quad \ldots\ldots\ldots\ldots\ldots (13b)$$

For equal spans and equal loads

$$p_m = \frac{2\,P_i}{l} - p_i = -\frac{48\,M_i}{l^2} - \frac{3\,P_i}{l} \quad \ldots\ldots\ldots\ldots (13c)$$

MOMENT BETWEEN COLUMNS

By considering each part of a combined footing, extending from center to center of adjacent bays, separately, two minimum contact pressures are obtained at the middle of each bay. These contact pressures $p_{mr(l)}$ belonging to the left part and $p_{ml(r)}$ belonging to the right part are not necessarily alike because each was computed on a different basis. For the computation of the positive moment, they can be replaced by $\bar{\bar{p}}_m$ as shown in Fig. 8.

The moment M_o of the simple supported beam then becomes

$$M_o = \frac{l^2}{48}\left(p_{i(l)} - \bar{\bar{p}}_m\right) + \frac{l^2}{8}\bar{\bar{p}}_m + \frac{l^2}{48}\left(p_{i(r)} - \bar{\bar{p}}_m\right) \quad \ldots\ldots (14)$$

or

$$M_o = \frac{l^2}{48}\left(p_{i(l)} + 4\,\bar{\bar{p}}_m + p_{i(r)}\right) \quad \ldots\ldots\ldots\ldots (15)$$

and the positive moment results as

$$M_m = M_o + \bar{M}_i \quad \ldots\ldots\ldots\ldots\ldots\ldots (16)$$

in which $\bar{M}_i$ is the average of the negative moments under the columns at each end of the bay.

$$\bar{M}_i = \frac{1}{2}\left(M_{i(l)} + M_{i(r)}\right) \quad \ldots\ldots\ldots\ldots (17)$$

From the final distribution of the contact pressures, the shear can be determined for any location.

MOMENT UNDER EXTERIOR COLUMNS

Fig. 9 shows the condition at the end of a continuous footing strip. The moment under the exterior column P_e consists of the moment due to the exterior column load itself, the influence of the next interior columns P_{e+1} and the influence of the free end. The first two parts can be treated similarly to those for an interior column. The exact expression for the moment under an exterior column is

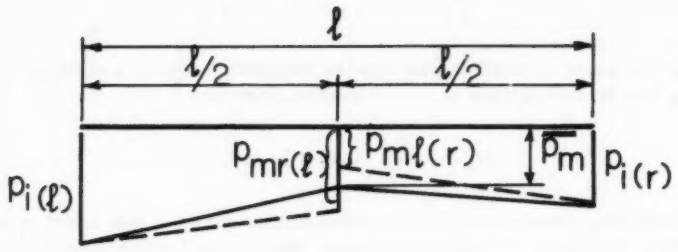

$$\overline{\overline{p_m}} = \frac{p_{mr\,(l)} + p_{ml(r)}}{2}$$

FIG. 8

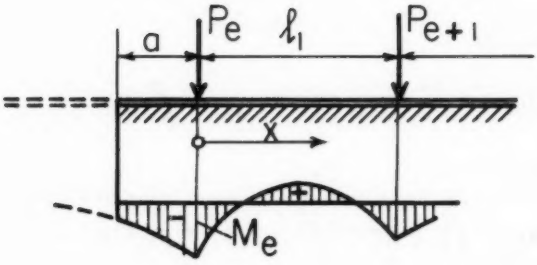

$$M'_e = -\frac{1}{4\lambda}\left(P_e C_{\lambda 0} + P_{e+1} C_{\lambda l_1} + \ldots\right)$$

FIG. 9

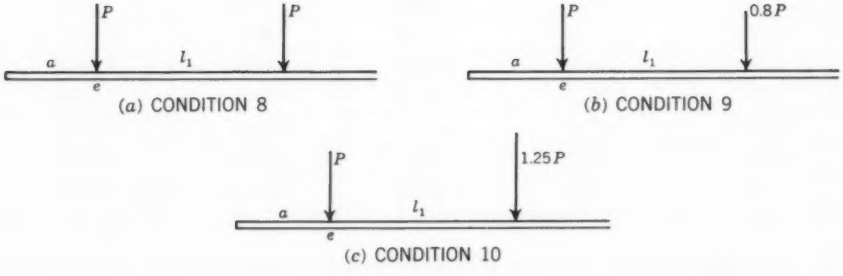

FIG. 10

$$M'_e = -\frac{1}{4\lambda}\left(P_e C_{\lambda 0} + P_{e+1} C_{\lambda l_1} + \dots\right) \quad \dots\dots\dots (18)$$

Using the same limitations as for the interior column, a straight-line expression can be substituted and the equation becomes

$$M'_e = -\frac{P_e}{4\lambda}\left(0.13\,\lambda\, l_1 + 0.56\right) \quad \dots\dots\dots (19)$$

The following equations give the relationship between the exact results for the various conditions of loadings, column spacing and stiffness ratios in comparison with those of the approximate Eq. 19.

$$M'_{e(7)} = -\frac{P}{4\lambda}\left(0.13\,\lambda\, l_1 + 0.56\right) = -\frac{P}{4\lambda} F_7 \quad \dots\dots\dots (19)$$

For condition 8 (Fig. 10a)

$$M'_{e(8)} = -\frac{P}{4\lambda}\left(C_{\lambda 0} + C_{\lambda l_1}\right) = -\frac{P}{4\lambda} F_8 \quad \dots\dots\dots (20a)$$

For condition 9 (Fig. 10b)

$$M'_{e(9)} = -\frac{P}{4\lambda}\left(C_{\lambda 0} + 0.8\, C_{\lambda l_1}\right) = -\frac{P}{4\lambda} F_9 \quad \dots\dots\dots (20b)$$

For condition 10 (Fig. 10c)

$$M'_{e(10)} = -\frac{P}{4\lambda}\left(C_{\lambda 0} + 1.25\, C_{\lambda l_1}\right) = -\frac{P}{4\lambda} F_{10} \quad \dots\dots\dots (20c)$$

The evaluation of loading conditions 8 to 10 for stiffness ratios $\lambda \bar{l}$ varying from 1.75 to 3.50 is recorded in Table 2 and diagrammatically shown in Fig.

TABLE 2.—TABLE OF MOMENT FACTORS F_7 TO F_{10}

$l_1\,\lambda$	F_7	F_8	F_9	F_{10}
1.75	0.7875	0.7980	0.8384	0.7475
2.00	0.8200	0.8207	0.8565	0.7758
2.25	0.8525	0.8518	0.8814	0.8147
2.50	0.8850	0.8851	0.9081	0.8563
2.75	0.9175	0.9165	0.9332	0.8956
3.00	0.9500	0.9437	0.9549	0.9293
3.25	0.9825	0.9657	0.9725	0.9571
3.50	1.0150	0.9823	0.9858	0.9778

11. The approximate formula furnishes results which deviate, for the most unfavorable combination of loading, column spacing, and stiffness, by about 6.5% from the exact values.

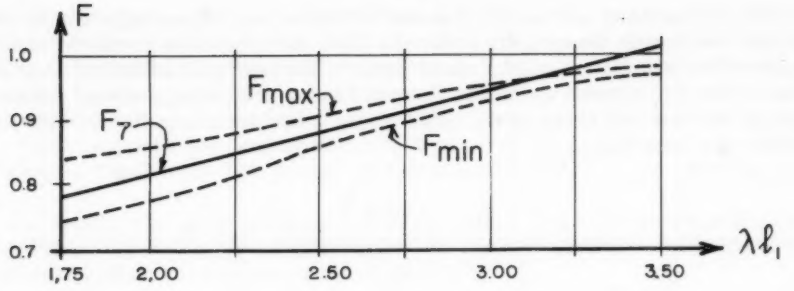

FIG. 11.–DEVIATIONS OF MOMENT FACTORS F_8 TO F_{10}

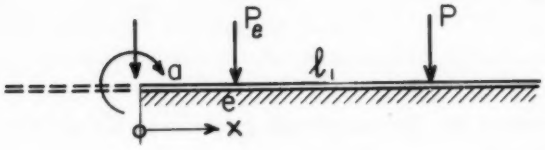

FIG. 12

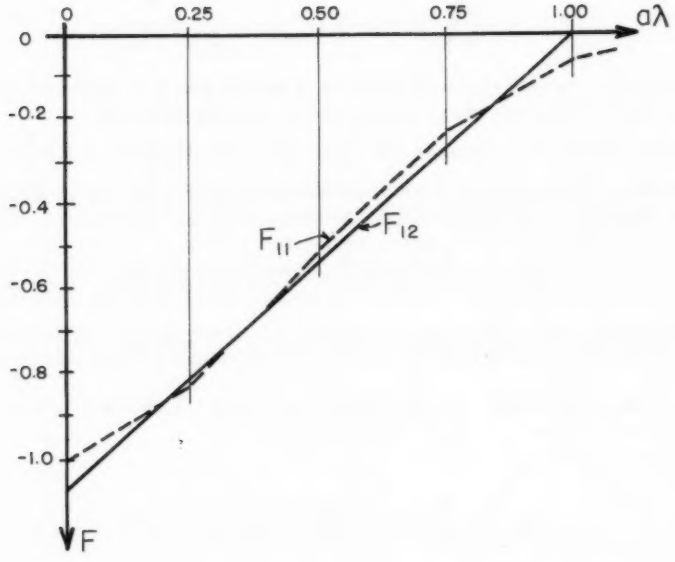

FIG. 13

The influence of a free end of a semi-infinite long beam supported by subgrade reaction on the moment under the first column can be found through the application of a moment and a shear force at the free end, as indicated in Fig. 12. These two forces, called by Hetenyi "end-conditioning-forces," make the actual moment and shear of the infinite long beam vanish to simulate the condition of a free end.

TABLE 3

$a\,\lambda$	F_{11}	F_{12}
0.00	- 1.0000	- 1.0600
0.25	- 0.8260	- 0.7950
0.50	- 0.5115	- 0.5300
0.75	- 0.2374	- 0.2650
1.00	- 0.0659	- 0.0000

The influence of the end-conditioning forces on the moment M_e under the exterior column is

$$M_e'' = -\frac{P_e}{4\lambda}\left[\left(C_{\lambda a} + 2\,D_{\lambda a}\right) C_{\lambda a} - 2\left(C_{\lambda a} + D_{\lambda a}\right) D_{\lambda a}\right]$$

$$= -\frac{P_e}{4\lambda}\left(C_{\lambda a}^2 - 2\,D_{\lambda a}^2\right) = -\frac{P_e}{4\lambda} F_{11} \quad \ldots\ldots\ldots \quad (21)$$

Evaluating this equation with the help of tables given by Hetenyi[5] the values given in Table 3 and the curve shown in Fig. 13 are obtained.

Moment factor F_{11} crosses the zero line at a distance $\lambda\, a = \frac{3}{8}\pi$. If $\frac{1}{\lambda}$ is stipulated as the maximum length for the end projection "a," a straight-line relation F_{12} can be substituted for the trigonometric expression of F_{11}.

$$M_e'' = -\frac{P_e}{4\lambda}\left(1.06\,\lambda\, a - 1.06\right) = -\frac{P_e}{4\lambda} F_{12} \quad \ldots\ldots\ldots \quad (22)$$

The final moment M_e consists of the sum of M_e' and M_e''.

$$M_e = M_e' + M_e'' = -\frac{P_e}{4\lambda}\left(0.13\,\lambda\, l_1 + 0.56 + 1.06\,\lambda\, a - 1.06\right)$$

or

$$M_e = -\frac{P_e}{4\lambda}\left(0.13\,\lambda\, l_1 + 1.06\,\lambda\, a - 0.50\right) \quad \ldots\ldots\ldots \quad (23)$$

Eq. 23 furnishes, especially for small end-projections, moments which require high subgrade reactions on the projecting part of the footing. Subsequent

settlement will reduce the moment at the exterior column and shift the resultant of the subgrade reactions for the exterior part towards the interior of the beam. This self-balancing action led to the assumption that for small projections the maximum contact pressure at the end of the projection (p_a) should not exceed the contact pressure under the exterior column. This is shown in Fig. 14, which indicates also the usually slight offset of the resultant of the contact pressures for the exterior footing part from the location of the exterior column.

To account for these adjustments, assumptions 1 and 2 have been changed to assumptions 1a and 2a, as given below, if used in connection with moments and contact pressures under exterior columns.

Assumption 1a.—Under exterior columns, the resultant of all subgrade reactions acting on the exterior part of a combined beam footing must be equal and opposite to the load of the exterior column.

(An exterior foundation part is that portion of a combined footing which primarily supports an exterior column load. It is assumed to extend from the center of the first bay to the tip of the projection.)

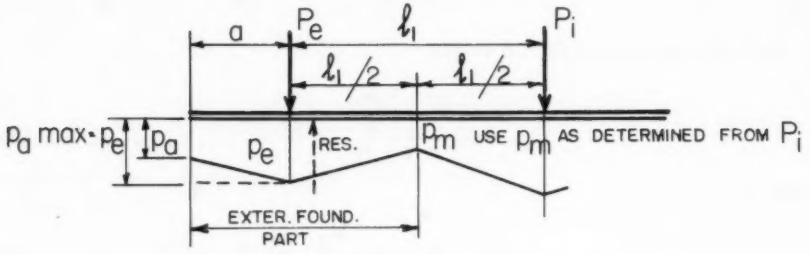

FIG. 14

Assumption 2a.—The contact pressures under an exterior foundation part are assumed to have a maximum value under the column, a minimum value at the tip of the projection and at the center of the first bay, and shall follow a straight-line distribution in between. The contact pressure at the tip of the projection shall never exceed the contact pressure under the exterior column.

The limitation for the contact pressure at the tip of the end projection leads to a second formula for the negative moment under an exterior column. From

$$P_e = p_e\, a + \left(\frac{p_e + p_m}{2}\right)\frac{l_1}{2} \qquad \text{.....(24a)}$$

and

$$p_e = \frac{4\,P_e - p_m\, l_1}{4\,a + l_1} \qquad \text{.....(24b)}$$

$$M_e = -\,p_e\,\frac{a^2}{2} = -\left(\frac{4\,P_e - p_m\, l_1}{4\,a + l_1}\right)\frac{a^2}{2} \qquad \text{..... (25)}$$

To assure the limitation the choice of Eq. 23 and 25 shall depend on which is the smaller.

CONTACT PRESSURE UNDER EXTERIOR COLUMNS

Based on assumptions 1a and 2a, the contact pressures under an exterior column can be determined as follows:

If Eq. 23 governs:

$$P_e = p_e \left(\frac{a}{2} + \frac{l_1}{4}\right) + p_a \frac{a}{2} + p_m \frac{l_1}{4} \quad \ldots\ldots\ldots (26)$$

$$M_e = - p_e \frac{a^2}{6} - p_a \frac{a^2}{3} \quad \ldots\ldots\ldots\ldots (27)$$

and

$$p_a = - \frac{3 M_e}{a^2} - \frac{p_e}{2} \quad \ldots\ldots\ldots\ldots (28)$$

Introducing P_a into Eq. 26 yields

$$p_e = \frac{4 P_e + \frac{6 M_e}{a} - p_m l_1}{a + l_1} \quad \ldots\ldots\ldots\ldots (29a)$$

and

$$p_a = - \frac{3 M_e}{a^2} - \frac{p_e}{2} \quad \ldots\ldots\ldots\ldots (29b)$$

If Eq. 25 governs

$$p_e = p_a = \frac{4 P_e - p_m l_1}{4 a + l_1} \quad \ldots\ldots\ldots (30)$$

MUTUAL INFLUENCE OF END CONDITIONS

Because the foundation shall be continuous over at least three bays, the minimum length of a beam, between exterior columns, is $\frac{5.25}{\lambda}$. Such beams can be considered as "long"; that is, they may be considered as semi-infinite beams and the end-conditions do not influence each other.

EXAMPLES

The following examples, which have been selected for average conditions, illustrate the practical application of the method. For reasons of clarity, any influence due to uneven settlements of the combined footing has been omitted.

Example on Mat Foundation Fig. 15.

Assume average 18 in. slab thickness (t), 0.225 kip per sq ft. Assume soil to be stiff clay, allowable soil pressure is 3000 psf., k_{si} = 100 tons per cu ft. P_i = 640 kips, P_e = 550 kips, l = 18 ft, b = 18 ft, a = 5 ft, k = 2 ρ k_{si} $\rho = \frac{1 + 0.5}{1.5}$ = 1.0 (see Appendix I) and f'_c = 3000 psi.

$$E_c = 432 \times 10^3 \text{ kips per sq ft, } I = 18 \times 1.5^3/12 = 5.06 \text{ ft}^4$$

$$\lambda = 2.9 \sqrt[4]{\frac{k_{si}\,\rho}{f'_c\,t^3}} = 2.9 \sqrt[4]{\frac{100}{3000 \times 18^3}} = 2.9 \frac{1}{\sqrt[4]{30 \times 18^3}} = 0.139 \text{ (see Appendix I)}$$

$$l \times \lambda = 18 \times 0.139 = 2.5 \begin{matrix} > 1.75 \\ < 3.50 \end{matrix}$$

Interior Columns and Bay.—From Eq. 5

$$M_i = -\frac{P_i}{4\lambda}(0.24\lambda\bar{l} + 0.16) = -\frac{640}{4 \times 0.139}(0.24 \times 0.139 \times 18 + 0.16) = -870 \text{ ft kips}$$

or

$$M_i = -\frac{P_i\, l}{12} = -\frac{640 \times 18}{12} = -960 \text{ ft kips}$$

for straight line contact pressure (870 < 960).

From Eq. 10

$$p_i = \frac{5\,P_i}{\bar{l}} + \frac{48\,M_i}{l^2} = \frac{5 \times 640}{18} - \frac{48 \times 870}{18^2} = 49 \text{ kips per ft}$$

and

$$p'_i = \frac{49}{18} + 0.225 = \underline{2.95} \text{ kips per sq ft total unit contact pressure.}$$

From Eq. 13c

$$p_m = -\frac{48\,M_i}{l^2} - \frac{3\,P}{l} = \frac{48 \times 870}{18^2} - \frac{3 \times 640}{18} = 22 \text{ kips per ft}$$

and

$$p'_m = \frac{22}{18} + 0.225 = \underline{1.45} \text{ kips per sq ft total unit contact pressure.}$$

From Eq. 15

$$M_o = \frac{l^2}{48}\left(p_{i_{left}} + 4\,p_m + p_{i_{right}}\right) = \frac{18^2}{48}(49 + 4 \times 22 + 49) = 1250 \text{ ft kips.}$$

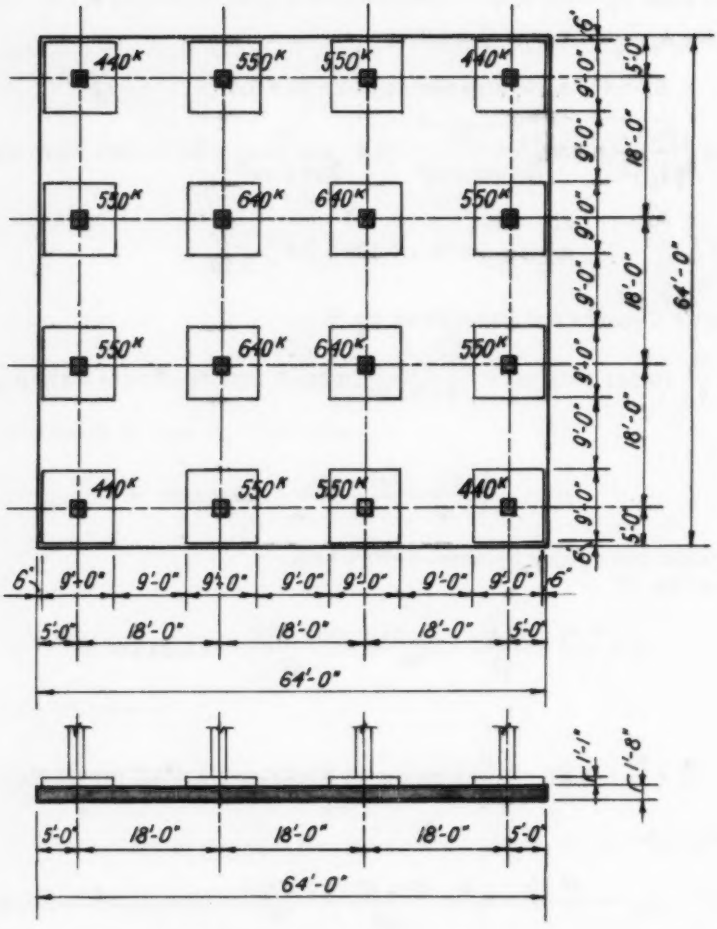

FIG. 15.–EXAMPLE ON MAT FOUNDATION

From Eq. 16

$$M_m = M_o + \overline{M}_i = 1250 - 870 = + \underline{380} \text{ ft kips.}$$

for the middle bay and

$$M_m = \frac{18^2}{48}(50 + 4 \times 22 + 49) + \left(\frac{-560 - 870}{2}\right) = 545 \text{ ft kips.}$$

for the end bay.

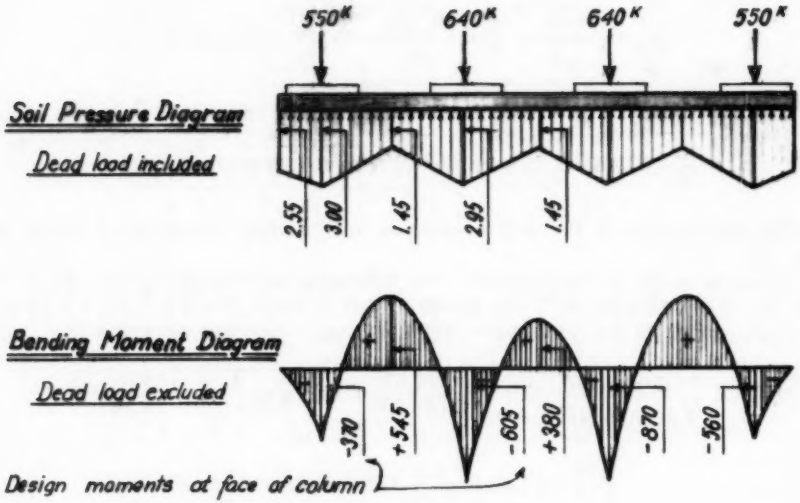

FIG. 16.–SOIL PRESSURE AND BENDING MOMENT DIAGRAMS FOR MAT FOUNDATION

Exterior Columns and Bay, (perpendicular to edge).–From Eq. 23

$$M_e = -\frac{P_e}{4\lambda}(0.13\,\lambda l_1 + 1.06\,\lambda a - 0.50) \quad \ldots\ldots\ldots \quad (23)$$

$$M_e = -\frac{550}{4 \times 0.139}(0.13 \times 0.139 \times 18 + 1.06 \times 0.139 \times 5 - 0.50) = -\underline{560} \text{ ft kips,}$$

or from Eq. 25

$$M_e = -\frac{a^2}{2}\left(\frac{4\,P_e - p_m\,l_1}{4\,a + l_1}\right) = -\frac{5^2}{2}\left(\frac{4 \times 550 - 22 \times 18}{4 \times 5 + 18}\right) = -595 \text{ ft kips, } 560 < 595$$

From Eq. 29a

$$p_e = \frac{4\,P_e + \frac{6\,M_e}{a} - p_m\,l_1}{a + l} = \frac{4 \times 550 - \frac{6 \times 560}{5} - 22 \times 18}{5 + 18} = 50 \text{ kip per ft}$$

and

$$p_e' = \frac{50}{18} + 0.225 = \underline{3.00} \text{ kip per sq ft total unit contact pressure.}$$

From Eq. 29b

$$p_a = -\frac{3\,M_e}{a^2} - \frac{p_e}{2} = \frac{3 \times 560}{5^2} - 25 = 4.2 \text{ kip per ft}$$

and

$$p_a' = \frac{42}{18} + 0.225 = \underline{2.55} \text{ kips per sq ft total unit contact pressure.}$$

The distribution of the soil pressures and bending moments is shown in Fig. 16.

Example on Strap Foundation.—The following data is given (see Figs. 17 and 18): $P_i = 640$ kips, $P_e = 550$ kips, $l = 18$ ft, $a = 5$ ft, $b = 6$ ft 6 in., $t = 24$ in. $\rho = 0.67$, allowable soil pressure = 8000 psf, $k_{si} = 250$ (see Appendix I).

$$\lambda = 2.9 \sqrt[4]{\frac{250 \times 0.67}{3000 \times 24^3}} = 2.9 \sqrt[4]{\frac{16.67}{4{,}147.200}} = 2.9 \sqrt[4]{\frac{1}{249.000}} = \frac{2.9}{22.34} = 0.13$$

$$\frac{1.75}{0.13} = 13.45 \text{ ft} \quad \frac{3.5}{0.13} = 26.9 \text{ ft (see Appendix I)}$$

From Eq. 5

$$M_i = -\frac{640}{4 \times 0.13}(0.24 \times 0.13 \times 18 + 0.16) = -\underline{886} \text{ ft kips,}$$

or

$$M_i = -\frac{640 \times 18}{12} = -960 \text{ ft kips for straight line contact pressure } (886 < 960).$$

From Eq. 10

$$p_i = \frac{5 \times 640}{18} - \frac{48 \times 886}{18^2} = 47 \text{ kips per ft}$$

and

$$p_i' = \frac{47}{6.5} + 0.3 = \underline{7.55} \text{ kips per sq ft total unit contact pressure.}$$

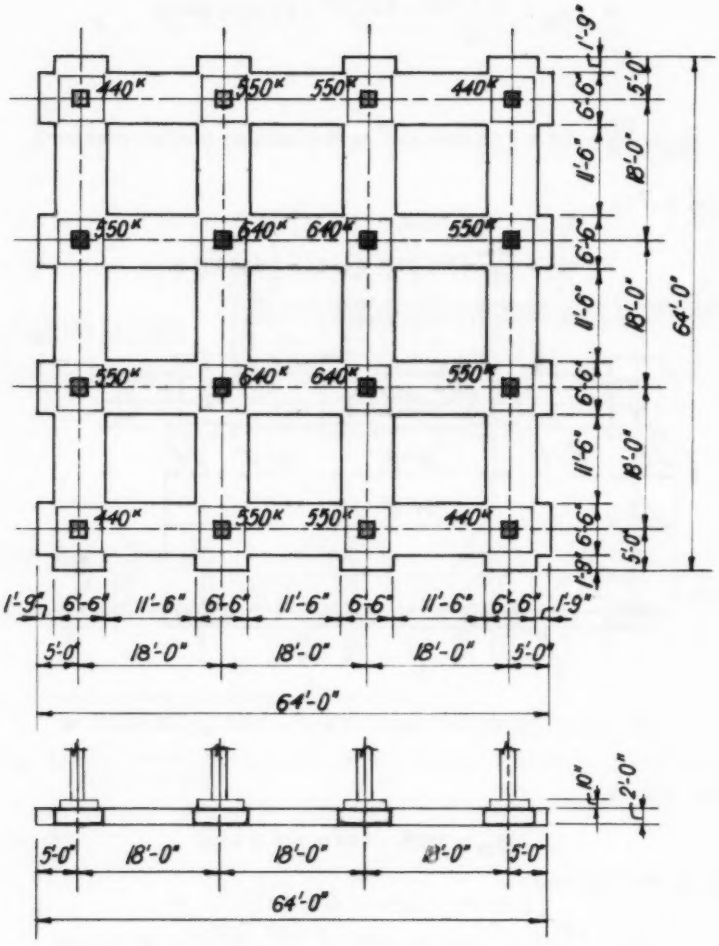

Plan and Section

FIG. 17.–EXAMPLE ON STRAP FOUNDATION

From Eq. 13c

$$p_m = \frac{48 \times 886}{18^2} - \frac{3 \times 640}{18} = 24 \text{ kips per ft}$$

and

$$p'_m = \frac{24}{6.5} + 0.3 = \underline{4.00} \text{ kips per sq ft total unit contact pressure.}$$

From Eq. 15

$$M_o = \frac{18^2}{48} (2 \times 47 + 4 \times 24) = 1280 \text{ ft kips}$$

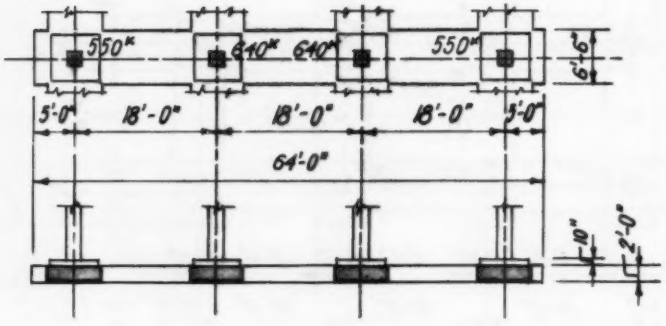

FIG. 18.–TYPICAL DESIGNED STRAP — PLAN AND SECTION

From Eq. 16

$$M_m = 1280 - 886 = \underline{394} \text{ ft kips}$$

for the middle bay and

$$M_m = \frac{18^2}{48} (50 + 4 \times 24 + 47) + \left(\frac{-513 - 886}{2}\right) = 600 \text{ ft kips}$$

for the end bay. From Eq. 23

$$M_e = \frac{550}{4 \times 0.13} \left(0.13^2 \times 18 + 1.06 \times 0.13 \times 5 - 0.50\right) = \underline{513} \text{ ft kips,}$$

or from Eq. 25

$$M_e = -\frac{5^2}{2} \left(\frac{4 \times 550 - 24 \times 18}{4 \times 5 + 18}\right) = 583 \text{ ft kips,} \quad 513 < 583$$

From Eq. 29a

$$p_e = \frac{4 \times 550 - \frac{6 \times 513}{5} - 24 \times 18}{5 + 18} = 50.2 \text{ kips per ft}$$

and

$$p'_e = \frac{50.2}{6.5} + 0.3 = \underline{8.00} \text{ kips per sq ft total unit contact pressure.}$$

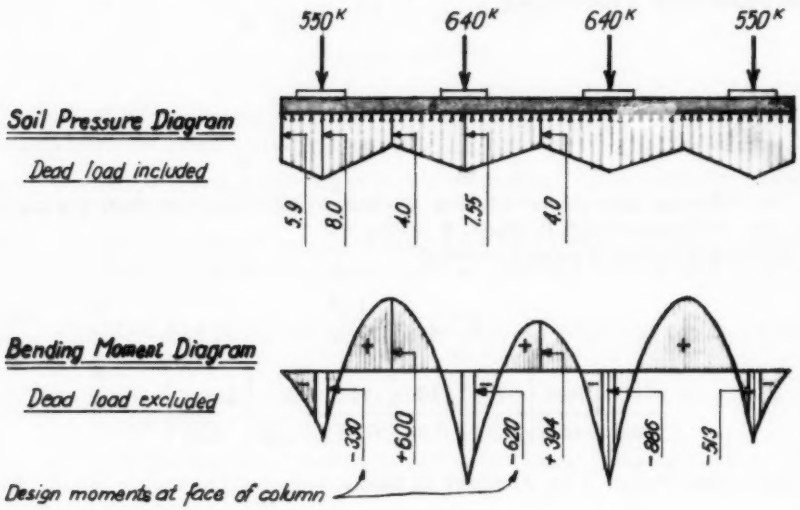

FIG. 19.–SOIL PRESSURE AND BENDING MOMENT DIAGRAMS FOR STRAP FOUNDATION

From Eq. 29b

$$p_a = \frac{3 \times 513}{25} - 25 = 36.5 \text{ kips per ft}$$

and

$$p'_a = \frac{36.5}{6.5} + 0.3 = \underline{5.9} \text{ kips per sq ft total unit contact pressure.}$$

The distribution of the soil pressures and bending moments is shown in Fig. 16.

CONCLUSIONS

This paper has shown that for continuous beam footings conforming to certain limitations, the moments due to subgrade reactions can be found by empirical method.

In making simplifying assumptions for the distribution of the contact pressures under the footing, the magnitude of the contact pressures can be found directly from the moments. The empirical formulae furnish results that are, for practical purposes, sufficiently close to those of an elastic analysis. Additional moments caused by uneven settlements (dishing) of the combined footings are not included in the formulae.

Liberal deviations from equal column loads and equal column spacings can be tolerated and permit wide application to practical design.

Grid and mat foundations can be treated as cases of intersecting beam foundations and can be solved by the same method. Examples illustrate the practical application of the method.

APPENDIX I

The following formulae and tables are based on the work of Karl Terzaghi Hon. M. ASCE and Ralph B. Peck, F. ASCE.[7,8]

Size Factor ρ for Footings on Sand.

$$\rho = \frac{1}{4}\left(1 + \frac{1}{\bar{b}}\right)^2 \qquad \ldots\ldots\ldots\ldots\ldots (31)$$

$\bar{b}$, in feet	5	10	15	20	large
value of ρ	0.36	0.30	0.28	0.275	0.25

Side-Ratio Factor ρ for Footings on Clay.

$$\rho = \frac{n + 0.5}{1.5\,n} \qquad \ldots\ldots\ldots\ldots\ldots\ldots (32)$$

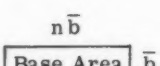

For Strips $\rho = 0.67$.

TABLE 4.—COEFFICIENT OF SUBGRADE REACTION k_{si}

	Sand			Clay		
	Loose	Medium	Dense	Stiff	Very Stiff	Hard
N	4 - 10	10 - 30	30 - 50	8 - 15	15 - 30	> 30
k_{si}	20 - 60	60 - 300	300 - 1000	50 - 100	100 - 200	>200

7 "Evaluation of Coefficients of Subgrade Reaction" by K. Terzaghi, published by The Institution of Civil Engineers, London, 1956.

8 "Soil Mechanics in Engineering Practice" by K. Terzaghi and R. B. Peck, Wiley, New York.

The values for the coefficient of subgrade reaction are given in Table 4.

$$\lambda = \sqrt[4]{\frac{k}{4\,E\,\bar{I}}} = \sqrt[4]{\frac{(2\,k_{si}\,\rho)\,\bar{b}}{4\left(\frac{1000\,f'_c\,144}{1000}\right)\left(\frac{\bar{b}\,t^3}{12 \times 1728}\right)}} = 2.9\sqrt[4]{\frac{k_{si}\,\rho}{f'_c\,t^3}} = \lambda\left(\frac{1}{ft}\right)$$

$$k = 2\,k_{sl}\,\rho \quad \ldots\ldots\ldots\ldots\ldots\ldots \quad (33)$$

APPENDIX II.—NOTATION

The following symbols have been adopted for use in the paper and are presented here for guidance of discussers:

- a = length of end projection of combined footing, measured from exterior column to tip of end projection, in feet;
- $\bar{b}$ = average width of combined footing (beam or strip), averaged between centers of bays or between center of first bay and tip of end projection, in feet;
- E = modulus of elasticity of concrete used for combined footing, in kips per square foot;
- f'_c = ultimate compressive strength of concrete at 28 days, in pounds per square inch;
- $\bar{I}$ = average moment of inertia of combined footing, based on average width $\bar{b}$, in feet to the fourth power;
- k = coefficient of vertical subgrade reaction for the width $\bar{b}$ (see Appendix I), in kips per square foot;
- k_{sl} = basic coefficient of vertical subgrade reaction for a square area 1 ft wide (see Appendix I) in tons per cubic foot;
- l = distance between two adjacent columns, in feet;
- $\bar{l}$ = average of two adjacent column distances, in feet;
- M_e = moment at exterior column for entire width of combined footing, in kip feet;
- M_i = moment at interior column, for entire width of combined footing, in kip feet;
- $\bar{M}_i$ = average of column moments at each end of a bay, in kip feet;
- M_m = moment at center of bay, for entire width of combined footing, in kip feet;
- M_o = simple span beam moment (for the entire width of the combined footing) for a beam supported by two adjacent columns acted upon by contact pressure due to column loads only, in kip feet;
- N = number of blows in Standard penetration soil test;

P_e = load of exterior column, consisting of weight of superstructure (D.L. + L.L.) excluding weight of footing and surcharge, in kips

P_i = load of interior column, consisting of weight of superstructure (D.L. + L.L.) excluding weight of footing and surcharge, in kips;

p_a = contact pressure at tip of end projection due to column loads only, for entire width of combined footing, in kips per foot;

p_e = contact pressure at exterior column due to column loads only, for entire width of combined footing, in kips per foot;

p_i = contact pressure at interior column due to column loads only, for entire width of combined footing, in kips per foot;

p_m = contact pressure at center of bay, due to column loads only, for entire width of combined footing, in kips per foot;

$\bar{p}_m$ = average between the p_m values at the centers of two adjacent bays, in kips per foot;

$\bar{\bar{p}}_m$ = average between the p_m values at the center of same bay as determined from adjacent bays, in kips per foot;

p' = total unit contact pressure, due to column loads plus footing weight plus surcharge, in kips per square foot;

t = thickness of combined footing, in inches;

λ = characteristic in classical theory of beam supported by subgrade reactions; and

ρ = size-or side-ratio factor of subgrade reaction (see Appendix I).

Journal of the
SOIL MECHANICS AND FOUNDATIONS DIVISION
Proceedings of the American Society of Civil Engineers

DISPLACEMENT OF LONG FOOTINGS BY DYNAMIC LOADS

By William L. Wallace[1]

SYNOPSIS

A mathematical expression for the displacement of a long footing subjected to a peak triangular force pulse is developed from theoretical considerations. The solution is presented in a manner convenient for the computation of the ultimate static shear resistance as well as the displacement under dynamic loading.

INTRODUCTION

Background.—With the advent of nuclear weapons, great interest has been shown in the study of construction capable of protecting personnel and equipment from the effects of nuclear detonations. For the civil engineer the primary requirement is to design structural elements and structures capable of withstanding the high, time-dependent loads associated with the shock waves emitted from such large energy releases. The rate of change of load within these blast loadings is so rapid that the response of a structure would be appreciably different from its response to static loads of a similar magnitude. The design of such protective construction has therefore emphasized the study of structural dynamics.

Structural dynamics investigations had been pioneered by studies of designs for earthquake-resistant structures, and this work served as the natural starting place for further study. Both analytical and experimental work have been

Note.—Discussion open until March 1, 1962. To extend the closing date one month, a written request must be filed with the Executive Secretary, ASCE. This paper is part of the copyrighted Journal of the Soil Mechanics Division, Proceedings of the American Society of Civil Engineers, Vol. 87, No. SM 5, October, 1961.

[1] Capt., U. S. Army, Corps of Engrs., U. S. Army Engr. Waterways Experiment Sta., Vicksburg, Miss.

done to determine the response of structural materials, structural elements, and total structures to blast-type loadings. It is only natural that these studies were started with better-defined building materials such as steel and reinforced concrete, and left the less understood, nonhomogeneous materials such as soil to later investigators. Current knowledge of the dynamic response of foundations is, therefore, greatly behind that of the superstructure.

Purpose and Scope.—Only one aspect of the many problems involving the dynamic properties and response of soils, that of the load-displacement response of long footings is presented. Specifically, the objective of the work described herein was to derive a mathematical expression for predicting the large permament displacements of long footings in terms of soil properties and blast-type dynamic loads. Additional information is presented elsewhere.[2,3,4,5,6]

The writer became interested in the dynamic behavior of footings while on duty at the U. S. Army Engineer Waterways Experiment Station (WES). The Soils Division, WES, is invextigating the dynamic properties and response of soils through several research studies being conducted or supervised by the WES staff.

At meetings involving representatives of the WES Soils Division and consultants, various possibilities for mode of failure of footings under dynamic loading were studied; among these were total shear failures involving rotation and punching of the footing. Rotation and punching as used herein distinguish between failures where the failure surface is to one side of the footing (one-sided), causing the footing to rotate as it displaces downward, and where the failure surface is symmetrical about the center line of the footing so that no rotation occurs as the footing displaces downward. The writer felt that a study of a failure surface giving a punching-type failure would be worthwhile in order that the displacements predicted during rotational and punching failures under similar soil and loading conditions could be compared. Also, a failure surface for the punching failure could be chosen to allow displacement computations for both frictional and cohesive soils.

There was reason to believe that a two-sided (punching) surface would prove more critical than the one-sided (rotational) surface, at least theoretically. The difference in ultimate static shear resistance between the two types of failure surfaces can be shown to be quite small. On the other hand, the mass of soil contained within the two types of surfaces would not be the same. If each half of the two-sided surface were exactly similar to the one-sided surface, the mass of soil contained within the one-sided surface would be twice as great as that contained within the two-sided surface (Fig. 1). Under dynamic loading

---

2 "The Behavior of Soils Under Dynamic Loadings," by R. V. Whitman, Final Report of Lab. Studies, Contract DA-49-129-eng-227, Massachusetts Inst. of Tech., August, 1954.

3 "Studies of Investigations into the Dynamic Bearing Properties of Cohesionless Soils," by T. D. Landale, thesis, presented to the Massachusetts Inst. of Tech., September, 1954.

4 "Design of Structures to Resist the Effects of Atomic Weapons; Strength of Materials and Structural Elements," U. S. Army, Corps of Engrs., EM 1110-345-414, March 15, 1957.

5 "Report on Survey of Literature in Connection with the Dynamic Bearing Capacity of Soils," by N. Kachaturian, Contract DA-22-079-eng-240, Univ. of Illinois, October, 1959.

6 "Analytical Study of Dynamic Bearing Capacity of Foundations," by G. E. Triandafilidis, Contract DA-22-079-eng-240, Univ. of Illinois, June, 1960.

it should be expected that the system with the least mass would displace further and therefore be the more critical.

THE PROBLEM

General Approach.—The predicted permanent displacement (Δ_{MAX}) of a long footing subjected to a vertical dynamic load is obtained by deriving an equation for footing displacement (Δ) versus time (t) and then solving the equation at the time of maximum displacement (t_{MAX}). The maximum occurs when the velocity of the footing first becomes zero. After this time, the motion tends to reverse in direction causing a similar reverse in the shear forces acting

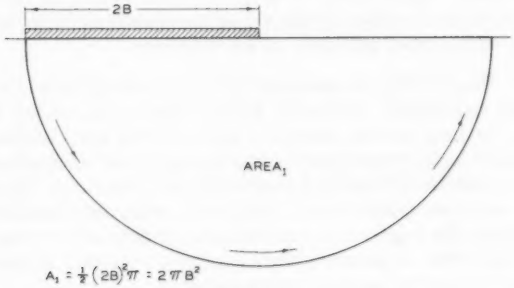

(a) ROTATIONAL FAILURE

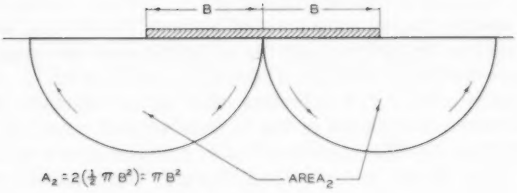

(b) PUNCHING FAILURE

FIG. 1.—SOIL WITHIN FAILURE SURFACES

along the failure surface. Footing displacement ceases at this time because the reversed shear forces available are greater than forces acting to cause motion. As mentioned subsequently, this assumption does not consider elastic rebound.

The equation relating footing displacement to time is obtained directly from the differential equation describing the movement. The dynamic resisting forces acting on the soil mass and footing are expressed in differential form as effective resisting forces acting vertically at the footing. These effective resisting forces are then equated to the loading function to obtain the differ-

ential equation. The total loading on the footing is considered to comprise: the dynamic load, the ultimate static shear resistance of the footing (p), the inertial force of the accelerated soil mass (IF), and the displacement-dependent restoring force created by the movement of the center of gravity of the soil mass (RF). This procedure will yield a second-order, nonhomogeneous differential equation for which the particular solution can be obtained by conventional mathematical means.

Assumptions.—Solution of problems relating to the static bearing capacity of footings is complicated by the nonhomogeneous, anelastic properties of the soil. In attempting to develop equations for the dynamic response of footings the problem is further complicated by strain-rate effects on shear strength, inertial effects due to mass movement, and the time history of the imposed footing load. Greatly simplifying assumptions are therefore necessary before any kind of solution is feasible. The basic assumptions used in the development of the equations and a brief analysis of each follow:

1. Footing.—The footing is assumed long relative to its width (2 B), and the end effects are neglected. Although square and rectangular footings are of great interest, the long footing seems a logical first step because of the simplification inherent in the two-dimensional system. The footing is assumed to be weightless and to impart a uniform load to the soil surface. The assumption of weightlessness is conservative since the force required to accelerate the footing would decrease the load on the soil surface. If deemed necessary, the mass of the footing and other superstructure could be included in the system, however, this is not within the scope of this paper.

2. Failure Surface.—Bearing failure occurs when the shear stress at all points along the failure surface has exceeded the ultimate shear strength of the soil. The dynamic failure surface assumed is the static failure surface first described by Prandtl and later modified by K. Terzaghi, Hon. M. ASCE (Fig. 2). It is composed of two spiral curves of varying radius (R) starting at the point of a wedge-shaped zone located beneath the footing and terminating in two passive wedges which intersect the soil surface at an angle of $45° - \phi/2$, in which ϕ equals the angle of internal friction for the soil.[7,8] As stated previously, the primary reason for selecting this failure surface is that it hypothesizes the downward movement of the footing without rotation.

3. Center of Spiral.—The center of each spiral surface (0) is assumed to lie on line ad (Fig. 2) or an extension thereof. The selection of the critical location of the spiral center is a prerequisite to precise computation of the ultimate shear resistance and of the mass of soil contained within the failure surface. The published data commonly used in determining the static bearing capacity are not based on an exact determination of the critical spiral center because simplifying assumptions are available which do not greatly affect the accuracy of the static computations. The same assumptions are not believed permissible in the dynamic solution because of the added significance of the moving mass contained within the failure surface. The added labor to obtain the more accurate failure surface and mass is believed quite necessary.

4. Stress-strain Relation.—The soil is assumed to be a rigid-plastic material, that is, the ultimate shear strength is reached without deformation

7 "Theoretical Soil Mechanics," by K. Terzaghi, John Wiley and Sons, Inc., New York, 1948.

8 "Soil Mechanics, Foundations, and Earth Structures," by G. P. Tschebotarioff, McGraw-Hill Company, Inc., New York, 1956, p. 221.

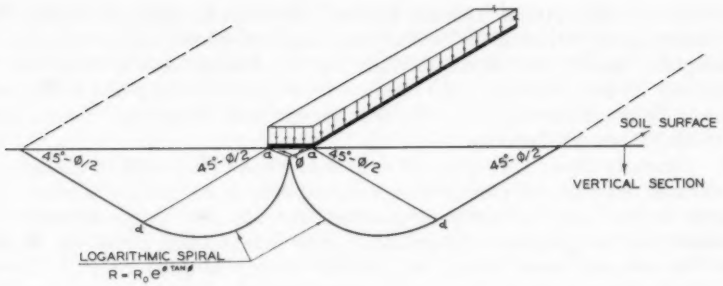

FIG. 2.—FAILURE SURFACE

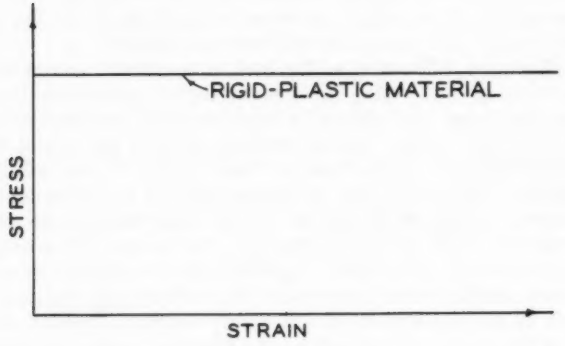

FIG. 3.—STRESS-STRAIN RELATION

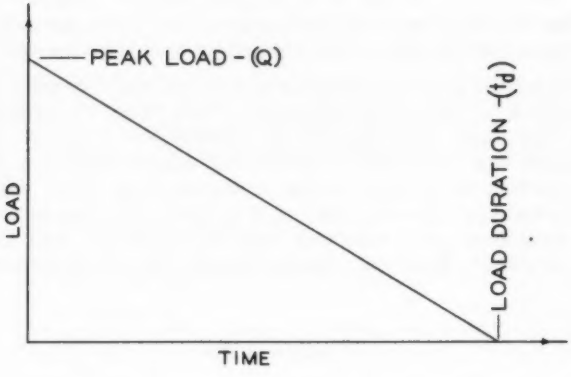

FIG. 4.—LOADING FUNCTION

and then the soil yields with no further increase in shear strength (Fig. 3). The discrepancy between the actual and computed deformations because of this assumption should be small as long as the deformation is relatively large compared to deformations that would occur prior to ultimate static bearing failure. This assumption also implies that the soil is incompressible and that the footing does not rebound.

5. Ultimate Shear Strength.—The ultimate shear strength is assumed equal to cohesion (c) plus the product of normal stress on the failure surface and the tangent of the angle of internal friction. The ultimate shear strength is also assumed, for the purposes of this paper, to be independent of the rate of strain, since the present knowledge of strain-type effects is quite limited. Certainly, the rate-of-strain effect will modify the footing displacement, and with further information on the effect of strain rate on shear strength such effects could and must be incorporated into the solution. For example, the ultimate shear resistance could be multiplied by a strain-rate coefficient and substituted into the solution in the same manner, if the strain-rate effect is constant throughout the loading cycle. If the effect is more complicated, the incorporation may require substantial changes in the differential equation.

6. Soil Mass and Movement.—The soil is assumed to be of uniform density and to deform as a rigid body. This assumption is necessary in order to compute the inertial force, and should be approximately correct provided the displacement is not excessive, that is does not destroy the initial geometry.

7. Loading Function.—The dynamic load applied to the footing is an initial-peak triangular force pulse (Fig. 4). Such a function is convenient for computations and approximates the probable footing loads under some practical conditions. As was true with other assumptions, the choice of loading function does not affect the over-all procedure. Another function could be substituted, if it is felt that such would better represent the actual load applied to the footing.

8. Effect of Displacement on Ultimate Bearing Capacity.—Any downward movement of the footing will displace the effective center of gravity of the soil contained within the failure surface in such a manner as to increase the ultimate bearing capacity. This is not accounted for as a change in bearing capacity, but as a displacement-dependent force acting to decrease the displacement, that is to restore the footing to its original position. Displacement will also slightly shorten the length of shearing surface from the original assumed failure surface, but this effect is neglected in the computations.

When all simplifying assumptions are considered together, they certainly put restrictions on the footing-soil system described. Nevertheless, it is believed that the model they describe is worth study. It should not be expected that the system will accurately predict small displacements of footings. However, the predictions of long footing displacements under vertical dynamic loads should be approximately correct if (1) the displacements are large compared to displacements associated with static failure, and (2) the strength properties assigned to the soil closely describe the actual dynamic properties of the soil.

EQUATIONS

Notation.—The letter symbols adopted for use in this paper are defined where they first appear and are arranged alphabetically, for convenience of reference, in the Appendix.

In the following paragraphs mathematical expressions for the forces acting on the soil mass are derived as effective forces acting vertically at the footing. These forces are then equated to the loading function to determine the differential equation for the footing motion. Since the assumed failure surface is symmetrical about the center line of the footing, only one-half of the footing and associated failure surface is necessary to compute all forces. A unit length of footing is also assumed for all computations.[9]

Ultimate Static Shear Resistance.—The ultimate static shear resistance of the footing may be defined as the footing load that will bring the soil beneath the footing into plastic equilibrium, that is, the condition in which the shear stress along all of the failure surfaces is at the ultimate (plastic) value. To determine the ultimate static shear resistance, a condition of ultimate shear stress is assumed along all failure surfaces and the footing load required to maintain equilibrium is evaluated. This footing load is the ultimate static shear resistance (p).

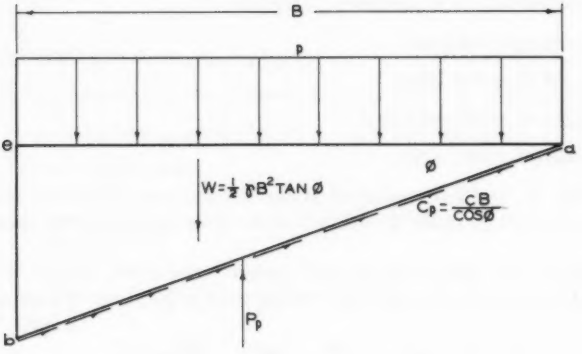

FIG. 5.—FORCES ACTING ON MASS abe

Consider soil mass abe (Fig. 5), and equate the sum of the vertical components of all static forces acting on the mass to zero. These forces include the ultimate shear resistance, the weight of soil mass abe, the cohesion along line ab (C_p), and the passive pressure force acting on face ab (P_p). The passive pressure force is considered to intersect line ab at an angle of $90° - \phi$, and therefore includes the frictional shear resistance along ab due to the normal force at that face

$$\Sigma \text{ Vertical forces} = 0 \qquad \uparrow +$$

$$P_p + c\,B \tan\phi - \frac{1}{2}\gamma\,B^2 \tan\phi - p\,B = 0 \quad \ldots\ldots\ldots (1a)$$

and

$$p = \frac{P_p}{B} + c \tan\phi - \frac{1}{2}\gamma\,B \tan\phi \quad \ldots\ldots\ldots\ldots\ldots (1b)$$

9 "Theoretical Study of the Displacement of Long Footings by Dynamic Loads," U.S. Army Engr. Waterways Experiment Sta., Miscellaneous Paper No. 3-418, March, 1961.

Eq. 1 is expressed in terms of known basic parameters except for the passive earth-pressure force (P_p). To evaluate P_p, the force is separated into two components (P'_p and P''_p), specifically defined so that their points of application along line ab are known. Force P'_p is the passive pressure force considering the soil to be weightless and to have cohesion and a surcharge pressure at the surface. Force P''_p is the passive pressure force considering the soil weight and neglecting the cohesion and surcharge (q). The forces are evaluated separately by equating to zero the moments from all forces acting on mass abdf (Fig. 6). The sum of $P'_p + P''_p$ then equals P_p.

Considering mass abdf to be in plastic equilibrium, the following forces contribute to the moment about point 0 (M^O) :

P'_d = passive force along df neglecting weight of soil;

P''_d = passive force along df when c and q are zero;

C_s = cohesive shear resistance along bd;

C_p = cohesive shear resistance along ab;

q = surcharge along ac;

W_1 = weight of mass b0d;

W_2 = weight of mass adf; and

W_3 = weight of mass ab0.

Note in Fig. 6 that the resultant of the normal and frictional shear forces (N) along bd is through point 0 and therefore does not enter the moment computations.

Determine P'_p: By assuming the soil weight to be zero, forces W_1, W_2, W_3, P''_d, and P''_p become zero. P'_p will act through the mid-point of line ab.

$$\Sigma M^O = 0 = M^O_{P'_p} + M^O_{P'_d} + M^O_{C_s} + M^O_q + M^O_{C_p} \quad \ldots\ldots\ldots \quad (2a)$$

and

$$-P'_p\left(\frac{1}{2}B + k\,B\sin\psi\right) + \frac{1}{2}\left(R_2^2 - k^2B^2\right)\left(c\cos\phi + q\sin^2\psi\right)$$

$$+\frac{c}{2\tan\phi}\left(R_2^2 - R_0^2\right) + \frac{1}{2}q\left(R_2^2 - k^2B^2\right)\sin^2\psi - \frac{c\,k\,B^2}{2\cos\psi} = 0 \quad . . \quad (2b)$$

in which k is the ratio of a0/B, dimensionless; R_0 is the initial radius of spiral, in feet; R_2 is the radius of spiral at point d, in feet; $\psi = 45 + \phi/2$.

$$P'_p = \frac{1}{\frac{1}{2}B + k\,B\sin\psi}\left[\left(R_2^2 - k^2B^2\right)\left(\frac{1}{2}c\cos\phi + q\sin^2\psi\right)\right.$$

$$\left.+\frac{c}{2\tan\phi}\left(R_2^2 - R_0^2\right) + \frac{c\,k\,B^2}{2\cos\psi}\right] \quad \ldots\ldots\ldots\ldots \quad (2c)$$

Determine P''_p: By assuming the cohesion and surcharge to be zero, forces P'_d, C_s, C_p, and P'_p become zero. P''_p will act through the two-thirds point of

line ab

$$\Sigma M^{O} = 0 = M^{O}_{P''_p} + M^{O}_{P''_d} + M^{O}_{W_1} + M^{O}_{W_2} + M^{O}_{W_3} \quad \ldots\ldots\ldots \quad (3a)$$

and

$$\begin{aligned} &- P''_p\left(\frac{2}{3}\,B + k\,B\sin\psi\right) + \frac{1}{6}\,\gamma\,\left(R_2 + k\,B\right)^2\left(R_2 - \frac{1}{2}\,k\,B\right)\cos\phi\sin\psi \\ &+ \frac{\gamma}{27\tan^2\phi + 3}\left\{R_2^{\,3}\left[3\tan\phi\sin\left(\theta_2 - \theta_1\right) - \cos\left(\theta_2 - \theta_1\right)\right]\right. \\ &\left. + R_0^{\,3}\left(\cos\theta_1 + 3\tan\phi\sin\theta_1\right)\right\} \\ &+ \frac{1}{6}\,\gamma\left(R_2 + k\,B\right)^2\left(R_2 - \frac{1}{2}\,k\,B\right)\cos\phi\sin\psi \\ &- \frac{1}{6}\,\gamma\,R_0\cos\left(\phi - \alpha\right)\left[\tan\phi - \tan\left(\phi - \alpha\right)\right]\left[R_0^{\,2}\cos^2(\phi - \alpha)\right. \\ &\left. - k^2\,B^2\sin^2\psi\right] = 0 \quad \ldots\ldots\ldots\ldots\ldots\ldots\ldots\ldots\ldots\ldots \quad (3b) \end{aligned}$$

in which θ_1 is the internal angle between R_o and vertical line through 0;

θ_2 is the internal angle between R_o and line 0d; and

α denotes angle ab0.

$$\begin{aligned} P''_p = &\frac{1}{\frac{2}{3}\,B + k\,B\sin\psi}\left[\frac{1}{3}\,\gamma\left(R_2 + k\,B\right)^2\left(R_2 - \frac{1}{2}\,k\,B\right)\cos\phi\sin\psi\right. \\ &+ \frac{\gamma}{27\tan^2\phi + 3}\left\{R_2^{\,3}\left[3\tan\phi\sin\left(\theta_2 - \theta_1\right) - \cos\left(\theta_2 - \theta_1\right)\right]\right. \\ &\left. + R_0^{\,3}\left(\cos\theta_1 + 3\tan\phi\sin\theta_1\right)\right\} \\ &- \frac{1}{6}\,\gamma\,R_0\cos\left(\phi - \alpha\right)\left[\tan\phi - \tan\left(\phi - \alpha\right)\right]\left[R_0^{\,2}\cos^2\left(\phi - \alpha\right)\right. \\ &\left.\left. - k^2\,B^2\sin\psi\right]\right] \quad \ldots\ldots\ldots\ldots\ldots\ldots\ldots\ldots\ldots\ldots \quad (3c) \end{aligned}$$

Examination of the equation for P'_p and P''_p shows them to be dependent on the value of k, which is the ratio of length a0 to B (Fig. 6), and therefore locates the center of the spiral which is the center of rotation. Obviously, the correct value of the center of rotation is that which yields the minimum passive earth-pressure force $\left(P_p = P'_p + P''_p\right)$ and therefore the minimum value of ultimate static shear resistance. Since there is no convenient way to obtain and substitute this correct value and eliminate k from the equations, it must be determined by trial and error for each set of problem parameters.

The equation for the static shear resistance is obtained by direct substitution of the sum $P'_p + P''_p$ into Eq. 1. This equation is then modified into a more convenient form (Eq. 4) by separation of terms into those dependent on γ, c, and q. The terms N_γ N_c, and N_q designate coefficients of static shear

resistance

$$P = N_\gamma \gamma B + N_c c + N_q q \quad \ldots\ldots\ldots\ldots\ldots \quad (4)$$

in which $\phi \neq 0$

$$N_\gamma = \frac{1}{\frac{2}{3} B^3 + k B^3 \sin \psi} \left\{ \frac{1}{3} (R_2 + k B)^2 \left(R_2 - \frac{1}{2} k B\right) \cos \phi \sin \psi \right.$$

$$+ \frac{1}{27 \tan^2 \phi + 3} \left[R_2^3 (3 \tan \phi \sin \psi - \cos \psi) \right.$$

$$\left. + R_0^3 (\cos \theta_1 + 3 \tan \phi \sin \theta_1) \right]$$

$$- \frac{1}{6} R_0 \cos (\phi - o) [\tan \phi - \tan (\phi - o)] \left[R_0^2 \cos^2 (\phi - o) \right.$$

$$\left. \left. - k^2 B^2 \sin^2 \psi \right] \right\} - \frac{1}{2} \tan \phi \quad \ldots\ldots\ldots\ldots\ldots\ldots \quad (5a)$$

$$N_c = \frac{1}{\frac{1}{2} B^2 + k B^2 \sin \psi} \left[\left(R_2^2 - k^2 B^2\right) \left(\frac{1}{2} \cos \phi\right) \right.$$

$$\left. + \frac{1}{2 \tan \phi} \left(R_2^2 - R_0^2\right) - \frac{k B^2}{2 \cos \psi} \right] + \tan \phi \ldots\ldots \quad (5b)$$

and

$$N_q = \frac{1}{\frac{1}{2} B^2 + k B^2 \sin \psi} \left(R_2^2 - k^2 B^2\right) \sin^2 \psi \quad \ldots\ldots\ldots\ldots\ldots \quad (5c)$$

in which $\phi = 0$

$$N_c = \frac{1}{\frac{1}{2} B^2 + k B^2 \sin \psi} \left[\frac{1}{2} \left(R_0^2 - k^2 B^2\right) + \left(\frac{3\pi}{4} + o\right) R_0^2 - \frac{k B^2}{2 \cos \psi} \right] \ldots (5d)$$

Inertial Forces.—Any acceleration of soil mass aebdc due to the downward movement of the footing will cause inertial forces which will resist such movement. The inertial forces are directly proportional to the acceleration of each individual soil mass and thereby dependent on the displacements. As the best first-order approximation of the motion, masses abe, acd, and ab0 are assumed to translate, and mass b0d to rotate about point 0 (Fig. 7). The prime (') designates point locations after displacement. Note that it is kinematically impossible for there to be an abrupt transition from translation to rotation along lines 0b and 0d, making the assumptions not exact but approximate.

After establishing the type of movement of each soil mass, it is necessary to express the relative displacements. This is accomplished by assuming the soil to be incompressible, from which it follows that equal volumes of each soil mass will be displaced by a unit displacement of the footing. For example, volume aca'c' must equal volume aea'e', giving a relation of the relative displacement of masses abe and acd. From similar volume considerations it is seen that the two edges R_0 and R_2 (Fig. 6) of mass b0d can not rotate the same

amount per unit footing displacement. The rotation of mass b0d is therefore considered to be the average of the angular rotations computed for each edge of the mass.

The effective total inertial force is obtained by combining the inertial forces acting on each separate mass using energy considerations. To be equivalent, the total inertial force must do the same total work when displaced downward as the sum of the work done by the individual inertial forces as they are

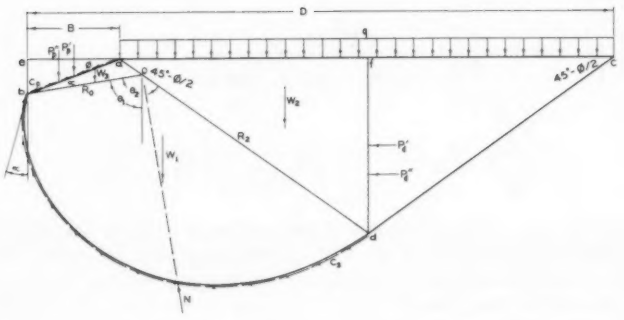

FIG. 6.—FORCES ACTING ON MASS abdf

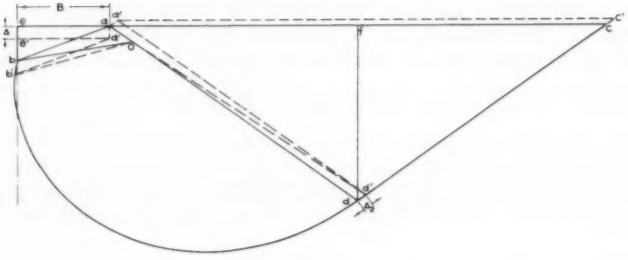

FIG. 7.—DISPLACEMENTS

displaced by the same footing movement. This procedure yields Eq. 6. The term N_I designates coefficient of dynamic inertial shear resistance

$$I\,F = N_I\,\gamma\,B^2\,\frac{d^2\Delta}{dt^2} \quad \ldots\ldots\ldots\ldots\ldots \quad (6)$$

in which $\phi \neq 0$,

$$N_I = \frac{1}{g}\left[\tan\phi - \frac{1}{2}\tan(\phi - \alpha) + \frac{1}{2\cos\phi}\left\{1 + \frac{k\,B^2\,[\tan\phi - \tan(\phi - \alpha)]}{2(R_2 + k\,B)^2\cos\psi}\right\}\right.$$
$$\left. + \frac{R_2^4 - R_0^4}{18\,B^2\tan\phi}\left[\frac{\cos(\phi - \alpha)}{R_0} + \frac{B}{R_2(R_2 + k\,B)}\right]^2\right] \quad \ldots\ldots (7)$$

in which $\phi = 0$,

$$N_I = \frac{1}{g}\left\{\frac{1}{2}\tan\alpha + \frac{1}{2}\left[1 + \frac{k\,B^2\tan\alpha}{2(R_2 + k\,B)^2\cos\psi}\right]\right.$$
$$\left. + \frac{R_0^4}{8\,B^2}(\theta_2 + \sin\theta_2)\left[\frac{B}{R_0(R_0 + k\,B)} + \frac{\cos\alpha}{R_0}\right]^2\right\} \quad \ldots\ldots (8)$$

Restoring Force.—Displacement of the soil mass within the failure surface due to downward movement of the footing will increase the restoring moment about point 0, and the increase in moment will be proportional to the magnitude of the displacement provided the angle changes do not become excessive. Only masses b0d and adf are assumed to contribute to the increase in restoring moment. Mass cdf is excluded from computations because of its consideration as a passive wedge and the shortening of length cd with displacement make its effect more problematical. The increase in restoring moment from the two masses is converted to an effective restoring force acting on the footing to retard motion. The expression is given as Eq. 9. The term N_R designates coefficient of dynamic shear resistance due to gravity restoring forces.

$$R\,F = N_R\,B\,\gamma\,\Delta \quad \ldots\ldots\ldots\ldots\ldots (9)$$

in which

$$N_R = \frac{1}{\frac{2}{3}B^2 + k\,B^2\sin\psi}\left[\left(\frac{1}{27\tan^2\phi + 3}\right)\left(\frac{\cos(\phi - \alpha)}{R_0} + \frac{B}{R_2(R_2 + k\,B)}\right)\right.$$
$$\left\{R_2^3\,(3\tan\phi\cos\psi + \sin\psi) + R_0^3\,(\sin\theta_1 - 3\tan\phi\cos\theta_1)\right\}$$
$$\left. + \frac{1}{4}B(R_2 + k\,B)\sin\psi\right] \quad \ldots\ldots\ldots\ldots\ldots (10)$$

Loading Function.—The fourth force acting on the footing is the loading function. For this treatise, the applied load is assumed to be an initial-peak triangular force pulse which decays to zero at time t_d (Fig. 4). The peak load Q is expressed in pressure units. Since the function is discontinuous at time t_d, two equations are necessary.

For $0 \leq t \leq t_d$: Loading function $= Q\,B\left(1 - \frac{t}{t_d}\right)$ ..... (11a)

For $t \geq t_d$: Loading function $= 0$ ..... (11b)

Differential Equations.—The differential equations are set up by equating the four vertical forces to zero. There must be separate equations for before and

after time t_d, since the loading function is defined in that manner.

For $0 \leq t \leq t_d$

$$N_I \gamma B^2 \frac{d^2\Delta}{dt^2} + N_R \gamma B \Delta + p B - Q B \left(1 - \frac{t}{t_d}\right) = 0 \quad \ldots \quad (12a)$$

and

$$\frac{d^2\Delta}{dt^2} + \frac{N_R}{N_I B} \Delta = \frac{Q - p}{N_I \gamma B} - \frac{Q}{N_I \gamma B t_d} t \quad \ldots\ldots \quad (12b)$$

For $t \geq t_d$

$$N_I \gamma B^2 \frac{d^2\Delta}{dt^2} + N_R \gamma B \Delta + p B = 0 \quad \ldots\ldots\ldots \quad (12c)$$

and

$$\frac{d^2 \Delta}{dt^2} + \frac{N_R}{N_I B} \Delta = - \frac{p}{N_I \gamma B} \quad \ldots\ldots\ldots\ldots \quad (12d)$$

Displacement Equations.—The solution of the differential equations will yield equations of footing displacement versus time. The forms of the particular solutions of Eq. 12(b) and Eq. 12(d) are found to be

$$\Delta = C_1 \cos (K t) + C_2 \sin (K t) + \left(\frac{Q - p}{N_R \gamma}\right) - \left(\frac{Q}{N_R \gamma t_d}\right) t \quad \ldots \quad (13a)$$

and

$$\Delta = C_3 \cos (K t) + C_4 \sin (K t) - \frac{p}{N_R \gamma} \quad \ldots\ldots\ldots \quad (13b)$$

respectively, in which $K = \sqrt{\frac{N_R}{N_I B}}$; and C_1, C_2, C_3, and C_4 are coefficients of integration. The coefficients C_1 and C_2 are evaluated by the initial conditions. The coefficients C_3 and C_4 are evaluated by the conditions of displacement and velocity at t_d as defined by Eq. 13(a). Solution and substitution of the coefficients yield nondimensional Eqs. 14.

For $0 \leq t \leq t_d$

$$\left(\frac{N_R \gamma}{p}\right) \Delta = \left(\frac{Q}{p} - 1\right) \left[1 - \cos (K t)\right] + \frac{\frac{Q}{p}}{t_d K} \left[\sin (K t) - K t\right] \ldots (14a)$$

For $t_d \leq t$

$$\left(\frac{N_R \gamma}{p}\right) \Delta = \left[1 - \frac{Q}{p} + \frac{\frac{Q}{p}}{t_d K} \sin \left(K t_d\right)\right] \cos (K t) + \left\{\frac{\frac{Q}{p}}{t_d K} \left[1 - \cos \left(K t_d\right)\right]\right\} \sin (K t) - 1 \quad \ldots\ldots \quad (14b)$$

NUMERICAL SOLUTION OF EQUATIONS

Coefficients.—The coefficients N_γ, N_c, N_q, N_I, and N_R (Eqs. 4, 6 and 9) are dependent only on values of ϕ and k. Using magnitudes of ϕ from 0° to

TABLE 1.—BEARING CAPACITY COEFFICIENTS AS FUNCTIONS OF k AND ϕ

k	N_γ	N_c	N_q	N_I	N_R	$\sqrt{N_R/N_I}$
			$\phi = 0.00$			
-0.05	0.0000	5.7277	1.0000	0.0633	2.0125	5.6366
0.00	0.0000	5.7124	1.0000	0.0631	1.9723	5.5887
0.05	0.0000	5.7258	1.0000	0.0633	1.9433	5.5394
			$\phi = 5.00$			
-0.65	0.1454	79.6255	7.9664	0.3755	8.9076	4.8709
-0.60	0.1445*	29.8163	3.6086	0.2280	6.4362	5.3126
-0.55	0.1481	18.9958	2.6619	0.1579	5.0332	5.6460
-0.50	0.1553	14.3469	2.2552	0.1213	4.1699	5.8636
-0.45	0.1655	11.8179	2.0339	0.1011	3.6088	5.9750
-0.40	0.1786	10.2699	1.8985	0.0897	3.2299	6.0020
-0.35	0.1945	9.2580	1.8100	0.0833	2.9674	5.9698
-0.30	0.2131	8.5723	1.7500	0.0799	2.7828	5.9005
-0.25	0.2344	8.1007	1.7087	0.0786	2.6523	5.8108
-0.20	0.2585	7.7778	1.6805	0.0785	2.5604	5.7116
-0.15	0.2855	7.5629	1.6617	0.0793	2.4969	5.6099
-0.10	0.3154	7.4291	1.6500	0.0809	2.4547	5.5096
-0.05	0.3483	7.3580	1.6437	0.0829	2.4288	5.4128
0.00	0.3843	7.3366	1.6419	0.0853	2.4155	5.3205
0.05	0.4233	7.3553	1.6435	0.0881	2.4122	5.2330
			$\phi = 10.00$			
-0.60	0.5700	53.9491	10.5127	0.1120	5.7922	7.1922
-0.55	0.5588*	28.9945	6.1125	0.0935	4.8411	7.1943
-0.50	0.5645	20.5266	4.6194	0.0833	4.2238	7.1228
-0.45	0.5832	16.3539	3.8837	0.0779	3.8095	6.9932
-0.40	0.6127	13.9337	3.4569	0.0757	3.5264	6.8273
-0.35	0.6521	12.4031	3.1870	0.0755	3.3323	6.6445
-0.30	0.7008	11.3881	3.0080	0.0767	3.2008	6.4587
-0.25	0.7586	10.7004	2.8868	0.0790	3.1147	6.2781
-0.20	0.8253	10.2345	2.8046	0.0821	3.0625	6.1071
-0.15	0.9012	9.9267	2.7503	0.0858	3.0360	5.9474
-0.10	0.9863	9.7361	2.7167	0.0901	3.0294	5.7994
-0.05	1.0807	9.6352	2.6990	0.0948	3.0386	5.6626
0.00	1.1848	9.6049	2.6936	0.0999	3.0604	5.5360
0.05	1.2986	9.6313	2.6983	0.1053	3.0923	5.4187
			$\phi = 25.00$			
-0.50	8.5665	73.8778	35.4499	0.0732	7.2347	9.9384
-0.45	8.3599*	51.2706	24.9079	0.0835	6.8363	9.0503
-0.40	8.3728	40.7056	19.9814	0.0954	6.6214	8.3291
-0.35	8.5541	34.7663	17.2119	0.1094	6.5339	7.7297
-0.30	8.8760	31.1015	15.5029	0.1254	6.5404	7.2223
-0.25	9.3230	28.7315	14.3977	0.1437	6.6199	6.7864
-0.20	9.8871	27.1750	13.6720	0.1646	6.7584	6.4075
-0.15	10.5646	26.1681	13.2024	0.1882	6.9462	6.0748
-0.10	11.3542	25.5533	12.9157	0.2148	7.1761	5.7803
-0.05	12.2569	25.2309	12.7654	0.2445	7.4429	5.5178
0.00	13.2745	25.1345	12.7205	0.2775	7.7423	5.2825
0.05	14.4095	25.2180	12.7594	0.3139	8.0710	5.0704
			$\phi = 30.00$			
-0.45	19.3095	80.8644	47.6872	0.1064	9.3123	9.3540
-0.40	19.1315*	62.4470	37.0539	0.1267	9.0899	8.4705
-0.35	19.3718	52.5548	31.3426	0.1506	9.0494	7.7518
-0.30	19.9490	46.6067	27.9084	0.1787	9.1446	7.1533
-0.25	20.8187	42.8208	25.7226	0.2116	9.3473	6.6458
-0.20	21.9566	40.3597	24.3017	0.2500	9.6392	6.2095
-0.15	23.3512	38.7778	23.3884	0.2944	10.0081	5.8303
-0.10	24.9984	37.8159	22.8330	0.3456	10.4452	5.4979
-0.05	26.8993	37.3127	22.5425	0.4041	10.9441	5.2044
0.00	29.0580	37.1624	22.4558	0.4706	11.4998	4.9436
0.05	31.4810	37.2926	22.5309	0.5457	12.1084	4.7107

ϕ = 15.00

-0.55	1.5462	46.5473	13.4724	0.0707	5.2677	8.6324
-0.50	1.5198*	30.2759	9.1124	9.0696	4.7177	8.2310
-0.45	1.5342	23.2038	7.2175	0.0707	4.3564	7.8481
-0.40	1.5806	19.3483	6.1844	0.0734	4.1189	7.4903
-0.35	1.6540	16.9964	5.5542	0.0773	3.9669	7.1622
-0.30	1.7520	15.4722	5.1458	0.0823	3.8766	6.8645
-0.25	1.8730	14.4550	4.8732	0.0881	3.8322	6.5961
-0.20	2.0166	13.7730	4.6905	0.0947	3.8232	6.3542
-0.15	2.1825	13.3257	4.5706	0.1020	3.8418	6.1361
-0.10	2.3710	13.0501	4.4968	0.1101	3.8825	5.9388
-0.05	2.5823	12.9048	4.4579	0.1188	3.9413	5.7596
0.00	2.8168	12.8613	4.4462	0.1282	4.0149	5.5961
0.05	3.0750	12.8991	4.4563	0.1383	4.1008	5.4463

ϕ = 20.00

-0.50	3.6745	46.2884	17.8477	0.0673	5.6658	9.1768
-0.45	3.6419*	33.8986	13.3381	0.0728	5.3067	8.5380
-0.40	3.6943	27.6099	11.0492	0.0796	5.0886	7.9941
-0.35	3.8151	23.9213	9.7067	0.0877	4.9684	7.5267
-0.30	3.9952	21.5875	8.8572	0.0970	4.9199	7.1214
-0.25	4.2298	20.0542	8.2992	0.1076	4.9258	6.7672
-0.20	4.5161	19.0369	7.9289	0.1194	4.9746	6.4552
-0.15	4.8533	18.3742	7.6877	0.1325	5.0582	6.1783
-0.10	5.2413	17.9678	7.5398	0.1470	5.1704	5.9309
-0.05	5.6804	17.7542	7.4620	0.1629	5.3068	5.7084
0.00	6.1717	17.6903	7.4388	0.1802	5.4638	5.5072
0.05	6.7161	17.7457	7.4589	0.1989	5.6386	5.3243

ϕ = 35.00

-0.45	46.2942	134.3023	95.0397	0.1527	13.4981	9.4021
-0.40	45.4427*	100.6609	71.4837	0.1887	13.2639	8.3844
-0.35	45.6687	83.4477	59.4308	0.2323	13.3114	7.5703
-0.30	46.7356	73.3676	52.3727	0.2849	13.5708	6.9017
-0.25	48.5145	67.0529	47.9511	0.3481	14.0015	6.3419
-0.20	50.9356	62.9887	45.1052	0.4237	14.5786	5.8661
-0.15	53.9640	60.3926	43.2874	0.5133	15.2859	5.4569
-0.10	57.5868	58.8199	42.1862	0.6191	16.1127	5.1018
-0.05	61.8051	57.9989	41.6113	0.7428	17.0515	4.7911
0.00	66.6296	57.7539	41.4398	0.8868	18.0970	4.5175
0.05	72.0773	57.9662	41.5884	1.0529	19.2451	4.2753

ϕ = 40.00

-0.40	115.7097	172.8231	146.0161	0.3229	20.8738	8.0404
-0.35	115.5504*	141.1002	119.3973	0.4107	21.1136	7.1701
-0.30	117.6386	123.0124	104.2199	0.5195	21.7125	6.4650
-0.25	121.5875	111.8576	94.8599	0.6535	22.6077	5.8817
-0.20	127.1879	104.7472	88.8935	0.8175	23.7629	5.3914
-0.15	134.3346	100.2323	85.1051	1.0168	25.1570	4.9741
-0.10	142.9868	97.5069	82.8181	1.2572	26.7775	4.6152
-0.05	153.1451	96.0866	81.6263	1.5450	28.6173	4.3038
0.00	164.8391	95.6630	81.2709	1.8870	30.6724	4.0317
0.05	178.1176	96.0303	81.5791	2.2904	32.9409	3.7924

ϕ = 45.00

-0.40	327.6781	322.2748	323.2752	0.6576	36.2961	7.4295
-0.35	325.4943*	259.1345	260.1349	0.8611	37.0113	6.5559
-0.30	329.9754	224.0769	225.0772	1.1194	38.3965	5.8568
-0.25	339.8627	202.7837	203.7840	1.4447	40.3468	5.2846
-0.20	354.4804	189.3358	190.3361	1.8515	42.8070	4.8083
-0.15	373.4871	180.8450	181.8452	2.3565	45.7496	4.4062
-0.10	396.7473	175.7358	176.7361	2.9784	49.1634	4.0628
-0.05	424.2605	173.0775	174.0778	3.7386	53.0475	3.7669
0.00	456.1177	172.2851	173.2853	4.6607	57.4067	3.5096
0.05	492.4763	172.9729	173.9732	5.7709	62.2499	3.2843

* Computed minimum N_y.

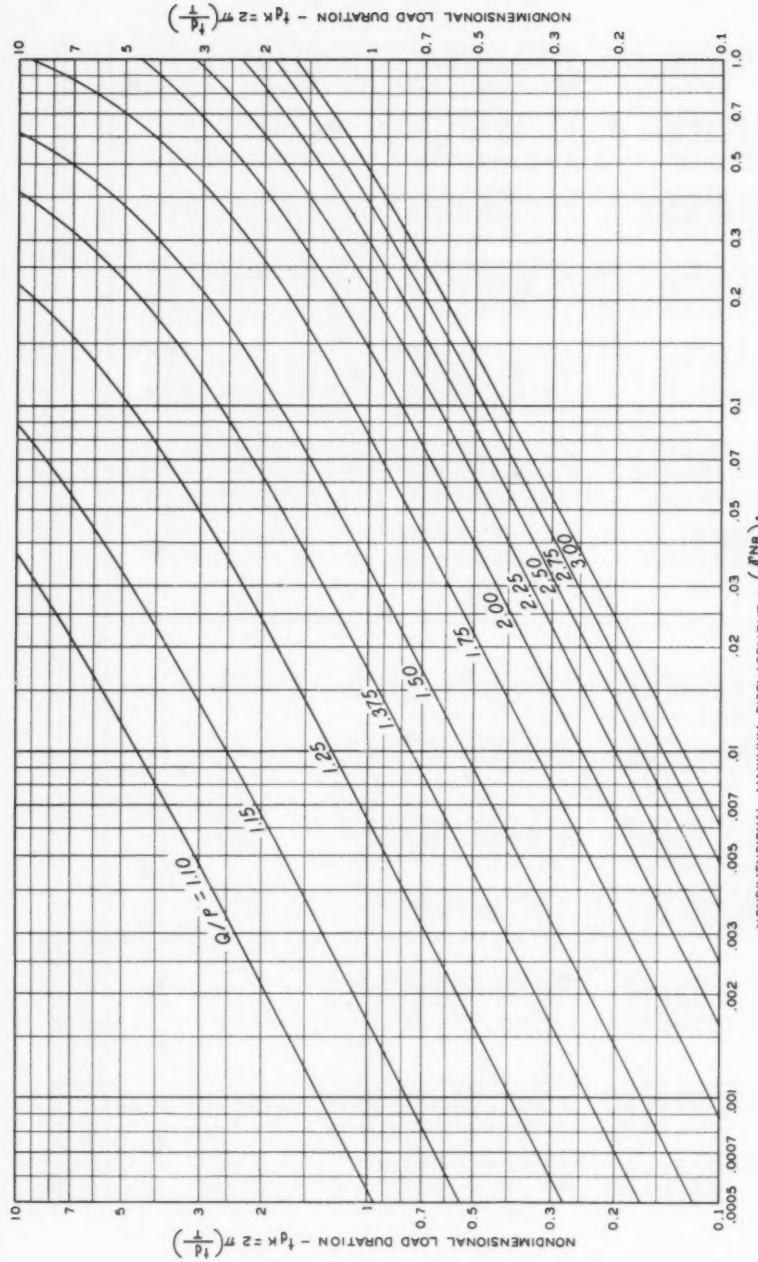

FIG. 8.—NONDIMENSIONAL MAXIMUM DISPLACEMENT

45° and of k for the region where the ultimate static shear resistance could be a minimum, these coefficients were evaluated on an IBM 650 digital computer. The values obtained are given in Table 1 for every fifth degree. A complete solution for each degree can be found elsewhere.[9]

Maximum Displacement.—As previously stated, the maximum displacement from Eq. 14(a) and Eq. 14(b) is the predicted permanent footing displacement, since downward motion ceases at the time of maximum displacement and rebound is not considered. The electronic computer was used to determine the nondimensional maximum displacement for ranges of Q/p of 1.10 to 3.00 and of t_d K from 0.10 to 10.00. These data along with the times of maximum displacement is also plotted in Fig. 8.

PROCEDURE FOR PROBLEM SOLUTION

Footing Displacement under a Specific Load.—Footing displacement under a dynamic load may be computed in the following manner. Given the following data:

B = half width of footing, in feet;
γ = unit soil weight, in pounds per cubic foot;
c = cohesive shear strength, in pounds per square foot;
ϕ = angle of internal shear resistance, in degrees;
q = surcharge, in pounds per square foot;
Q = peak dynamic load, in pounds per square foot; and
t_d = duration of load pulse, in seconds.

Determine (1) the ultimate static shear resistance (p); (2) the values of N_R and N_R/N_I; and (3) the value of Δ_{max}.

(1) To determine the ultimate static shear resistance (p), assume a value of k (which determines the failure surface) and determine coefficients N_γ, N_c, and N_q from Table 1. Compute p for this k by substitution into Eq. 4. Repeat this procedure with different values of k until the minimum value of p is found. This value will be the ultimate static shear resistance, and the associated k will define the correct center of rotation.

Note: The correct value of k is within a limited range for any particular value of ϕ. Only these ranges are shown in Table 1.

(2) To determine the values of N_R and $\sqrt{N_R/N_I}$, use ϕ and the critical value of k found in step (1) and determine N_R and $\sqrt{N_R/N_I}$ from Table 1.

(3) To determine the value of Δ_{max}, compute $K\left(K=\sqrt{N_R/N_I}B\right)$, Q/p, t_d K, and $N_R\gamma/p$. Determine $(N_R\gamma/p)\Delta_{max}$ from Fig. 8, using Q/p and t_d K to enter the plot. Divide $(N_R\gamma/p)\Delta_{max}$ by the constant $(N_R\gamma/p)$ to determine the value of footing displacement, Δ_{max}.

Effect of Load Parameters on Footing Displacement.—The effect of peak dynamic load or load duration on displacement can be determined by repeating the procedure given previously for several values of Q/p or t_d K. Plots of displacement versus Q or t_d may then be developed to show the relation of footing displacement to either load parameter.

TABLE 2.—SOLUTION OF EQ. 6(a) FOR NONDIMENSIONAL MAXIMUM DISPLACEMENTS

Q/p (1)	t_d K (2)	t_{max} K (3)	$\left(\frac{N_R \gamma}{p}\right) \Delta_{max}$ (4)
1.10	0.100	0.019	0.00000550
	0.300	0.056	0.00004955
	1.000	0.182	0.0005482
	3.000	0.534	0.004748
	10.000	1.490	0.03768
1.15	0.100	0.027	0.00001699
	0.300	0.079	0.0001530
	1.000	0.260	0.001684
	3.000	0.747	0.01404
	10.000	1.840	0.08915
1.25	0.100	0.041	0.00006664
	0.300	0.121	0.0005987
	1.000	0.396	0.006511
	3.000	1.082	0.04965
	10.000	2.220	0.2232
1.375	0.100	0.056	0.0001858
	0.300	0.167	0.001665
	1.000	0.534	0.01781
	3.000	1.376	0.1214
	10.000	2.510	0.4140
1.50	0.100	0.068	0.0003701
	0.300	0.200	0.003313
	1.000	0.645	0.03475
	3.000	1.572	0.2146
	10.000	2.570	0.6162
1.75	0.100	0.087	0.0009173
	0.300	0.257	0.008184
	1.000	0.811	0.08288
	3.000	1.820	0.4386
	10.000	2.690	1.030
2.00	0.100	0.101	0.001664
	0.300	0.299	0.01480
	1.000	0.928	0.1454
	3.000	1.967	0.6896
	10.000	2.760	1.451
2.25	0.100	0.113	0.002573
	0.300	0.335	0.02281
	1.000	1.015	0.2181
	3.000	2.062	0.9544
	10.000	2.800	1.873
2.50	0.100	0.126	0.003637
	0.300	0.370	0.0321
	1.000	1.088	0.2981
	3.000	2.128	1.227
	10.000	2.820	2.297
2.75	0.100	0.138	0.004855
	0.300	0.405	0.04268
	1.000	1.152	0.3843
	3.000	2.178	1.505
	10.000	2.840	2.722
3.00	0.100	0.151	0.006227
	0.300	0.438	0.05446
	1.000	1.208	0.4754
	3.000	2.215	1.786
	10.000	2.850	3.147

Solution of Sample Problems.—

Problem 1.—Determine the maximum footing displacement for the following footing, soil, and loading conditions. Given:

$B = 10$ ft $\qquad q = 100$ lb per sq ft

$\gamma = 100$ lb per cu ft $\qquad Q = 60{,}000$ lb per sq ft

$c = 1000$ lb per sq ft $\qquad t_d = 0.50$ sec

$\phi = 25°$

Determine p, N_R, $\sqrt{N_R/N_I}$, and Δ_{max}.

Solution.—

1. $p = N_\gamma B\gamma + N_c c + N_q q = 1000\, N_\gamma + 1000\, N_c + 100\, N_q$

   Using Table 1,

   for $k = 0$, $\quad p = 13{,}274 + 25{,}134 + 1{,}272 = 39{,}680$

   $k = -0.10$, $\quad p = 11{,}354 + 25{,}553 + 1{,}292 = 38{,}199$

   $k = -0.20$, $\quad p = 9{,}887 + 27{,}175 + 1{,}367 = 38{,}429$

   $k = -0.15$, $\quad p = 10{,}564 + 26{,}168 + 1{,}320 = 38{,}052$

   Therefore $p = 38{,}052$ lb per sq ft at $k = -0.15$

2. Using Table 1,

   $N_R = 6.9462$ and $\sqrt{N_R/N_I} = 6.0748$

3. To determine Δ_{max}:

   $K = \dfrac{6.0748}{\sqrt{10}} = 1.921 \qquad t_d K = 0.50 \times 1.921 = 0.96$

   $\dfrac{N_R \gamma}{p} = \dfrac{6.9462 \times 100}{38{,}052} = 0.01825 \qquad \dfrac{Q}{p} = \dfrac{60{,}000}{38{,}052} = 1.57$

   Using Fig. 8,

   $\left(\dfrac{N_R \gamma}{p}\right)_{\Delta max} = 0.040 \qquad \Delta max = \dfrac{0.040}{0.01825} = 2.2$ ft

Problem 2.—Determine the effect of various magnitudes of peak dynamic load on the maximum footing displacement for the given footing, soil, and duration of load. Given:

$B = 4$ ft $\qquad c = 1000$ lb per sq ft $\qquad q = 0$

$\gamma = 100$ lb per cu ft $\qquad \phi = 0 \qquad t_d = 0.32$ sec

Determine p, N_R, $\sqrt{N_R/N_I}$, and Δ_{max}.

Solution.—

1. $p = N_\gamma B\gamma + N_c c + N_q q = 400\, N_\gamma + 1000\, N_c$

   For $k = 0$, $p = 0 + 5712 = 5712$

Therefore $p = 5712$ lb per sq ft at $k = 0$

Note: For $\phi = 0$, there is only one possible location of the critical surface.

2. Using Table 1,

$$N_R = 1.972 \text{ and } \sqrt{N_R/N_I} = 5.588$$

3. To determine Δ_{max} as a function of Q:

$$K = \frac{5.588}{\sqrt{4}} = 2.794 \qquad t_d K = 0.32 \times 2.794 = 0.894$$

$$\frac{N_R \gamma}{p} = \frac{1.972 \times 100}{5712} = 0.0345$$

TABLE 3.—TABULATION USING FIG. 8

Q/p (1)	$\left(\frac{N_R \gamma}{p}\right) \Delta_{max}$ (2)	Δ_{max}, in feet (3)	Q, in pounds (4)
1.25	0.0052	0.15	7,140
1.50	0.028	0.81	8,568
1.75	0.068	2.0	9,996
2.00	0.12	3.5	11,424
2.25	0.18	5.2	12,852

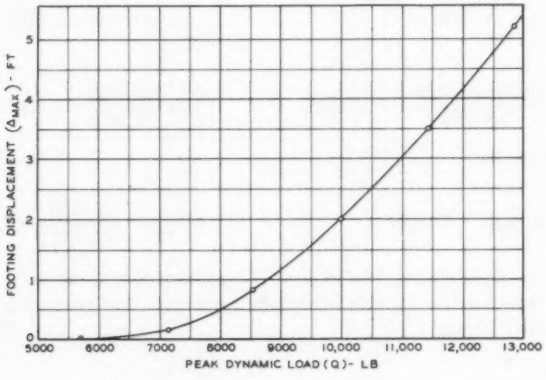

FIG. 9.—FOOTING DISPLACEMENT—SAMPLE PROBLEM 2

Using Fig. 8, construct a tabulation as given in Table 3. Results of sample problem 2 are plotted in Fig. 9.

COMMENTS

The primary objective of developing a mathematical expression for the displacement of long footings based on a punching failure and applicable to

any soil type has been obtained. However, the theory as defined by the derived equations cannot be regarded as more than a preliminary attempt to theorize a complex physical phenomenon. The assumptions have been restrictive to the extent that precise correlation between the predicted and measured values of footing displacement should not be expected. At this time even the magnitude of the deviations cannot be assessed because of the lack of experimental data. Laboratory tests are needed to furnish such information and to supplement further theoretical development.

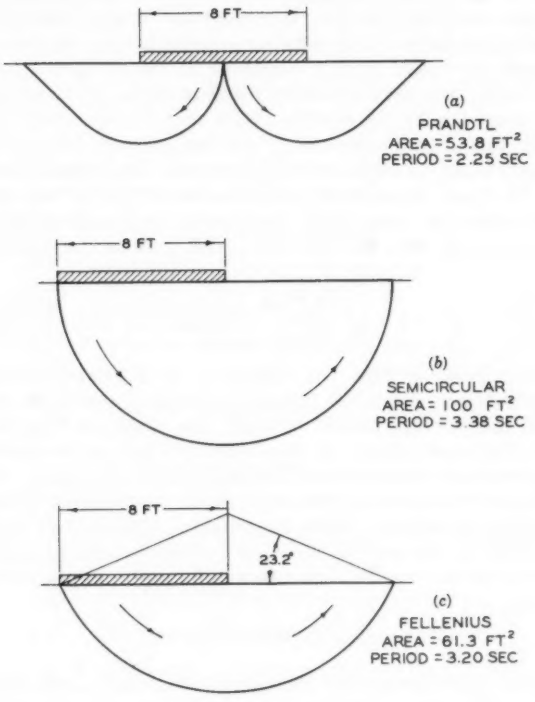

FIG. 10.—COMPARISON OF FAILURE SURFACES

Although the predicted displacements cannot be compared with measured values, it is possible to assess the difference between predictions using rotational—and punching-type failures. Both sets of equations were developed using similar assumptions and procedures. Comparison of the displacements predicted in sample problem 2 with the predicted displacements for the same problem using a rotational failure shows the displacements for the punching failure to be larger.[10] For example, at a peak dynamic load of 9000 lb per sq ft the modified Prandtl failure surface gives a displacement 5.5 times that for

10 "Analytical Study of Dynamic Bearing Capacity of Foundations," by G. E. Triandafilidis, Contract DA-22-079-eng-240. Univ. of Illinois, June, 1960.

a semicircular failure surface and 2.3 times that for a Fellenius failure surface. The shapes of these surfaces are shown in Fig. 10. Since the general assumptions on which the mathematical model is based will result in smaller computed displacements than expected in the prototype (a lower-bound solution), the greater displacements associated with the punching failure indicate that it is theoretically the more representative of the prototype. However, this does not mean that the punching failure using a modified Prandtl failure surface is the most critical failure condition.

To determine why the punching failure yields larger displacements, a closer look at the three failure surfaces and the mathematical systems which represent them seems desirable. In the "Introduction" it was stated that the punching failure should be expected to give larger displacements, since for similar failure surfaces the mass of soil displaced in the rotational failure would be larger. It is important here to realize that mass alone is not the only factor affecting the response of the system. With only a slight oversimplification it can be shown that two parameters, natural period (T) and ultimate shear resistance, determine the response of the system. Assuming the ultimate shear resistance to be equal, the system with the shorter period will have the larger displacements under the same load. The period is dependent on the resistance with displacement as well as the mass, and radius of gyration in which the mass rotates $\left(T = \frac{2\pi}{K} = 2\pi\sqrt{\frac{N_I B}{N_R}}\right)$. Although the mass is important in determining the period, it does not appear to be the predominant parameter.

The area bounded by the three failure surfaces (Prandtl, semicircular, and Fellenius) and the natural period of each are shown in Fig. 10. Even though the area (and therefore mass) of the Fellenius failure is close to that of the Prandtl, its period is closer to that of the semicircular failure. For the punching failure, the soil mass is distributed closer to the centers of rotation, giving a smaller moment of inertia. Since the moment of inertia is in the numerator of the expression for the period, the effect of the two-sided failure surface is to give a shorter period system and therefore larger displacements.

SUMMARY

Mathematical procedures are developed to predict large displacements of long footings subjected to dynamic loads, assuming ultimate failure and a punching-type failure surface. The expressions are presented in a manner convenient for computation of displacement under initial-peak triangular load pulses. Since the work is based on rather broad assumptions and is not substantiated by experimentation, the expressions should be regarded as a research vehicle rather than a design method for dynamically loaded foundations.

Predictions of footing displacement are compared for assumed rotational- and punching-type failures. The displacements associated with punching failure were found to be larger, primarily because of the shorter natural period of that failure mode. For both types of failure, approximations were such that computed displacements should be theoretically less than the true displace-

ments, and therefore it is concluded that the punching failure is a better approximation of the true failure conditions.

ACKNOWLEDGMENTS

Acknowledgment is made to R. V. Whitman, M. ASCE, Massachusetts Institute of Technology; R. B. Peck, F. ASCE, H. O. Ireland, M. ASCE, and G. E. Triandafilidis, M. ASCE, University of Illinois; and Messrs. W. J. Turnbull, F. ASCE, W. G. Shockley, F. ASCE, and R. W. Cunny, M. ASCE, Waterways Experiment Station, for their comments and advice.

APPENDIX - NOTATIONS

a, b, c, etc. = points used for identification;

a', b', c' = points after displacement;

B = half width of footing, in feet;

C_1, C_2, C_3, C_4 = constants of integration;

C_s = cohesive shear resistance along line bd, in pounds per foot;

C_p = cohesive shear resistance along line ab, in pounds per foot;

c = cohesive shear strength of soil, in pounds per square foot;

D = distance from center line to point of passive wedge, in feet;

g = acceleration due to gravity, in feet per square second;

I F = total inertial force, pounds per foot;

K = coefficient related to natural period of footing;

k = ratio of a0/B, dimensionless;

$M^o_{C_s}$, $M^o_{C_p}$, etc. = moment of forces C_s, C_p, etc., about point 0, in pound-feet per foot;

N = resultant of normal and frictional shear forces along line bd, in pounds per foot;

N_γ, N_c, N_q, N_R, N_I = coefficients of static and dynamic shear resistance;

0 = center of spiral shear surface and center of rotation;

p = ultimate static shear resistance, in pounds per square foot;

P'_d = passive earth-pressure force on line df neglecting weight of soil, in pounds per foot;

P''_d = passive earth-pressure force on line df when c and q are zero, in pounds per foot;

P_p = total passive earth-pressure force on line ab, in pounds per foot;

P'_p = passive earth-pressure force on line ab neglecting soil weight, in pounds per foot;

P''_p = passive earth-pressure force on line ab when c and q are zero, in pounds per foot;

q = surcharge on soil surface, in pounds per square foot;

Q = peak dynamic load, in pounds per square foot;

R_0 = initial radius of spiral, in feet;

R_2 = radius of spiral at point d, in feet;

RF = total restoring force, in pounds per foot;

t = time, in seconds;

T = natural period, in seconds;

t_d = duration of load pulse, in seconds;

t_{max} = time at Δ_{max}, in seconds;

W_1, W_2, etc. = weight of soil masses, in pounds per foot;

α = angle ab0;

γ = unit weight of soil, pounds per cubic foot;

Δ = downward transient displacement of footing, in feet;

Δ_{max} = maximum displacement of footing, in feet;

θ = internal angle between R_0 and any radius, R;

θ_1 = internal angle between R_0 and vertical line through 0;

θ_2 = internal angle between R_0 and line 0d;

ϕ = angle of internal friction for soil; and

ψ = $45° + \phi/2$.

Journal of the
SOIL MECHANICS AND FOUNDATIONS DIVISION
Proceedings of the American Society of Civil Engineers

TANK FOUNDATIONS IN EASTERN VENEZUELA

By Emery D. Carlson[1] and Stephen P. Fricano,[2] A. M. ASCE

SYNOPSIS

The foundation experience obtained from over 500 oil storage tanks constructed in Eastern Venezuela is presented in summary form. The 20 yr settlement record of a twenty-eight-tank terminal constructed on soft clay soils is given. It is observed that large steel storage tanks can be successfully operated with shell settlements as large as 3 ft and bottom settlements as much as 2 ft greater than those of the shell.

Continuous settlement records of three 150,000 bbl tanks over a 10 yr period, including controlled test loadings are shown. The three tanks are located adjacent to each other on deep soft clay and have experienced unusually large settlements. The foundation of one tank failed resulting in a maximum shell settlement of 5.75 ft with a differential settlement of 2.8 ft along the shell. Soil conditions and analysis calculations of the failure are presented along with the remedial measures taken and the subsequent 8 yr service record.

Basic criteria used in the design of the company's standard tank base is outlined. Except in the most unusual conditions a compacted earth base is used

Note.—Discussion open until March 1, 1962. To extend the closing date one month, a written request must be filed with the Executive Secretary, ASCE. This paper is part of the copyrighted Journal of the Soil Mechanics and Foundations Division, Proceedings of the American Society of Civil Engineers, Vol. 87, No. SM 5, October, 1961.

[1] Division Engr. of Eastern Venezuela, Creole Petroleum Corp., Caripito, Venezuela.
[2] Soils and Foundation Engr., Creole Petroleum Corp., Caripito, Venezuela.

without concrete ring wall topped by a 2 in. compacted cold mix sand-asphalt blanket.

INTRODUCTION

From June 1928, when commercial oil deposits were discovered in Eastern Venezuela, until mid-1960 the firm with which the writers are associated has constructed tanks ranging in size from 100 bbl to 150,000 bbl capacity within

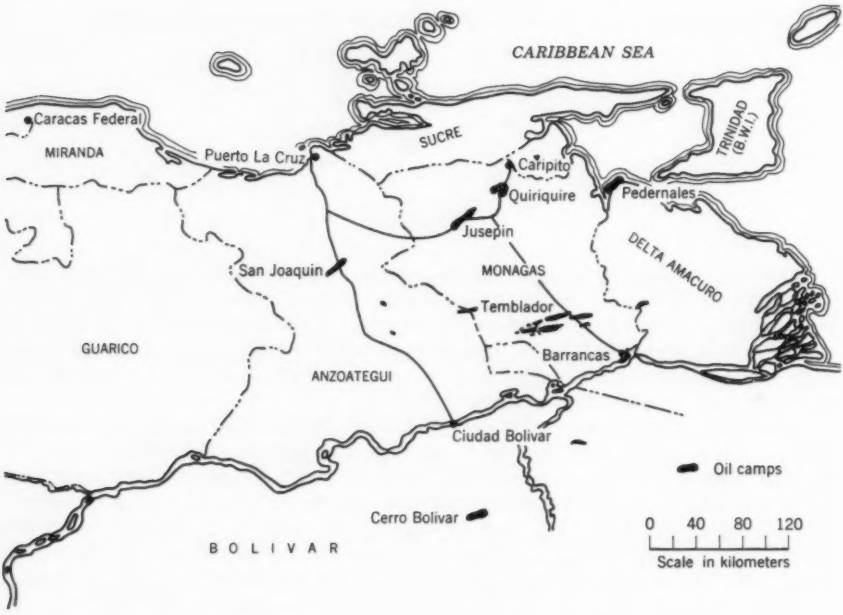

FIG. 1.—OIL CAMPS IN EASTERN VENEZUELA

an area extending southward from the Caribbean Coast to the Orinoco River and from the Eastern coast 180 miles inland. It includes the Venezuelan states of Monagas, Sucre and most of Anzoátegui. The low mountains of the state of Sucre and the central plains area directly south make up a water shed area which drains toward the south and east to the Orinoco River, and toward the west to the Unare River. The eastern half of this area, principally in the state of Monagas, forms part of the great Orinoco alluvial delta which drains into the Gulf of Paria adjacent to Trinidad, and into the Atlantic Ocean. The annual rainfall varies from 30 in. over the inland plain area to 80 in. to 100 in. in the Delta area. The majority of the tanks built are located at Ciudad Bolivar,

Barrancas, Pedernales, and Caripito (Fig. 1) and are constructed on the Orinoco Delta sedimentary fine sands, silts, and clays.

Some of the most difficult soil conditions encountered in the Eastern Venezuelan tank farms are those in the Caripito terminal located next to the Caripe River two miles from where it joins the San Juan River. In this area foundations have been principally of compacted fills, some having concrete ring walls. Settlement data, obtained as early as 1940, has been compiled for approximately twenty tanks in the Caripito tank farm.

The detailed time-settlement curves for the initial load tests and subsequent eight year service records of three 150-ft diameter tanks are presented. The failure of one of the three foundations is explained with a description of the remedial measures taken to restore it to service. The standard compacted-fill tank base, used where conditions permit, is presented.

SUMMARY OF TANKS CONSTRUCTED

A total of 555 tanks of all sizes are still in service in Eastern Venezuela, built by the company with which the writers are involved from 1928 to 1960. Numerous others have been built and dismantled or replaced. Of the total present tankage, 395 are 1,000 bbl to 150,000 bbl capacity, and 160 tanks range in capacity from 100 bbl to 1,000 bbl. This tankage represents a total capacity of 11,173,200 bbl. Table 1 summarizes the tank sizes and types of foundations built. It is particularly significant that only twelve tanks were built on foundations other than compacted-fill when one considers the varying soil conditions on which they were built.

20 YR SETTLEMENT EXPERIENCE OF THE CARIPITO TANK FARM

Description.—The Caripito tank farm is a crude oil and refined products terminal located within a large curve of the Caripe River just two miles west of the San Juan River. This is shown in Figs. 2(a) and 2(b). Construction of the terminal began in 1931. Additions have been made periodically until today there are 28 tanks with a total capacity of 2,752,000 bbl. The tanks range in capacity from 30,000 bbl. to 150,000 bbl. with diameters from 70 ft to 150 ft. The dimensions, capacities, and elevations of each tank are shown in Table 2.

Soil Profiles.—Numerous borings have been taken in the tank farm area since the 1930's. The soil profile shown in Fig. 3(a), is representative of the underlying strata. The whole area is underlain with soft gray clay varying from 6 ft to 30 ft in thickness. Under this there are intermixed sand and clay strata down to a depth of 90 ft where sand, gravel, and boulders are encountered.

Settlement Data.—It may be noted that for the twenty tanks for which there are elevation records in the 1940–1950 period, the average shell settlement varied from 0.03 ft to 1.16 ft. The mean settlement for the twenty tanks was 0.46 ft. The same twenty tanks registered total settlements from 1940 to 1960 from 0.00 ft to 1.24 ft with a mean of 0.66 ft as shown in Table 2.

All tanks were constructed on compacted earth bases except Tanks 22 and 29, which have concrete ring walls. Between the years 1940 and 1960 these two tanks had average shell settlements of 0.62 ft and 0.16 ft, respectively. No significant advantage can be seen for the concrete ring except that it pro-

vides a level base for the original erection of the tank shell. The ring may also provide some protection against differential settlements along the shell due to soft pockets. However, the experience in Venezuela has not revealed

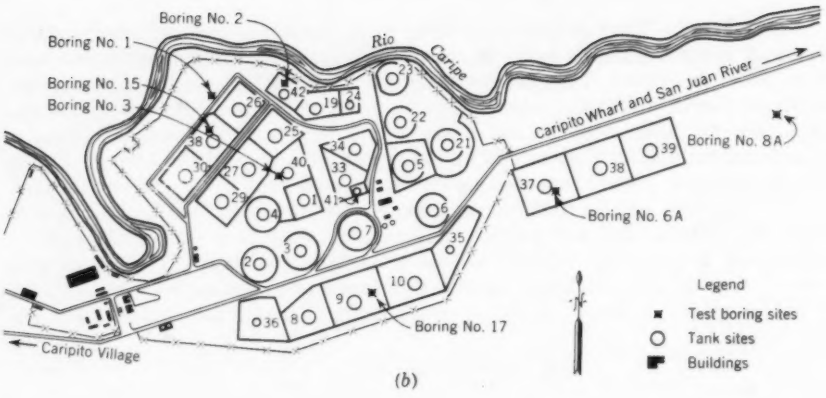

FIG. 2.—TERMINAL TANK FARM

any distressed tank shells resulting from local soft pockets along the shell of the other tanks constructed on compacted bases. The center portions of all tanks in this area have settled an additional 1.0 ft to 2.0 ft and have required lengthening of the roof columns during periods of repair and painting. Con-

TABLE 1.—SUMMARY OF TANKS BUILT IN EASTERN VENEZUELA

Tank Size Diameter x Height, in feet (1)	Capacity, in barrels (2)	Quantity Built (3)	Foundation	
			Quantity (4)	Type (5)
Various	< 1,000	162	4	Timber Mat
			158	Compacted Fill
24.75 x 12	1,000	92		↑
21.5 x 24	1,500	65		|
25 x 24	2,100	11		|
25 x 36	3,000	9		|
48 x 12	3,800	4		|
30 x 32	4,000	6		↓
35 x 30	5,000	54	2	Timber Mat
			2	Timber Piles
			50	Compacted Fill
36 x 30	5,400	15	15	↑
40 x 42	9,400	7	7	|
42 x 40	10,000	10	10	|
50 x 42	15,000	3	3	|
60 x 42	21,000	5	5	|
67 x 40	25,000	1	1	|
70 x 42	30,000	3	3	|
80 x 40	35,000	1	1	|
83 x 42	40,000	1	1	|
88 x 40	43,000	1	1	|
114.5 x30	55,000	19	19	↓
117 x 42	80,000	12	2	Concrete Ring
			10	Compacted Fill
118 x 42	82,000	4	4	Compacted Fill
128 x 42	96,000	15	2	Concrete Ring
			13	Compacted Fill
128 x 42	96,765	36	36	↑
144 x 40	116,000	3	3	|
150 x 40	125,000	1	1	|
150 x 45	139,300	8	8	|
150 x 48	150,000	5	5	|
155 x 45	162,500	2	2	↓
Total 555 Tanks				
Total Capacity—11,173,200 Bbl				

tinuous data on individual tanks is not available except for three 150,000 bbl tanks built in 1950.

SETTLEMENT RECORDS OF THREE 150,000 BBL TANKS

The most interesting tank experience in the Caripito Terminal has been the settlement performance of three 150,000 bbl tanks constructed in the southeast corner of the tank farm. Prior to construction of the tanks, soil samples were taken from two deep borings at the site. Laboratory tests, performed in the field, were limited by the test equipment available locally at that time. They included blow counts of sampler, moisture content, Atterberg limits and

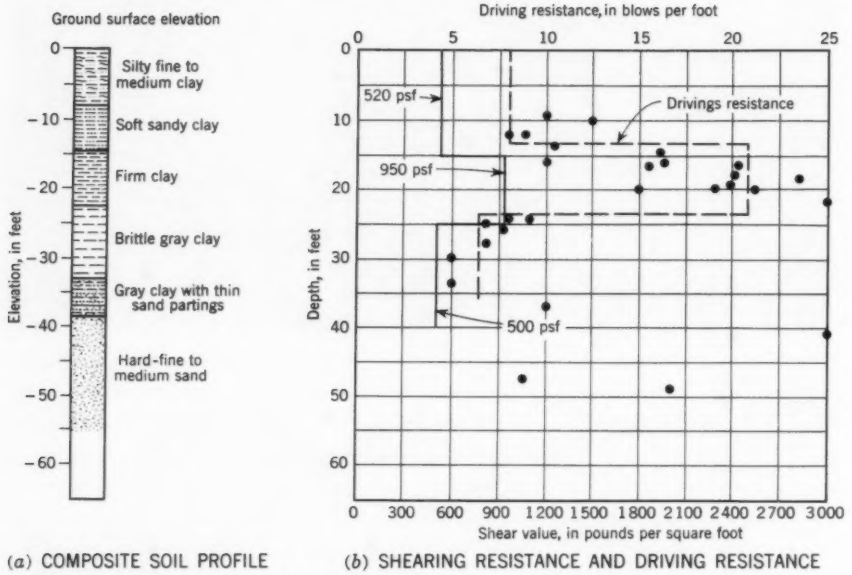

(a) COMPOSITE SOIL PROFILE (b) SHEARING RESISTANCE AND DRIVING RESISTANCE

FIG. 3

classification. From the results of these tests and from the general experience of tank bases in the same area, it was felt that settlement would be experienced and close observation of the three tanks would be especially important. Consequently, both short and long term observation schedules were established to record the movement of these tanks.

The terrain in the general area slopes slightly to the southeast. In order to obtain approximately the same base elevations for each of the three tank sites, for operational purposes, it was necessary to construct fills for the bases with heights of 2.4 ft, 2.6 ft, and 3.7 ft for Tanks 37, 38, and 39, respectively. The bases were constructed with a sandy clay gravel mixture brought from a point 2 km (1.24 miles) inland. No record of compaction of base material is available. The three tanks constructed were API (American Petroleum Institute)

TABLE 2.—CARIPITO TERMINAL TANK FARM DATA

Tank No	Capacity, in barrels	Diameter, in feet	Height, in feet	Month-Year Built	Average Shell Settlement, in feet	
					1950 to 1960	1940 to 1960
(1)	(2)	(3)	(4)	(5)	(6)	(7)
1	55,000	116	30	04-32		0.15
2	80,000	116	42	11-33		0.00
3	80,000	116	42	05-31		0.10
4	80,000	116	42	12-33		0.05
5	55,000	116	30	05-32		0.25
6	80,000	116	42	10-35		0.58
7	80,000	116	42	11-30		0.30
8	116,000	144	40	11-40		0.74
9	116,000	144	40	11-40		0.91
10	116,000	144	40	11-40		1.24
19	55,000	116	30	01-55		
21	96,000	128	42	02-38		0.96
22[a]	96,000	128	42	08-38		0.62
23	96,000	128	42	08-38		0.75
24	30,000	70	42	10-39		0.35
25	96,000	128	42	10-39		0.26
26	96,000	128	42	10-39		1.17
27	96,000	128	42	10-39		0.73
28	96,000	128	42	10-39		0.56
29[a]	96,000	128	42	10-39		0.16
30	96,000	128	42	10-39		0.21
33	80,000	116	42	06-46	0.21	
34	80,000	116	42	06-46	0.22	
35	80,000	116	42	06-46	0.46	
36	80,000	116	42		0.42	
37	150,000	150	48	03-50	1.88	
38	150,000	150	48	03-50	2.56	
39	150,000	150	48	03-50	1.54	

[a] Bases with Concrete Ring Walls

welded cone-roof type, 150 ft in diameter and 48 ft high. To facilitate settlement readings, clip angles were welded to the shells at the quarter points.

Tank No. 37.—This tank was test loaded with water beginning September 9, 1949. A total of 46.5 ft of water was pumped into the tank at a fairly uniform rate over a 30 day period for a gross pressure on the sub-soil (including the tank at 75 psf, and the base at 250 psf) of 3,235 psf. The load was held for 90 days from October 9, 1949 until January 7, 1950. The water was then pumped out at a nearly uniform rate in 16 days.

The time-settlement curve in Fig. 4 shows fairly uniform settlement of the shell which averaged 60 cm (1.96 ft) after 90 days loading. Points 1, 2, 3 and 4 are observation points on the tank shell. Their orientation is indicated. Maximum differential settlement of the shell was only 9 cm (0.30 ft). Rebound of the shell after unloading averaged 5 cm (0.17 ft). Cross sections showing the settlement of the tank interior are shown in Fig. 5, with point orientation as shown in Fig. 4. Examination of the settlement profiles of the tank interior

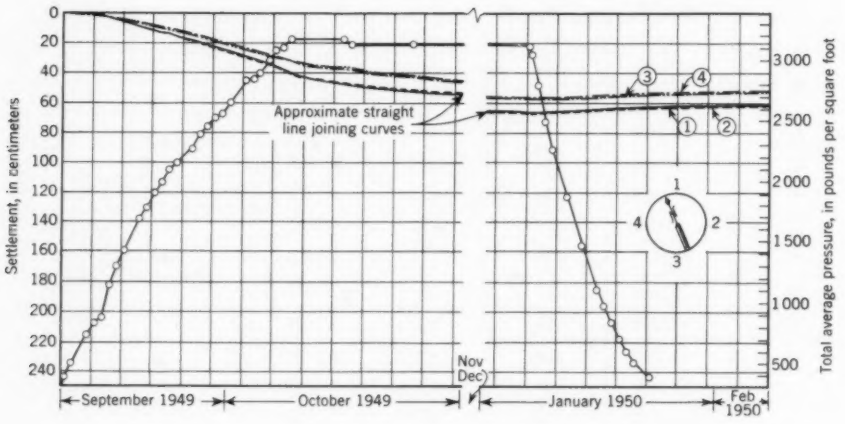

FIG. 4.—TIME-SETTLEMENT AND TIME LOAD FOR WATER LOAD TEST ON TANK NO. 37

shows settlements near the center of the tank of over 50 cm (1.67 ft) more than along the shell. No evidence of general shear failure is apparent, although some local shearing of the compacted base took place as the tank punched into it. This tank was placed in service in 1950 and has, throughout the year, an average soil loading of 2,700 psf. The time-settlement curve from 1952 to 1960 is shown in Fig. 6(a). Total additional settlement of the shell while in normal service averages approximately 42 cm (1.40 ft).

Tank No. 38.—This tank was test loaded with water beginning November 1, 1949. Again, approximately 46.0 ft of water was pumped into the tank at a uniform rate over a 30 day period for a gross pressure of 3,230 psf. The load was held for a 60 day period from December 1, 1949 until February 1, 1950. The water was then removed at a uniform rate in 15 days. The time-settlement curve showed an increasing rate of settlement as the point of full load

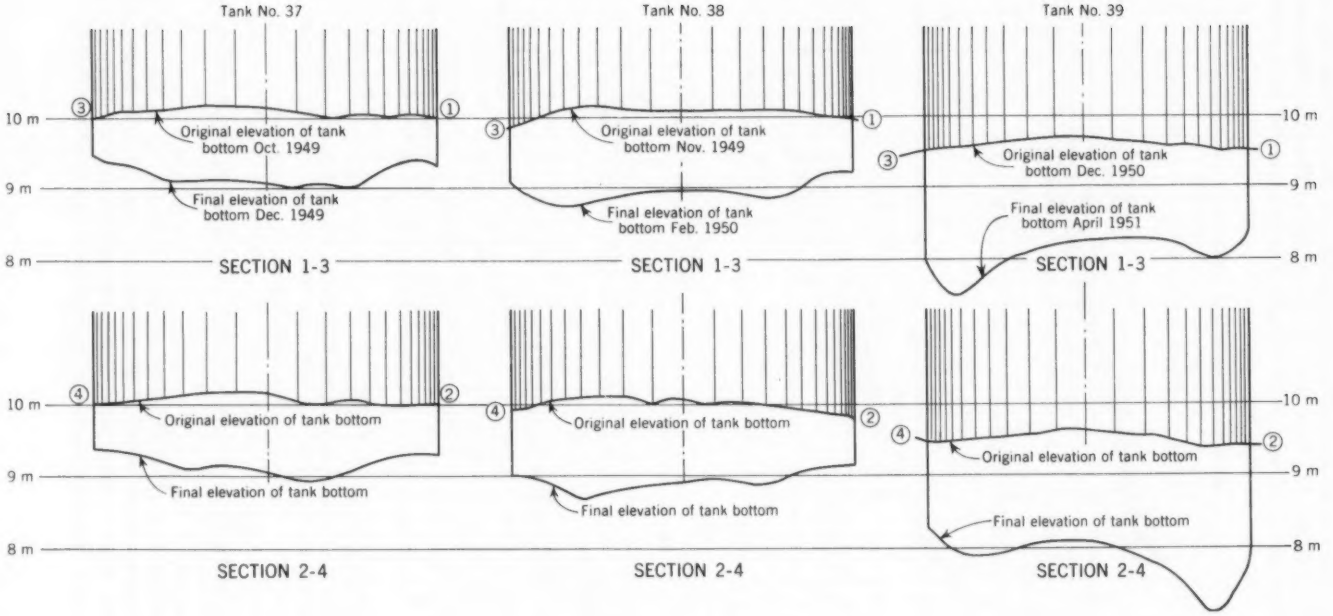
Tank No. 37
Tank No. 38
Tank No. 39
10 m
9 m
8 m
Original elevation of tank bottom Oct. 1949
Final elevation of tank bottom Dec. 1949
Original elevation of tank bottom Nov. 1949
Final elevation of tank bottom Feb. 1950
Original elevation of tank bottom Dec. 1950
Final elevation of tank bottom April 1951
SECTION 1-3
SECTION 1-3
SECTION 1-3
Original elevation of tank bottom
Final elevation of tank bottom
Original elevation of tank bottom
Final elevation of tank bottom
Original elevation of tank bottom
Final elevation of tank bottom
SECTION 2-4
SECTION 2-4
SECTION 2-4

FIG. 5.—SETTLEMENT OF TANK INTERIOR

was approached. However, about 20 days after the full load was placed the rate of settlement decreased and stayed so uniform that the test was discontinued after 60 days in order to place the tank in service. The tank shell showed an average settlement of 82 cm (2.67 ft) at the end of the test with a maximum

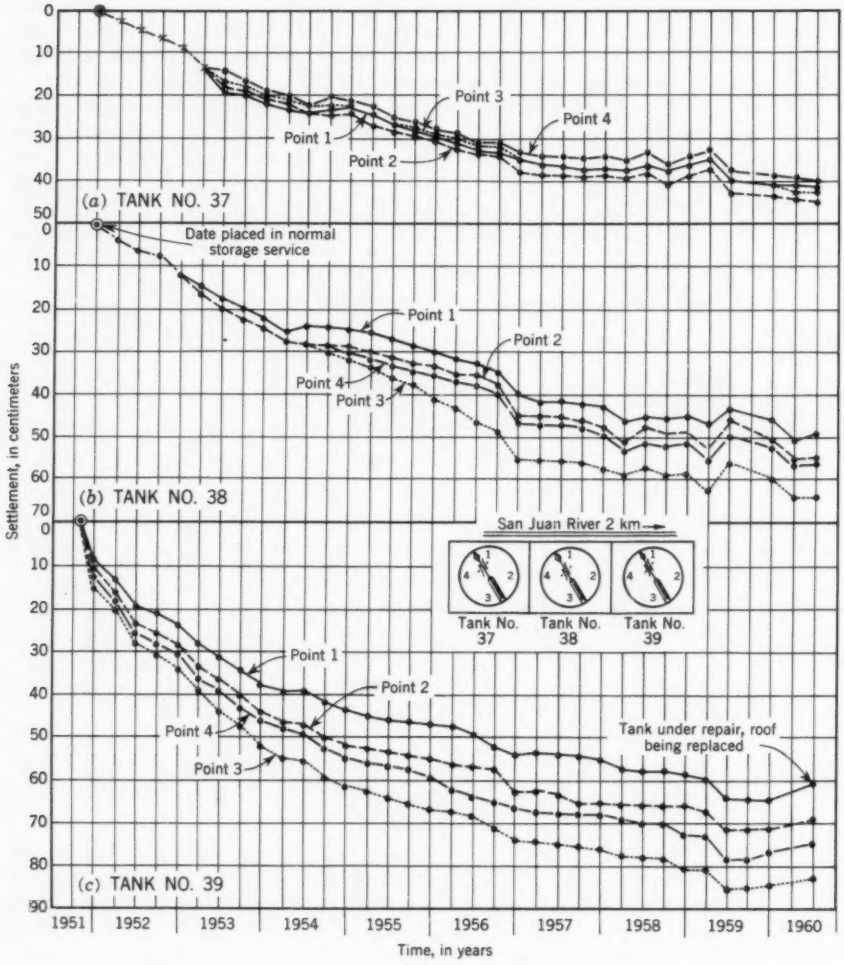

FIG. 6.—CURVES OF TIME SETTLEMENT AND LONG TERM SETTLEMENT

differential settlement along the shell of 12 cm (0.40 ft). As in the case of Tank No. 37 the interior shows settlements of about 40 cm (1.33 ft) more than along the shell Fig. 6(a) . Again, no evidence of general shear failure is apparent although the tank "punched" into the base approximately 30 cm (1.0 ft). In 1950

it was placed in service similar to Tank 37. Its time-settlement curve from 1952 to 1960 is shown in Fig. 6(b). Total additional settlement of the shell to date averages 57 cm (1.90 ft).

Tank No. 39.—The tank was first loaded with water beginning December 5, 1950. A total of 45.75 ft of water was pumped into the tank at a uniform rate (with one 4 day interruption) over a period of 33 days for a gross pressure of 3,350 psf. This load was held until February 2, 1951 when it was increased to 3,500 psf. and held for 82 days until April 25, 1951. The water was then released by gravity flow.

An analysis of the loading and settlement curves reveals a rapidly increasing differential settlement immediately after the 3,350 psf gross load was placed. However, after several days, the rate of settlement decreased considerably until February 2 when the total load pressure was increased to 3,500 psf. About four days following this load increase, the settlement rate of points 2 and 3 on the southeast side of the tank speeded up for a period of four weeks. The tank tilted badly to the southeast until it stabilized with a maximum differential settlement along the shell of 85 cm (2.8 ft). Total settlement on April 25 varied between 90 cm and 175 cm (3 ft and 5.75 ft) at the shell. The tank was considered unsafe for general service.

Examination of the settlement profiles of the tank interior (Fig. 5) indicated greater settlements were concentrated along the tank edge between points 2 and 3. Settlement along the southeast edge was nearly 1.0 cm (3.3 ft) more than at the center of the tank. A shear failure was definitely indicated. The failure appeared to be confined to the base and upper strata. However, no general upheavel of the surrounding ground could be detected.

ANALYSIS OF TANK No 39 FOUNDATION FAILURE

Description of Foundation Soils.—The original foundation of Tank No. 39 consisted of a relatively uncompacted fill of clayey gravel in the shape of a wedge varying in thickness from 2 ft to 4 ft. This compensated for gentle slope toward the southeast. The subsoil conditions are represented by the soil profile shown in Fig. 7. These data were collected from two deep borings taken in January, 1951. The top 6 ft consists of a medium brown clay with undrained shear values of about 720 psf. Shear values are one-half the compression strength from the unconfined compression test. Below this is a stiff blue clay stratum down to -19 ft with an undrained shear value of 1,860 psf. From -19 ft to 52 ft there are sands and soft clays with undrained shear values of only 350 psf.

From -52 ft down, shear strength[3] increases up to 700 psf at the northwest side of the tank. Penetration resistance required to drive a spoon sampler 12 in. with a 140 lb hammer varied up to 14 blows. Water contents ranged from 30% to 74% of dry weight. Dry weight varied from 55 pcf to 90.8 pcf.

Analysis of Failure Conditions.—The foundation analysis of the failure, made in 1950, was done by the Housel block shear method using shear planes at 45° from the horizontal. Shear values were those obtained from Housel transverse shear tests.[4] Overload ratios of the failure condition varied from

3 "Notes on Basic Principles of Shear Strength," by R. V. Whitman, 1959.

4 "Design Memorandum on Bearing Capacity of Spread Footings on Cohesive Soil," By W. S. Housel, 1952.

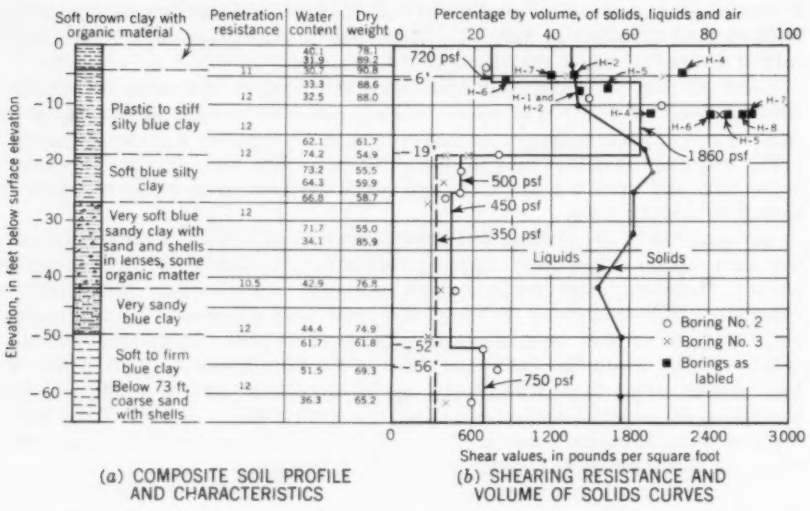
Soft brown clay with organic material
Penetration resistance
Water content
Dry weight
Percentage by volume, of solids, liquids and air
Elevation, in feet below surface elevation
Plastic to stiff silty blue clay
Soft blue silty clay
Very soft blue sandy clay with sand and shells in lenses, some organic matter
Very sandy blue clay
Soft to firm blue clay
Below 73 ft, coarse sand with shells
720 psf
1 860 psf
500 psf
450 psf
350 psf
750 psf
Liquids
Solids
Boring No. 2
Boring No. 3
Borings as labled
Shear values, in pounds per square foot
(a) COMPOSITE SOIL PROFILE AND CHARACTERISTICS
(b) SHEARING RESISTANCE AND VOLUME OF SOLIDS CURVES

FIG. 7.—SOIL PROFILE TANK NO. 39

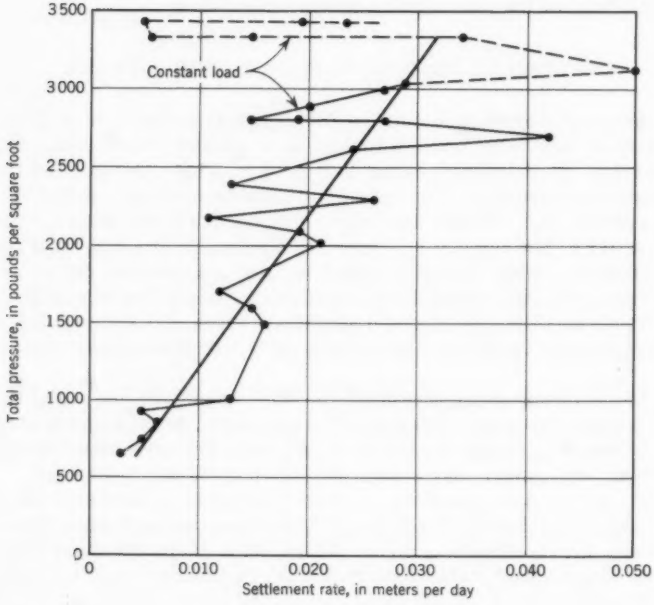

FIG. 8.—LOAD VERSUS SETTLEMENT RATE FOR POINT 3 TANK NO. 39; FIRST WATER LOAD TEST

2.0 to 3.8 in the various strata. These are approximately equivalent to Terzaghi-Peck[5] safety factors[6a] of 1.0 to 2.0. The reconstructed tank foundation was calculated to have an overload ratio of 2.5, equivalent to a Terzaghi-Peck safety factor of 1.66.

Because unconfined compression strength tests were made on the original soil samples at the same time as the Housel transverse shear values were taken, it is possible to make an analysis using undrained shear strengths equal to one-half the unconfined compression strength using the stability analysis formula of A. W. Skempton.[7]

The stability analysis was done by considering three cases. Case I assumes a failure of the base and the soft top stratum from 0 ft to -6.0 ft, with the base having a shear value equal to the top stratum, 720 psf. Case II assumes a failure circle extending down through the next stratum to -19.0 ft, with a shear value of 1,860 psf. Case III assumed a failure circle extending down through the soft weak stratum having a shear value of only 350 psf and extending to -73.0 ft.

Because the three assumed failure cases varied from an annular strip to a full half circular base, the Nc value in the bearing capacity formula

$$q_d = N_c C + p \quad \ldots\ldots\ldots\ldots\ldots\ldots \quad (1)$$

as proposed[6] by A. W. Skempton in 1951 was modified from 5.2 to 5.69 as suggested by L. Bjerrum.[8] The calculations are given in Appendix I for each case. The results are summarized in Table 3.

It is readily apparent from the safety factor found in the failure condition that the foundation could have failed in both the 0 ft to -6.0 ft stratum and the -19.0 ft to 73.0 ft stratum. From field observations and study of the settlement curves and sections of tank bottoms, as well as the stability analysis, the writers believe there are three factors involved in the foundation failure.

1. The tank punched through the relatively poorly compacted clayey gravel base, failing it and the top soft clay stratum. This was evident from field observations of the failure.
2. The foundation stratum, -19.0 ft to -73.0 ft, also failed in shear. The cross section showing the settlement of the tank interior plainly indicated the failure area extended nearly to the tank center, approximately 70.0 ft from the shell.
3. The entire tank base settled considerably as a result of rapid consolidation of the underlying strata. The load-settlement curves indicate a fairly rapid settlement rate, however a settlement rate versus load plot (Fig. 8) shows the settlement rates rapidly decreasing under constant load. It seems logical to assume that the underlying strata were undergoing a constant consolidation process with corresponding shear strength increases, even immediately before and after the two periods of apparent overload and failure.

Remedial Measures.—The tank was floated off the base by flooding the area within the fire walls and then towed to a new location within the area.

---

5 "Soil Mechanics in Engineering Practice," by K. Terzaghi and R. B. Peck, John Wiley, 1948.

6 "Soil Mechanics, Foundations, and Earth Structures," by G. P. Tschebotarioff, McGraw-Hill, New York, 1951, (a) p. 405.

7 "The Bearing Capacity of Clays," by A. W. Skempton, Building Research Cong., 1951.

8 "Foundation Failure of an Oil Tank in Fredrickstad, Norway," by L. Bjerrum and A. Overland, 4th Internatl. Conf. on Soil Mech., August, 1957.

After draining the area the gravel fill was removed from the base and the soft brown clay layer from 0 ft to -6 ft was excavated. The base was then rebuilt to its original elevation with a well compacted shale. The area was then reflooded and the tank floated back to its original position. After the area was again drained, an earth surcharge varying from 4 ft to 6 ft was placed around the tank Fig. 9.

Although considerable long term settlements were expected in Tank No. 39, due to deformation of the very soft deep clay stratum and consolidation of the silty sandy clay stratum, it was believed that the rebuilt base and shaped surcharge would reduce the differential settlement to serviceable proportions.

The safety factors, 2.98 to 3.02, obtained in the top strata by modifying the base, preclude failure in these strata. It seems that consolidation of the -19.0 ft to -73.0 ft stratum, with subsequent increase in shear strength, is a logical answer to why the tank foundation has performed satisfactorily after being modified. The safety factor of only 1.05 in this stratum is based on the original borings taken during the first load test and do not reflect the subsequent consolidation due to both the first and second load tests.

TABLE 3.

Stratum Checked, in feet	Failure Condition			Modified Base	
	Modified Nc Value	Calculated Bearing Capacity, in psf	Safety Factor	Calculated Bearing Capacity, in psf	Safety Factor[a]
(1)	(2)	(3)	(4)	(5)	(6)
0 to - 6.0	5.24	4000	1.14	10,380	2.98
0 to - 19.0	5.32	8840	2.52	10,580	3.02
0 to - 73.0	5.69	2930	0.84	3,650	1.05

[a] Before allowance for increase in shear resistance with consolidation

Second Load Test on the Modified Foundation.—The testing of the modified foundation began November 10, 1951 with the addition of 5 ft increments of water. Each increment was added over a two-day period and left in place 4 days before adding the next increment. This method of loading was used in order to allow more time for consolidation to take place in the underlying strata than had been allowed in the previous test. It also made it simpler to detect any changes in rate of settlement which would indicate impending failure or unacceptable differential settlements. Actual loading rates and resulting settlements are shown in Fig. 10. The total settlement of the shell ranged from 15.4 cm to 21.4 cm (0.51 ft to 0.71 ft) with a maximum differential of 6.0 cm to (0.20 ft). Since the settlements were so small, the full load of 3,500 psf was held for only 10 days. After the water load was removed, the tank rebounded an average of 3.0 cm (0.10 ft). Cross section of the settlement of the tank interior are shown in Fig. 11. The long-term service time-settlement curve, Fig. 6(c), shows an average additional shell settlement of 75 cm, (2.5 ft), and a maximum differential of 21 cm (0.7 ft). The direction of tilting changed from southeast to southwest.

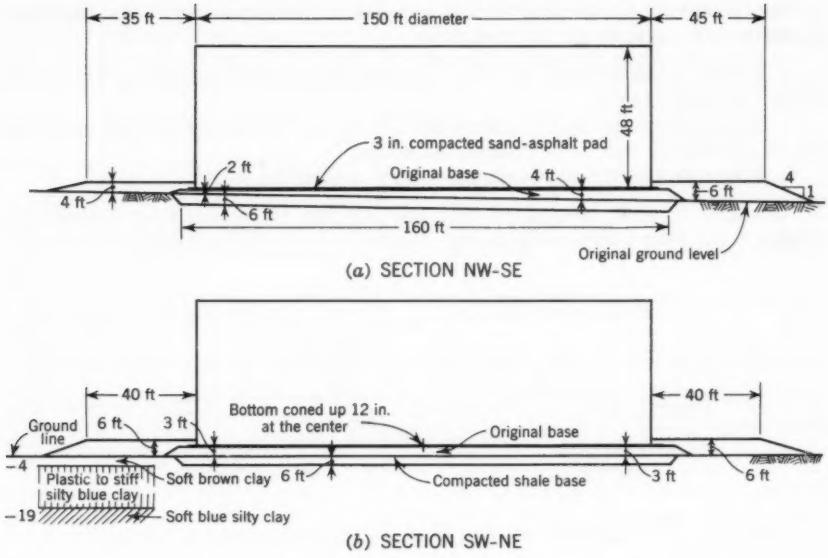

FIG. 9.—MODIFIED FOUNDATION FOR TANK NO. 39

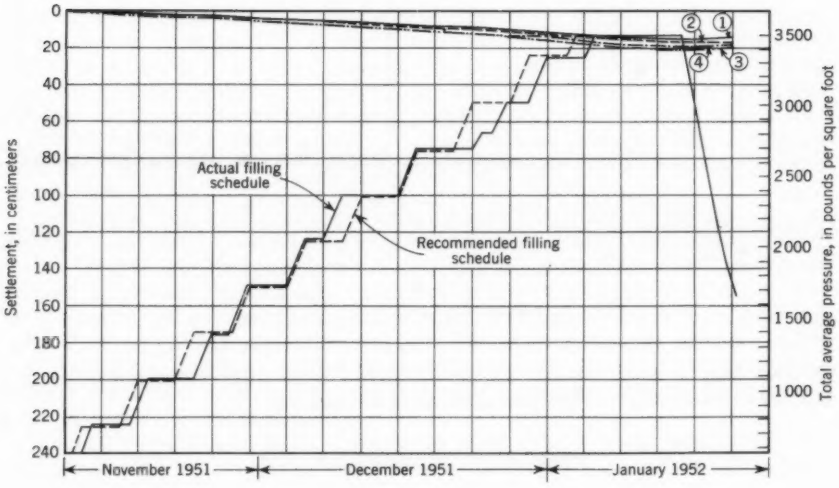

FIG. 10.—CURVES OF TIME SETTLEMENT AND TIME LOAD FOR SECOND WATER LOAD TEST FOR TANK NO. 39

The factors contributing to the successful performance of the modified foundation are assumed to be as follows:

1. Partial consolidation of some sub-soil strata from the preloading action of the two water tests;
2. Replacement of the 6 ft. thick soft brown clay layer and the uncompacted clayey gravel fill with well compacted shale;
3. Placement of the balanced surcharge around the tank.

Although it was recognized that the addition of the surcharge would increase total long term settlements, it was believed to be justified in view of

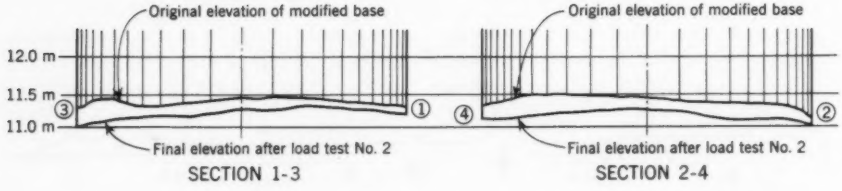

FIG. 11.—SETTLEMENT OF TANK NO. 39 WITH MODIFIED FOUNDATION

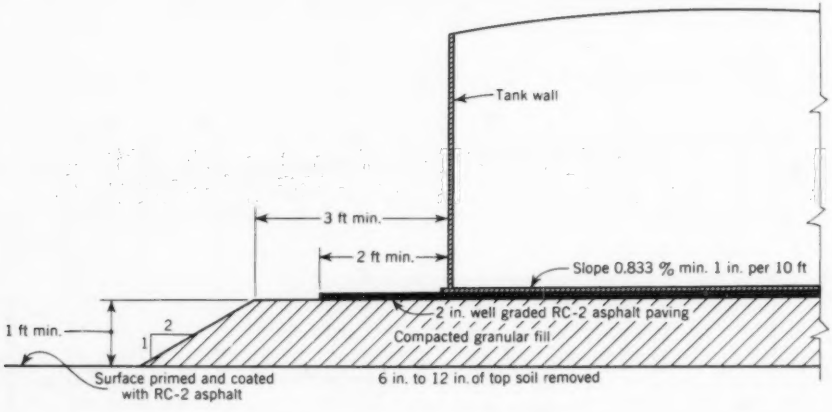
Tank wall
3 ft min.
2 ft min.
Slope 0.833 % min. 1 in. per 10 ft
2 in. well graded RC-2 asphalt paving
Compacted granular fill
1 ft min.
2
1
Surface primed and coated with RC-2 asphalt
6 in. to 12 in. of top soil removed

FIG. 12.—TYPICAL TANK FOUNDATION

the fact that it would reduce the possibility of large differential settlements, which are most critical for overall tank performance.

TYPICAL TANK BASE DESIGN

As a result of this experience in the construction of tanks of various sizes on sub-soils of varied characteristics the following general approach has been evolved. Prior to base construction it is now the company's standard practice

to investigate the site by taking one or more borings even though it may be within a well explored area. Because of the large investment in even a small tank, it has been found to be most economical to investigate the subsoil conditions of all sites to avoid costly failures. With this data, soil studies are made to determine the possibility of problems arising from one or more of the three critical types of tank foundation settlement resulting from either shear failure or from soil consolidation:

1. Differential settlements between opposite sides causing the shell to deform elliptically setting up excessive stresses in the shell;
2. Differential settlements closely spaced along the shell causing the shell itself to buckle;
3. Large differential settlements between the shell and the tank bottom causing the bottom to tear away from the shell.

The general stability of the entire tank foundation against shear failures causing slides, plastic flow and upheaval, or overturning failures is studied. After determining the soil characteristics and corrective action to be taken where necessary a typical base, as shown in Fig. 12, is constructed.

With the proper design of connected piping, a typical petroleum tank designed and constructed in accord with the API Standards can withstand several feet of uniform settlement. A large tank can also operate successfully with the center area settling 2 ft to 3 ft more than the shell because of its flexible bottom and roof. The columns supporting the roof can be adjusted in length from time to time to correct excessive deformation in the roof. Experience in the Caripito Tank Farm has amply demonstrated this fact. Nearly every tank which has been opened for inspection after several years service has had from 1 ft. to 2 ft more settlement near the center of the tank than at the shell.

Site Drainage.—The entire area enclosed within the limits of the firewalls is stripped of grass, roots, and topsoil. The outer edge of the tank base is built to a minimum of 1 ft above the elevation of the stripped ground surface. This insures drainage of the base even when the area enclosed by the firewalls is subjected to heavy rains before the operating personnel can open drain valves. A minimum slope of 1 in. in 10 ft is used to allow for possible greater settlements of the tank center than the tank shell. Both the base thickness and finish slope are frequently increased when it is known that the subsoil conditions may cause considerable settlement (3 in. or more) as in the Caripito Tank Farm area.

Base Material.—The material specifications for the compacted fill are generally limited to Casagrande classifications GW, GC, GF, SW, SC, and SF or better. Within the limitations of the material available, uniformity, moisture content, and density are closely controlled to insure a minimum of 90% maximum density and satisfactory shear strength. The (AASHO) American Assn. of State Highway Officials Specification M57-49 for embankments and subgrades is followed as a guide for construction. With these simple but flexible specifications it has been possible to build successful foundations utilizing local materials in remote areas at minimum cost.

Asphalt Blanket.—A 2 in. compacted cold mix sand-asphalt blanket is placed over the entire base and finished to within $\pm$ 1/4 in. of the final grade. This asphalt blanket insures that the finish grade is maintained during construction of the tank and insulates the tank bottom from the corrosive effects of the underlying moist soils during the normal life of the tank. Because one of the most critical settlement conditions of any tank is the differential

settlement along the tank shell, it is important that the asphalt pad be well compacted and true to grade along the shell line. The unit pressure directly beneath the tank wall are as high as 130 psi while it is only 22 psi over the interior of the tank bottom in a fully loaded 48 ft high tank. Some tanks' walls may "breathe," that is, move in or out horizontally as much as 1/2 in. under certain loading and temperature conditions. To prevent the outer edge of the tank bottom from gradually cutting through the sand asphalt pad, well-graded mixes using RC-2 asphalt are designed. A wide range of mixes may be utilized depending upon local materials. However, asphalt content and compaction are both closely controlled to insure adequate density and stability.

CONCLUSIONS

1. Careful subsoil exploration, laboratory analysis, and expert design together with close control of field construction will provide the most economical tank foundations, even in areas for which there is a great accumulation of data.
2. Large oil storage tanks can be successfully used in areas where several feet of settlement is probable, if the settlement is anticipated and provided for.
3. The greatest danger to the tank arises from excessive differential settlement, especially along the shell.
4. The use of concrete ring walls in tank foundations is generally not justified nor economical.
5. The successful construction of numerous tank foundations in Eastern Venezuela has led to the adoption of the compacted granular fill base with 2 in. sand-asphalt pad as the most economical and adaptable for general use.

ACKNOWLEDGMENTS

The writers wish to acknowledge that the information presented in this report was compiled from the engineering files of the Creole Petroleum Corporation Eastern Division.[9] The original subsoil explorations, laboratory analyses, and field supervision involved the efforts of many engineers, however, S. J. Mathis, F. ASCE, and C. A. Vickland, M. ASCE, contributed most to the foundation engineering examined herein. The work of analyzing the Tank 39 foundation failure and designing the modified foundation was accomplished[10] by W. S.

9 "Test Loading of 150,000 Bbl Storage Tanks, Caripito Terminal," Creole Petroleum Corp. Engrs., General Engrg. Report No. 9, January, 1951.

10 "Report on Tank No. 39, Caripito Terminal," Creole Petroleum Corp. Engrs. General Engrg. Report No. 15, July, 1952.

Housel, F. ASCE, and G. A. Oakes, M. ASCE, of the University of Michigan, Ann Arbor, Mich.

APPENDIX.—STABILITY CALCULATIONS - TANK 39

BASIC DATA

Loads.—The total test load pressure on original ground - S. E. side is composed of tank weight of 75 psf, 4 ft earth fill - 420 psf, and 48 ft of water or 2,995 psf for a total of 3,490 psf, say 3,500 psf. The total test load pressure on original ground - N. W. side is composed of the tank weight of 75 psf, 2 ft earth fill or 210 psf, and 48 ft of water or 2,995 psf, for a total of 3,280 psf, say 3,300 psf.

Bearing Capacity Formula.

$$qd = N_c\, c + \gamma\, d \quad \ldots\ldots\ldots\ldots\ldots\ldots \quad (2)$$

in which qd is the bearing capacity in pounds per square foot; N_c is a factor varying from 5.2 for strip footing to 6.2 for round or square footing - both on the ground surface; γ denotes density of surcharge, in pounds per cubic foot; d refers to the depth of surcharge; c is the undrained shear strength; and

$$qd\,\frac{b^2}{2} = \left(c_1\, L_1\, b + c_2 L_2\, b\right) + (\gamma\, d) \quad \ldots\ldots\ldots\ldots \quad (3)$$

gives qd by balancing moments between load pressure and the resisting shearing resistance along a circular failure plane.

Case I (Fig. 13).—Assume strip case modified

$$N_c = 5.2 + \frac{6}{150} \times 1.0$$

$$N_c = 5.24$$

or annular strip 6 ft wide.

Check along arc ABC

$$q\,d = N_c\, c + \alpha\, d = (5.24 \times 720) + (-1.3 \times 105 \text{ pcf})$$

$$3773 - 137 = 3636 \text{ psf}$$

$$(S\,F) = \frac{3638}{3080} = 1.17$$

Check arc A' B' C'

$$q\,d = (5.24 \times 720) + (2.2 \times 105) = 3773 + 231 = 4004 \text{ psf}$$

$$S\,F = \frac{4004}{3490} = 1.14$$

slightly worse case. In Fig. 13, b represents radius of assumed arc of shear failure.

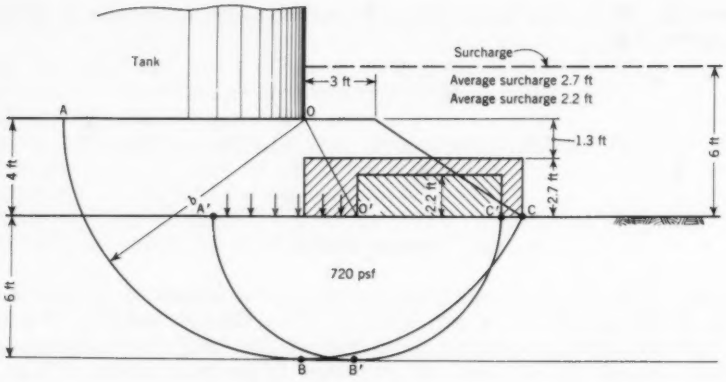

FIG. 13

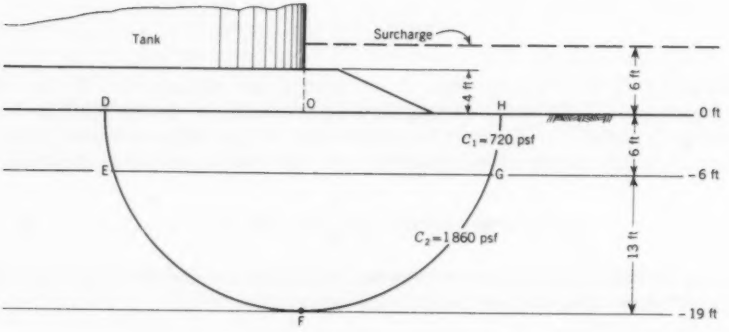

FIG. 14

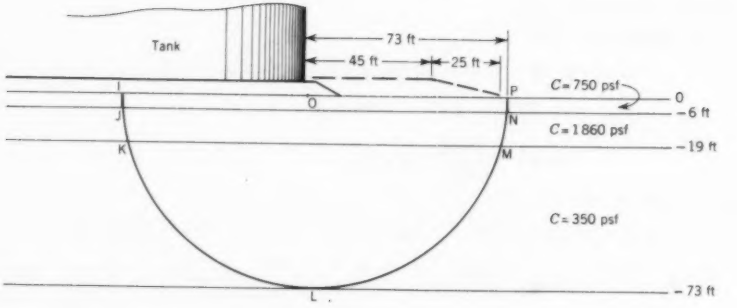

FIG. 15

Case IA.—Check stability to -6.0 ft with base and top stratum replaced with 1860 psf material and with 6 ft surcharge 45 ft wide.

$$q\,d = (5.24 \times 1860) + (6.0 \times 1.05) = 10.380 \text{ psf}$$

$$S\,F = \frac{10.380}{3490} = 2.98$$

Case II (Fig. 14).—Check stability from 0 ft to -19 ft by balancing moments about point 0 and reduce bearing value in accord with adjusted N_c value

$$\text{adjusted } N_c = 5.2 + \frac{19 \text{ ft}}{150 \text{ ft}} = 5.32$$

$$\text{reduction factor} = \frac{5.32}{6.20} = 0.86$$

$$q\,d\,\frac{b^2}{2} = (c_1 L_1 b + c_2 L_2 b)$$

$$q\,d = \frac{2}{b}(c_1 L_1 + c_2 L_2)$$

For b = 19.0 ft, c_1 = 720 psf, c_2 = 1860 psf, L_1 = 11.9 ft, and L_2 = 47.8 ft

$$q\,d = \frac{2}{19}(720 \times 11.9 + 1860 \times 47.8) = 10{,}250 \text{ psf}$$

Reduced bearing capacity = 0.86 x 10,250 = 8,840 psf

$$S\,F = \frac{8840}{3500} = 2.52$$

Case II A.—Check stability of modified base with 58 ft wide surcharge.

$$q\,d = \frac{2}{b}(c_1 L_1 + c_2 L_2) + \left(d \times \frac{2}{b} \times \frac{b^2}{2}\right) c_1 = 1860 \text{ psf}$$

$$q\,d = \frac{2}{19}(1860 \times 11.9 + 1860 \times 47.8) + (105 \times 6)$$

$$q\,d = 11{,}680 + 630 = 12{,}310 \text{ psf}$$

Reduced bearing capacity = 0.86 x 12,310 = 10,580 psf

$$S\,F = \frac{10{,}580}{3{,}500} = 3.02$$

Case III A (Fig. 15).—Check stability from 0 ft to -73 ft by balancing moments about point 0 and reducing bearing value in accord with Bjerrun method, that is adjusting N_c from 5.2 to 6.2 according to ratio of base width.

$$\text{adjusted } N_c = 5.2 + \frac{73 \text{ ft}}{150 \text{ ft}} \times 1.0 = 5.69$$

$$\text{bearing value factor} = \frac{5.69}{6.20} = 0.92$$

$$q\,d\,\frac{b^2}{2} = c_1 L_1 b + c_2 L_2 b + c_3 L_3 b$$

$$q\,d = \frac{2}{b}(c_1 L_1 + c_2 L_2 + c_3 L_3)$$

For c_1 = 720 psf, c_2 = 1860 psf, c_3 = 350 psf, L_1 = 12.8 psf, L_2 = 20.4 psf, and L_3 = 196.2 psf.

$$q\,d\,\frac{2}{73}\,(720 \times 12.8 + 1860 \times 20.4 + 350 \times 196.2) = 3180 \text{ psf}$$

bearing value reduced = (0.92 x 3180) = 2926 psf

$$S\,F = \frac{2926}{3500} \text{ psf} = 0.84$$

Case III B.—Check stability from 0 ft to -73 ft with 6 ft x 58 ft wide surcharge and stratum 0 ft to -6 ft replaced with material with shear value of 1860 psf $(c_1 = 1860)$

$$q\,d = \frac{2}{b}\left(c_1L_1 + c_2L_2 + c_3L_3\right) + (\gamma\,h) \times \left(\frac{2}{b^2}\right) \times \left(\frac{58^2}{2}\right)$$

$$q\,d = \frac{2}{73}\,(1860 \times 12.8 + 1860 \times 20.4 + 350 \times 196.2) +$$

$$\left(\frac{58}{2} \times 150 \times \frac{2}{73^2}\right) 6 = 3560 + 398 = 3968 \text{ psf}$$

Reduced bearing value = 0.92 x 3968 = 3650 psf

$$S\,F\,\frac{3650}{3500} = 1.05$$

Journal of the
SOIL MECHANICS AND FOUNDATIONS DIVISION
Proceedings of the American Society of Civil Engineers

ANALYSIS OF SEEPAGE PROBLEMS

By Milton E. Harr[1] M. ASCE and Robert C. Deen[2]

SYNOPSIS

A type of civil engineering problem involving the flow of groundwater is solved by making use of potential theory, elliptic integrals, the theory of complex variables, and conformal mapping. The results are summarized in chart form for ready use in analysis, allowing a rapid solution of a problem that requires much time and effort by conventional methods.

INTRODUCTION

Powerful analytical tools have been applied to the solution of a number of seepage problems (4)(5).[3] In the development of these methods, potential theory, elliptic integrals, the theory of complex variables and conformal mapping have been used to advantage. In spite of their great generality, these mathematical methods are not widely used in the analysis of structures for which the flow of ground water has a controlling influence on the design. It is the purpose of this paper to show how these methods can be adapted to obtain essentially exact solutions to a variety of civil engineering problems. Although an outline of the theoretical analysis is presented for those who may be interested, the primary purpose of this paper is to show how the essential results can be summarized in chart form for ready use in analysis.

Note.—Discussion open until March 1, 1962. To extend the closing date one month, a written request must be filed with the Executive Secretary, ASCE. This paper is part of the copyrighted Journal of the Soil Mechanics and Foundations Division, Proceedings of the American Society of Civil Engineers, Vol. 87, No. SM 5, October, 1961.

[1] Assoc. Prof. of Civ. Engrg., Purdue Univ., Lafayette, Ind.

[2] Research Engr. Senior, Materials Research Lab., Kentucky Dept. of Highways, Lexington, Ky.

[3] Numerals in parentheses refer to corresponding references in Appendix II.

The problem selected for illustration is shown in Fig. 1(a). The principal factors of interest in design are (a) the quantity of seepage, (b) the pressure in the water at any point, (c) the exit gradient which determines the possibility of piping and (d) the average gradient across a critical section that may be subject to heave. Fig. 1(a) represents a transformed section. The anisotropic case, in which the principal axes of permeability are parallel to the x- and y-coordinate axes, can be treated by applying the appropriate scaling factors (6).

THEORETICAL ANALYSIS

Notation.—The letter symbols adopted for use in this paper are defined where they first appear, in the illustrations or in the text, and are arranged alphabetically, for convenience of reference, in Appendix I.

Essentially, the procedure used in solving such a problem is to transform the problem from a geometrical domain in which a solution is sought into one for which the solution is known. The mathematical expedient permitting such a transformation is called conformal mapping, which in turn is a part of the theory of functions of complex variables (2).

If $w = \phi(x, y) + i\,\psi(x, y)$ is an analytic function of $z = x + i\,y$, i.e. $W = f(z)$ is analytic, then it can be shown that both ϕ and ψ satisfy Laplace's equation and that ϕ = constant and ψ = constant (except at singular points) intersect at right angles in the x-y plane. It can be shown that in the transformation from one plane to the other, the relationship $w = f(z)$ may, in general, alter both the scale and orientation of a line, but the angles formed by intersecting lines are preserved, thus "conformal" mapping.

The problem then is to find the particular functional relationship that will perform the desired transformation. This is generally provided by the Schwarz-Christoffel transformation (2). The Schwarz-Christoffel transformation will be used in this problem to map the polygonal regions of the z- or w-planes on the upper half of the auxilary t-plane.

The correspondence between the various points on the z-plane and the t-plane are as shown in Figs. 1(a) and 1(b). Applying the Schwarz-Christoffel transformation,

$$z = M_1 \int_0^t \frac{dt}{(t+1)^{1/2}\,(t+\sigma)^{-1}\,(t+m)^{1/2}\,(t-1)^{1/2}\,(t-\sigma)^{-1}\,(t-m)^{1/2}} + N \ldots \quad (1a)$$

and

$$z = M \int_0^t \frac{(\sigma^2 - t^2)\,dt}{(m^2 - t^2)(1 - t^2)} + N \quad \ldots\ldots\ldots\ldots \quad (1b)$$

Note that $z = 0$ when $t = 0$; thus, N must equal zero. Eqs. 1 can be expressed as the difference between two integrals in the following manner:

$$z = M\left[\sigma^2 \int_0^t \frac{dt}{\sqrt{(m^2 - t^2)(1 - t^2)}} - \int_0^t \frac{t^2\,dt}{\sqrt{(m^2 - t^2)(1 - t^2)}}\right] \ldots \quad (2a)$$

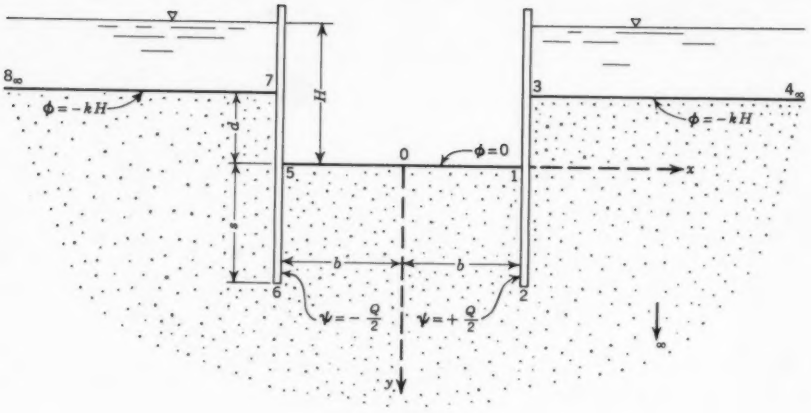

(a) z-PLANE

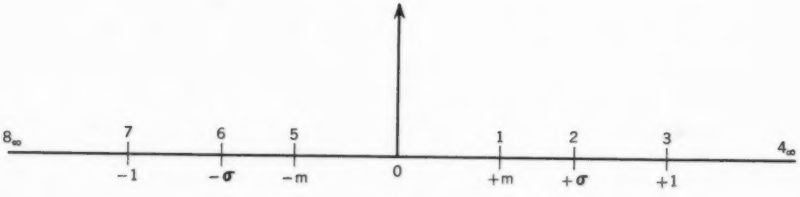

(b) t-PLANE

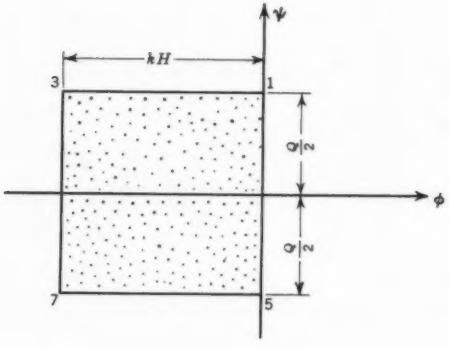

(c) w-PLANE

FIG. 1.—ILLUSTRATION OF THE PROBLEM

and

$$z = M\left(J_1 - J_2\right) \quad \ldots\ldots\ldots\ldots\ldots \quad (2b)$$

Letting $t = m\,\tau$, and thus $dt = m\,d\tau$,

$$J_1 = \sigma^2 \int_0^t \frac{d\,\tau}{\sqrt{\left(1 - \tau^2\right)\left(1 - m^2\,\tau^2\right)}} \quad \ldots\ldots\ldots \quad (3)$$

and

$$J_2 = \int_0^t \frac{d\,\tau}{\sqrt{\left(1 - \tau^2\right)\left(1 - m^2\,\tau^2\right)}} \quad \ldots\ldots\ldots\ldots \quad (4)$$

Substituting $\tau = \text{sn}\ u = \sin\theta = t/m$; $\theta = \text{am}\ u = \sin^{-1}(t/m)$, Eqs. 3 and 4 become in Legendre's notation

$$J_1 = \sigma^2\ F(m,\ \theta) \quad \ldots\ldots\ldots\ldots\ldots \quad (5)$$

and

$$J_2 = F(m,\ \theta) - E(m,\ \theta) \quad \ldots\ldots\ldots\ldots \quad (6)$$

where $F(m,\ \theta)$ and $E(m,\ \theta)$ are the elliptic integrals of the first and second kinds respectively with a modulus m.

Substituting Eqs. 5 and 6 into Eq. 2b, with $F(m,\ \theta) = u$,

$$z = M\left[\sigma^2\ u - u + E(u)\right] = M\left[\left(\sigma^2 - 1\right) u + E(u)\right] \quad \ldots\ldots \quad (7)$$

To determine the constants M, σ, and m, consider the relationship between the Points 1, 2, and 3 in the z- and t-planes.

At Point 1, $z = b$, $t = m$, $t/m = 1$, $u = K$, $E(u) = E(K) = E$, and

$$z = M\left[\left(\sigma^2 - 1\right) K + E\right] = b \quad \ldots\ldots\ldots\ldots \quad (8)$$

in which K and E are the complete elliptic integrals of the first and second kinds, respectively.

At Point 2, $z = b + is$, $t = \sigma$, $t/m = \sigma/m > 1$ but $< 1/m$. For this case, u will be a complex number of the form $u = K + iv\ (1)$. Thus

$$\frac{\sigma}{m} = \text{sn}\ u = \text{sn}\ (K + iv) = \frac{\text{cn}\ (iv,\ m)}{\text{dn}\ (iv,\ m)} = \frac{1}{\text{dn}\ (v,\ m')} \quad \ldots\ (9a)$$

and

$$\text{dn}\ (v,\ m') = \frac{m}{\sigma},\ v = \text{dn}^{-1}\left(\frac{m}{\sigma,\ m'}\right) \quad \ldots\ldots\ldots \quad (9b)$$

in which sn u, cn u and dn u are the Jacobian elliptic functions (4), and m' is the complementary modulus $\left(m' \sqrt{1 - m^2}\right)$. It can also be shown that

$$E(u) = E(K + iv) = E + i\left[v - E(v,\ m') + m'^2\ \text{sn}\ v'\ \frac{\text{cn}\ v'}{\text{dn}\ v'}\right] \ldots \quad (10)$$

(sn v', and so forth, designate sn (v, m'), . . .) Hence for Point 2,

$$z = M\left[\left(\sigma^2 - 1\right) K + E\right] + i\,M\left[\sigma^2 v + \left(m'^2\,\mathrm{sn}\,v'\,\frac{\mathrm{cn}\,v'}{\mathrm{dn}\,v'}\right) - E(v, m')\right] = b + is \quad \ldots\ldots\ldots (11a)$$

At Point 3, $z = b - id$, $t = 1$, $t/m = 1/m$, $u = K + iK'$, hence

$$E(u) = E(K + iK') = E + i(K' - E') \quad \ldots\ldots\ldots (11b)$$

in which K' and E' are the complete elliptic integrals of the first and second kinds respectively with modulus m'. Thus for Point 3 it is found that

$$z = M\left[\left(\sigma^2 - 1\right) K + E\right] + iM\left(\sigma^2 K' - E'\right) = b - id \quad \ldots\ldots (12)$$

On this basis, the three constants M, σ and m can be determined from

$$b = M\left[\left(\sigma^2 - 1\right) K + E\right] \quad \ldots\ldots\ldots\ldots (13a)$$

$$s = M\left[\sigma^2 v + \left(m'^2\,\mathrm{sn}\,v'\,\frac{\mathrm{cn}\,v'}{\mathrm{dn}\,v'}\right) - E(v, m')\right] \quad \ldots\ldots (13b)$$

and

$$-d = M\left(\sigma^2 K' - E'\right) \quad \ldots\ldots\ldots\ldots (13c)$$

Combining Eqs. 13c and 13a,

$$\sigma^2 = \frac{E' + \left(\frac{d}{b}\right)(K - E)}{K' + \left(\frac{d}{b}\right) K} \quad \ldots\ldots\ldots\ldots (14)$$

and σ thus can be determined readily once the modulus m is known.

Solving Eq. 13a for M,

$$M = \frac{b}{\left(\sigma^2 - 1\right) K + E} \quad \ldots\ldots\ldots\ldots\ldots (15a)$$

and substituting from Eq. 14

$$\sigma^2 - 1 = \frac{E' - K' - \left(\frac{d}{b}\right) E}{K' + \left(\frac{d}{b}\right) K} \quad \ldots\ldots\ldots\ldots (15b)$$

into Eq. 15a

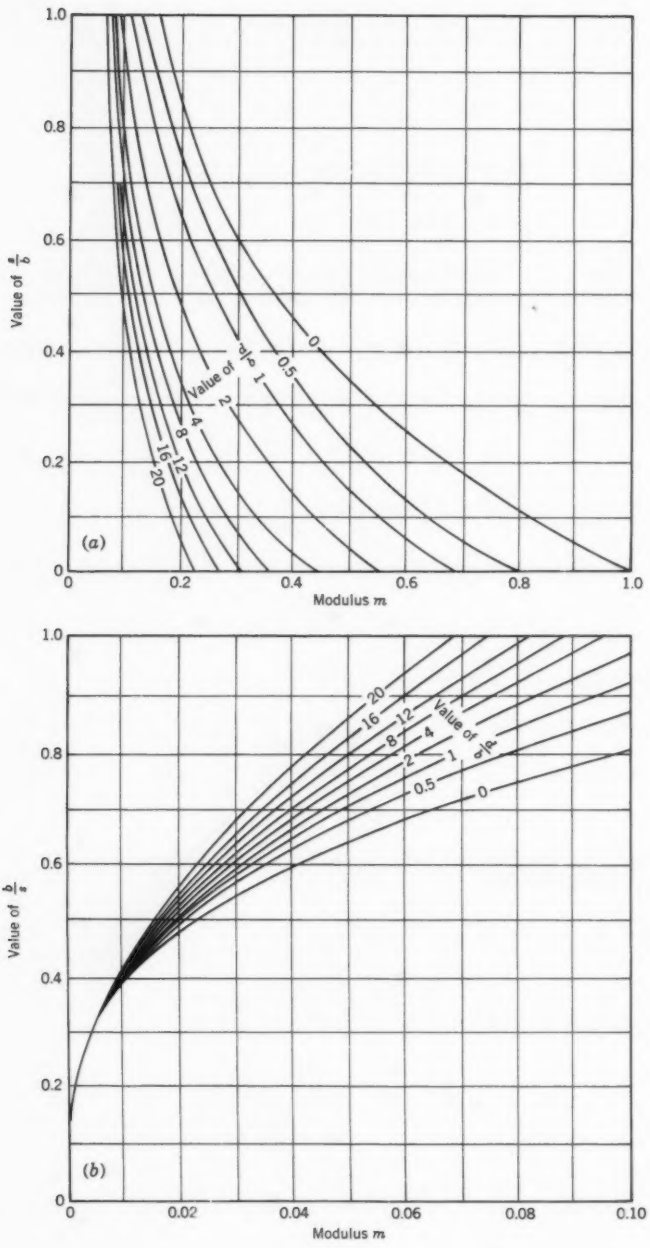

FIG. 2.—DETERMINING THE MODULUS

$$\frac{M}{b} = \frac{K' + \frac{d}{b} K}{E' K + E K' - K K'} \quad \ldots\ldots\ldots\ldots (15c)$$

which, recognizing Legendre's formula $(E'K + EK' - KK' = \pi/2)$, becomes simply

$$M = \left(\frac{2b}{\pi}\right) \left[K' + \left(\frac{d}{b}\right) K\right] \quad \ldots\ldots\ldots\ldots (15d)$$

Now, substituting the expressions for M and $(\sigma^2 - 1)$ into Eq. 7, the following is obtained for the required mapping function:

$$z = \left(\frac{2b}{\pi}\right) \left[\left(E' - K' - \frac{d}{b} E\right) u + \left(K' + \frac{d}{b} K\right) E(u)\right] \quad \ldots\ldots (16)$$

where the modulus remains to be determined.

From Eq. 13b,

$$\frac{s}{b} = \frac{\sigma^2 v + \left(m'^2 \, sn\, v' \, \frac{cn\, v'}{dn\, v'}\right) - E(v, m')}{(\sigma^2 - 1) K + E} \quad \ldots\ldots\ldots (17)$$

in which the left part, as noted from Eqs. 9 and 14, is a function of the modulus and the ratio d/b only. Because of the implicit nature of Eq. 17 a graphical procedure was devised whereby the modulus could be obtained for a wide range of d/b and s/b ratios. Such a plot is given in Fig. 2.

It is noted, in particular, that when s = 0 in Eq. 17, m = σ, hence Eq. 14 becomes

$$m^2 = \frac{E' + \left(\frac{d}{b}\right)(K - E)}{K' + \left(\frac{d}{b}\right) K} \quad \ldots\ldots\ldots\ldots (18a)$$

and

$$\frac{d}{b} = \frac{(E' - m^2 K')}{(E - m'^2 K)} \quad \ldots\ldots\ldots\ldots\ldots (18b)$$

Hence, for s/b = 0, the values of the modulus can be obtained directly from Fig. 3.

Thus Eq. 17 in conjunction with Fig. 2 allows for the complete mapping of the z-plane on the t-plane.

It is convenient in this problem to assume the w-plane as shown in Fig. 1(c). For symmetry, ψ is taken as zero along the y-axis. Applying the Schwarz-Christoffel transformation,

$$w = M \int_0^t \frac{dt}{\sqrt{(t^2 - m^2)(t^2 - 1)}} + N \quad \ldots\ldots\ldots (19)$$

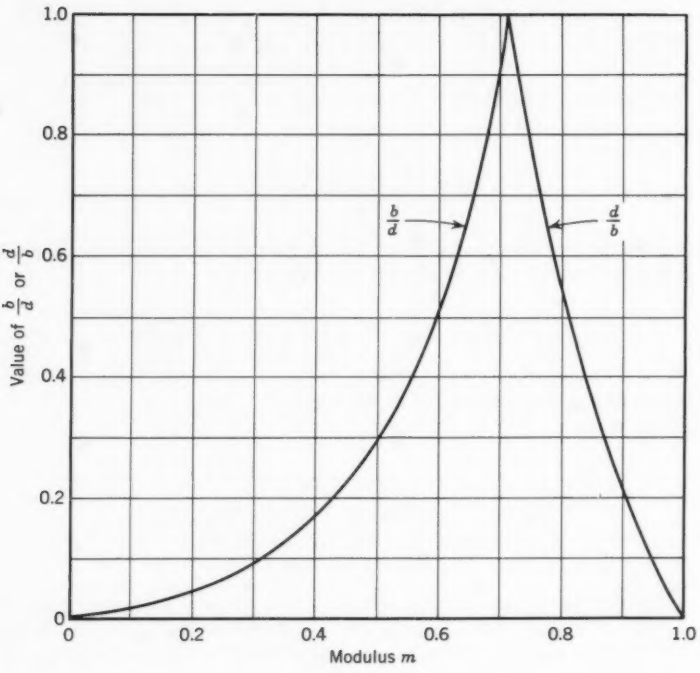

FIG. 3.—DETERMINING THE MODULUS WHEN s = 0

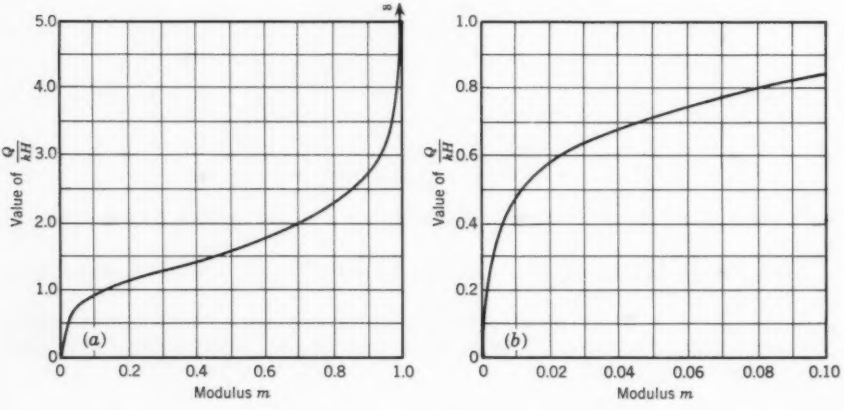

FIG. 4.—DETERMINING THE QUANTITY OF SEEPAGE

and because w = 0 when t = 0, N = 0. Making the substitution $t = m\,\tau$ in Eq. 19,

$$w = M_1 \int_0^{t/m} \frac{d\tau}{\sqrt{(1 - \tau^2)(1 - m^2\,\tau^2)}} \quad \ldots\ldots\ldots \quad (20)$$

Considering the correspondence between the two planes at Point 1; t = m, w = i Q/2 where Q is the quantity of seepage, then t/m = 1, and

$$M_1 = \frac{i\,Q}{2\,K} \quad \ldots\ldots\ldots\ldots\ldots \quad (21)$$

At Point 3, t = 1, $w = -k\,H + \frac{i\,Q}{2}$ where k is the coefficient of permeability, t/m = 1/m; hence

$$-k\,H + \frac{i\,Q}{2} = \frac{i\,Q}{2\,K} \int_0^{1/m} \frac{d\tau}{\sqrt{(1 - \tau^2)(1 - m^2\,\tau^2)}} = \frac{i\,Q}{2\,K}\,(K + iK') \quad \ldots (22a)$$

and

$$Q = \frac{2\,k\,H\,K}{K'} \quad \ldots\ldots\ldots\ldots\ldots (22b)$$

A plot of Eq. 22b, as a function of the modulus (Fig. 2), is given in Fig. 4.

In addition to the determination of the quantity of seepage the possibility of heaving and piping must also be investigated. Heaving of the soil prism 1256, Fig. 1(a), between the sheetpiles will be considered first. Using Legendre's notation for Eq. 20

$$w = \frac{i\,Q\,F(m,\,\theta)}{2\,K} \quad \ldots\ldots\ldots\ldots \quad (23)$$

in which $\theta = \sin^{-1}(t/m)$. Instead of computing the average gradient along the line $\overline{62}$ (Terzaghi's method) (7), the gradient along the line $\overline{12}$ will be obtained. The factor of safety with respect to heaving determined on this basis will always be slightly on the safe side.

At Point 2, $w = -\phi_2 + i\,Q/2$, t = σ and t/m = σ/m > 1. Because $F(m, \theta) = K + iv$ when t/m = σ/m, Eq. 23 becomes

$$-\phi_2 + \frac{i\,Q}{2} = \frac{i\,Q\,(K + iv)}{2\,K} \quad \ldots\ldots\ldots\ldots \quad (24)$$

hence

$$\phi_2 = \frac{-Qv}{2\,K} = \frac{-k\,H\,v}{K'} \quad \ldots\ldots\ldots\ldots \quad (25)$$

and for the gradient along the piling,

$$i_p = \frac{\left(\frac{1}{k}\right)(0 - \phi_2)}{s} = \frac{H\,v}{K'\,s} \quad \ldots\ldots\ldots\ldots \quad (26)$$

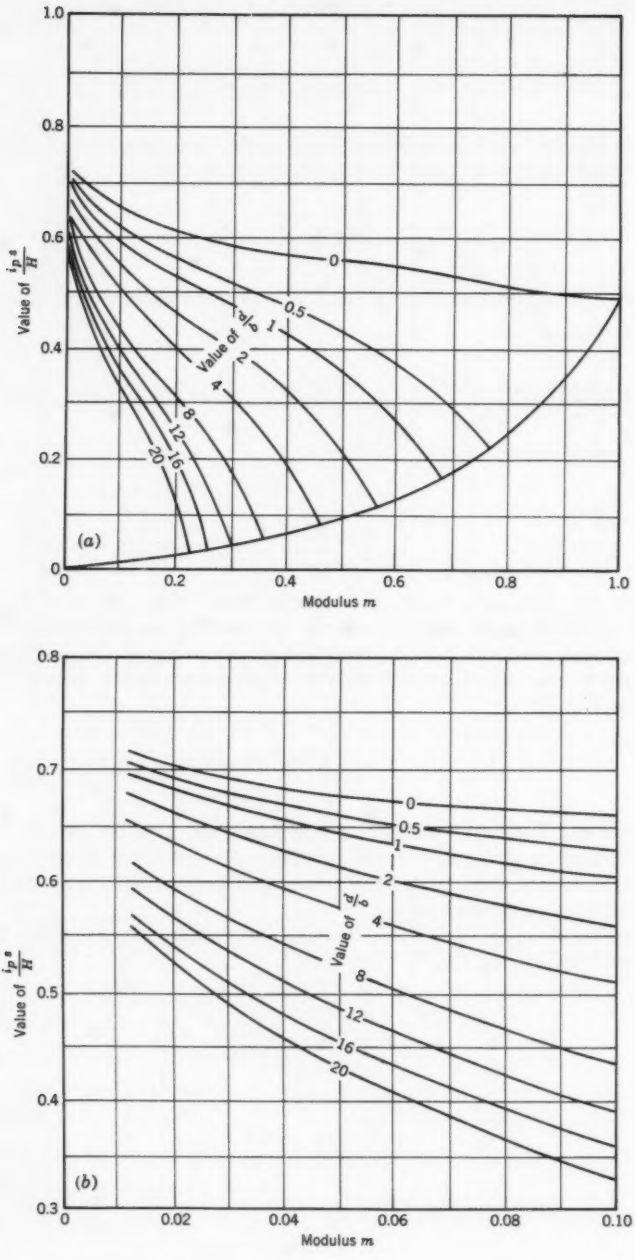

FIG. 5.—DETERMINING THE GRADIENT ALONG THE SHEET PILING

in which $v = dn^{-1}(m/\sigma, m')$, Eq. 9, with σ as determined from Eq. 14. Graphical solutions for $i_p\, s/H$ of Eq. 26 are given in Fig. 5 for various ratios of d/b. The modulus can be obtained from Fig. 2.

Considering next the exit gradient (Points 1 and 5),

$$i_e = \frac{1}{k}\frac{\partial\phi}{\partial t}\frac{\partial t}{\partial z}\frac{\partial z}{\partial y} = \frac{H\left[\left(\sigma^2 - 1\right) K + E\right]}{b\, K'\left(\sigma^2 - t^2\right)} \quad \ldots\ldots\ldots (27)$$

and at Point 1, t = m,

$$i_e = \frac{H\left[\left(\sigma^2 - 1\right) K + E\right]}{b\, K'\left(\sigma^2 - m^2\right)} \quad \ldots\ldots\ldots\ldots (28)$$

A plot of Eq. 28 for $i_e\, s/H$ is given in Fig. 6.

All the information necessary to effect a solution is now available in graphical form.

ILLUSTRATIVE PROBLEMS

To illustrate the use of the charts in solving particular problems, the conditions illustrated in Fig. 7 will be analysed. For example, when s = 5 ft, b/s = 1.00 and d/b = 2, from Fig. 2, m = 0.108. Entering Fig. 4 with this value for m, Q/kH = 0.90, from which the quantity of seepage is found to be 13.5 cu ft per day per ft of piling.

From Fig. 5 (with m = 0.108, $i_p\, s/H = 0.54$, that is, $i_p = 1.62$. The factor of safety against heaving (using the gradient along the inside of the sheet piles) is then

$$\text{F. S.} = \frac{i_{cr}}{i_p} = \frac{\gamma' m}{\gamma_w\, i_p} = \frac{54}{62.4} \times 1.62 = 0.53$$

From Fig. 6, $i_e\, s/H$ is found to be 0.40, whence $i_e = 1.20$, and the factor of safety (using the exit gradient) is equal to 0.72.

This procedure can be repeated for various depths of penetration of the sheet piling, and plots of the quantity of seepage and the factor of safety with respect to heaving versus the depth of penetration can be obtained as shown in Fig. 8.

The methods used in solving the illustrative problem (Figs. 1 and 7) can be extended to other situations, such as the one illustrated in Fig. 9. It is noted that the geometry of the z-plane is the same as that shown in Fig. 1, and thus the same mapping from the z-plane to the t-plane is as given in Eq. 17. However, it is noted that the w-plane is different. Fig. 9(c) indicates that the quantity of seepage is infinite whereas Fig. 1(c) indicates a finite quantity of seepage. For the mapping of the w-plane shown in Fig. 9(c) on the t-plane,

$$t = \cos\left(\frac{\pi\, w}{k\, H}\right) \quad \ldots\ldots\ldots\ldots\ldots (29a)$$

in which $w = \phi + i\,\psi$. Along the boundary of the weir ($\psi = 0$)

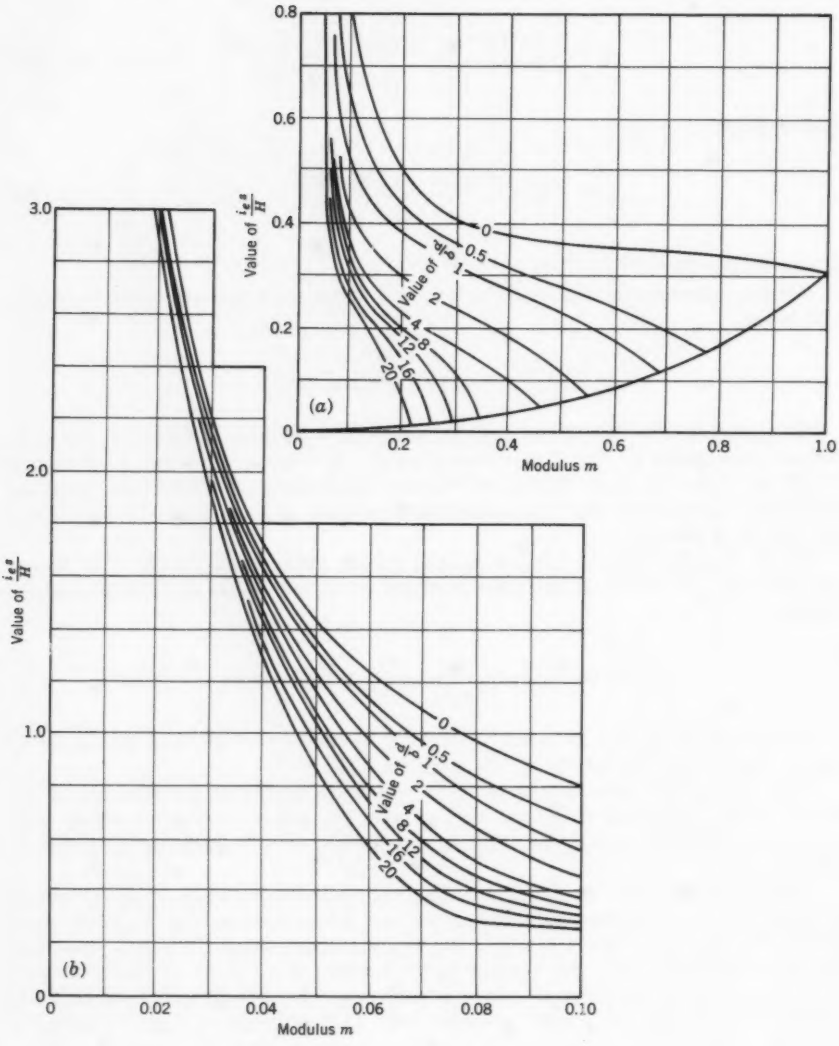

FIG. 6.—DETERMINING THE EXIT GRADIENT

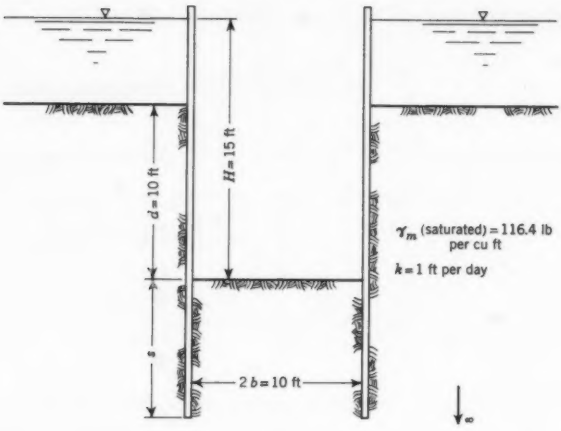

FIG. 7.—ILLUSTRATION OF A PARTICULAR PROBLEM

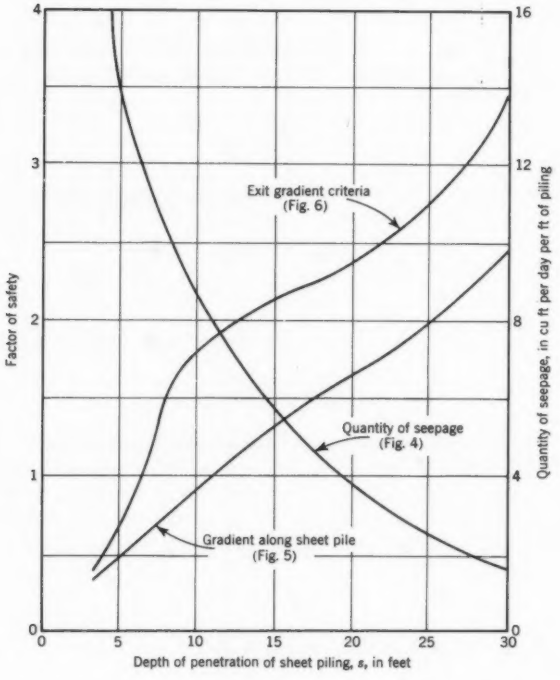

FIG. 8.—FACTORS OF SAFETY AND QUANTITY OF SEEPAGE AS A FUNCTION OF DEPTH OF SHEET PILE PENETRATION

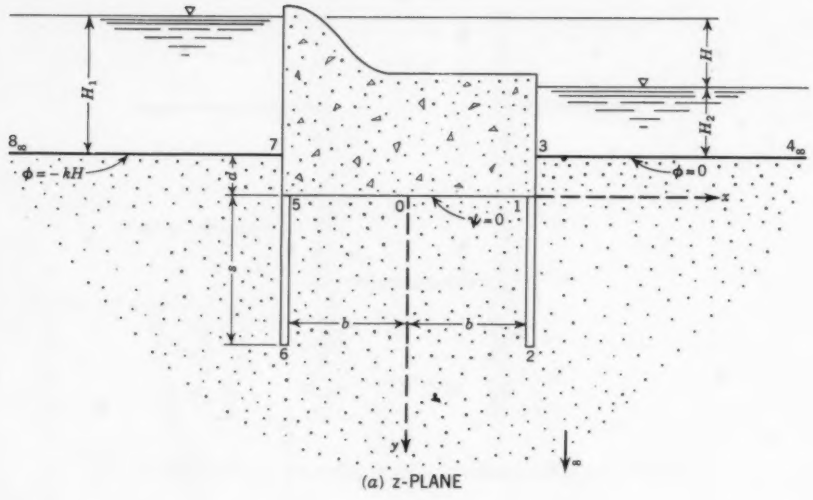

(a) z-PLANE

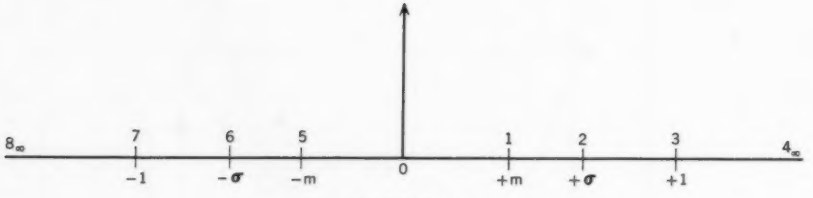

(b) t-PLANE

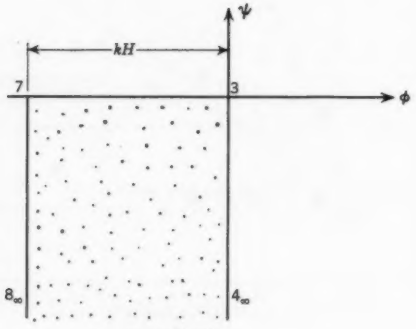

(c) w-PLANE

FIG. 9.—DEPRESSED WEIR WITH SHEET PILES

$$\phi = \frac{k\,H}{\pi} \cos^{-1} t \quad \ldots\ldots\ldots\ldots\ldots\ldots (29b)$$

and hence the pressure in the water, p, equals

$$p = -\gamma_w \left[\left(\frac{H}{\pi}\right) \cos^{-1} t - y - H_2 - d\right] \quad \ldots\ldots\ldots (29c)$$

where $-\pi \leq \cos^{-1} t \leq 0$.

For the exit gradient (at Point 3),

$$i_e = \frac{H\sqrt{t^2 - m^2}}{M\,\pi(t^2 - \sigma^2)} = \frac{H\sqrt{t^2 - m^2}}{2\,b\,(t^2 - \sigma^2)\left(K' + \frac{dK}{b}\right)} \quad \ldots\ldots\ldots (30)$$

Noting that $t = 1$ at the exit point and substituting for $(\sigma^2 - 1)$ from Eq. 15b, the exit gradient is given by

$$i_e = \frac{Hm'}{2\,b\left(K' - E' + \frac{dE}{b}\right)} \quad \ldots\ldots\ldots\ldots\ldots (31)$$

where the modulus can be obtained from Fig. 2.

Consider now the gradient along line $\overline{23}$. At Point 2, from Eq. 29b,

$$\phi_2 = \left(\frac{kH}{\pi}\right) \cos^{-1}\left(\frac{\sigma}{m}\right) \quad \ldots\ldots\ldots\ldots (32)$$

and for the gradient along the piling,

$$i_p = \frac{\left(\frac{1}{k}\right)(0 - \phi_2)}{(s - d)} = \frac{H}{\pi(s - d)} \cos^{-1}\left(\frac{\sigma}{m}\right) \quad \ldots\ldots\ldots (33)$$

where m is obtained from Fig. 2 and σ from Eq. 14.

CONCLUSIONS

It is hoped that this paper has illustrated how the powerful analytical tools available to civil engineers can be applied to obtain "design" curves for various problems. These methods have been used in this paper to develop a group of design curves that can be quickly and easily used to aid in the solution of a certain type of civil engineering problem involving the flow of groundwater.

APPENDIX I.—NOTATION

The following symbols have been adopted for use in this paper:

b = half the width of the weir or excavation between sheet piling;

d = depth weir is depressed or depth of excavation between sheet piling;

E = complete elliptic integral of the second kind with modulus m;

E' = complete elliptic integral of the second kind with modulus m';

$E(m,\theta)$ = elliptic integral of the second kind;

F.S. = factor of safety;

$F(m,\theta)$ = elliptic integral of the first kind;

H = head loss;

H_2 = tail water depth;

i = mathematical operator, the imaginary unit;

i_{cr} = critical gradient;

i_e = exit gradient;

i_p = gradient along the sheet piling;

J_1 = see Eq. 3;

J_2 = see Eq. 4;

k = coefficient of permeability;

K = complete elliptic integral of the first kind with modulus m;

K' = complete elliptic integral of the first kind with modulus m';

m = modulus;

m' = co-modulus;

M = constant;

M_1 = constant;

N = constant of integration;

p = pressure in the water;

Q = quanity of seepage;

s = depth of sheet pile penetration;

t = a complex variable, a point in the t-plane;

u = sn u = sin θ;

v = see Eqs. 9;

w = a complex variable, a point in the w-plane;

x = abscissa of point z;

y = ordinate of point z;

z = a complex variable, a point in the z-plane;

γ'_m = saturated unit weight;

γ_w = unit weight of water;

θ = $\theta = \sin^{-1}(k/m) = \text{am } u$;

σ = coordinate of a point in the t-plane;

τ = dummy variable;

ϕ = abscissa of point w; and

ψ = ordinate of point w.

APPENDIX II.—REFERENCES

1. "Handbook of Elliptic Integrals for Engineers and Physicists," by P. F. Byrd and M. D. Friedman, Springer-Verlag, Berlin, Germany, 1954.
2. "Introduction to Complex Variables and Applications," by R. V. Churchill, McGraw-Hill Book Co., Inc., New York, 1948.
3. "Uplift and Seepage Under Dams on Sand," by L. F. Hara, Transactions, ASCE, Vol. 100, 1935, p. 1352.
4. "Jacobian Elliptic Function Tables," by L. M. Milne-Thomson, Dover Publications, New York, 1950.
5. "The Flow of Homogeneous Fluids Through Porous Media," by M. Muskat, J. W. Edwards, Inc., Ann Arbor, Mich., 1946.
6. "Seepage in Homogeneous Medium," by F. B. Nelson-Skornyakov, Moscow, 1949.
7. "Collected Works," by N. N. Pavlovsky, Moscow-Leningrad, 1956.
8. "Fundamentals of Soil Mechanics," by D. W. Taylor, John Wiley and Sons, Inc., New York, 1948, p. 171-172.
9. "Theoretical Soil Mechanics," by Karl Terzaghi, John Wiley and Sons, Inc., New York, 1943, p. 257.

Journal of the
SOIL MECHANICS AND FOUNDATIONS DIVISION
Proceedings of the American Society of Civil Engineers

DISCUSSION

Note.—This paper is a part of the copyrighted Journal of the Soil Mechanics and Foundations Division, Proceedings of the American Society of Civil Engineers, Vol. 87, No. SM 5, October, 1961.

PILE DRIVING ANALYSIS BY THE WAVE EQUATION[a]

Closure by E. A. L. Smith

E. A. L. SMITH,[42]—Soderberg's discussion suggests certain changes in the method of computation that would not materially affect the final result but are intended to reduce the amount of computation required.

It is characteristic of approximate solutions that there is usually a choice as to how the approximation is to be made. Soderberg has developed a method somewhat different from that of the writer, and has set forth its essentials in his analysis. He should have full credit for this development.

Soderberg computes only the displacements. Forces or other information that may be wanted must be obtained by means of a supplementary computation, therefore in many cases the time saving might be much less than Soderberg has indicated. In any event, this is a subject for study primarily by mathematicians and computer experts as it does not affect the civil engineering aspects of the problem.

Gates examines the question of how the bearing capacity of piles should be determined. For this purpose Gates opposes the use of the wave equation, but advocates a pile driving formula (Eq. 37) which he has devised. The writer presented this general subject briefly in the paper under the headings "Introduction" and "Recommendations and Comments." The words were carefully chosen, and there is no wish to add to them herein or to amend them in any way.

In Gates discussion there are three statements that call for answers as follows:

A. The discussion states that previous investigators "unanimously cautioned against the use of the wave equation as a means of determining bearing capacity." No specific references are given to support this statement, and the writer has been unsuccessful in his attempt to confirm it. He did, however, find a statement exactly to the contrary in the writings of A. E. Cummings[43] whom both Gates and the writer have referred to as an authority. This same statement also appears in the last part of a paragraph on page 13 of Gates' reference No. 25. Cummings first refers to the wave equation developments of St. Venant, Boussinesq, Isaacs, and the British Building Research Board (Gates' references Numbers 11, 12, 17, and 18) and then writes as follows: "However, there is a considerable amount of field evidence available which shows that the stress transmission characteristics of a pile are of great importance not

---

[a] August, 1960, by E. A. L. Smith (Proc. Paper 2574).

[42] Chf. Mech. Engr., retired, Raymond Internatl. Inc., New York, N. Y.

[43] Discussion by A. E. Cummings of "Pile Driving Formulas," by Progress Report of the Committee on the Bearing Value of Pile Foundations, Proceedings, ASCE, Vol. 68, January, 1942, p. 172.

only in determining its behavior during driving but also with respect to its subsequent ability to carry static load." Cummings' paragraph concludes: "It is a new and promising field for investigation."

B. It is suggested in the discussion that the writer "should make a definitive statement concerning the limits of application of his presentation." The writer has no intention of doing this because he believes that there is no good reason for limitations beyond those already stated in the paper.

C. It is stated in the discussion that the writer is guilty of "qualification of his previous references to bearing capacity by mentioning in this paper soils which may either relax or set-up." However, the writer had previously mentioned these particular soil characteristics in the second paragraph of Gates' reference No. 16 published in 1957. No such "qualification" has occurred.

Gates has implied that the wave equation and a dynamic pile formula are the same, and that references whose authors had no thought of the wave equation may therefore be cited against it. The wave equation is a mathematical method.[7] Dynamic pile formulas appear to be mathematical, but their mathematics is defective as has been carefully explained by Cummings[3,43] in two separate articles devoted to the subject.

Passing completely from the subject of bearing capacity, the analysis next proceeds to criticize four technical features of the paper. In all four cases the analysis makes statements which, if taken together, leave the reader with the impression that the writer's method is quite inaccurate. These statements are presented in the following:

No. 1: The discussion lists six assumptions necessary in order to apply the wave equation to pile driving. These have been taken from a list[19] that applied specifically to the wave equation pioneering done almost 100 yr ago by St Venant[11] and Boussinesq.[12] This list is now (1961) out-of-date. Only assumptions No. 3 and No. 5 are necessary in accordance with the writer's method. Assumption No. 1 can be made if it appears to fit the actual ground conditions, but it is not necessary because side friction has been specifically provided in the writer's method. Assumption No. 2 involves negligible error if the ram is short and stubby, but a comparatively long ram may be represented by any suitable number of weight and springs as per Fig. 10(b). Assumption No. 4 is not necessary because piles of irregular section have been provided for. Assumption No. 6 is completely unnecessary.

No. 2: Immediately following the list of assumptions it is stated that the writer's method takes no account of propagation losses in the pile. The writer has presented Eq. 27 for this purpose. However, in piles of ordinary length the internal losses are negligible.

No. 3: Near the end of the discussion, the compressive forces computed in the writer's Illustrative Example are compared unfavorably with those obtained by strain gage measurement in certain field tests.[30] The discussion emphasizes that the computed forces increased rapidly towards the tip of the pile, and states "This conclusion is diametrically opposed to the results obtained from field tests." Gates has ignored the fact that in the Illustrative Example, side friction was completely absent, whereas the field measurements were made on piles in which side friction predominated. There is no reason whatever to expect the forces to be distributed in the same manner in these two radically different cases. The discussion also emphasizes that the computed forces are larger than the measured forces. Here again a vital fact is ignored, namely that in the two cases the pile weight per foot is different. The heavier and

stiffer pile used in the Illustrative Example will inevitably produce higher impact forces if the same hammer is used. A comparison of this kind should not have been made because the only major way in which the two cases resemble each other is that the same hammer was used.

No. 4: The discussion states that in the writer's method there is a "need to preassign not only the factor R_u but also the penetration at which this value occurs." As a matter of fact the penetration "s" is obtained by making the wave equation computation. It is never under any circumstances "preassigned." This appears in the paper as part of the first paragraph under the heading "Outline of Numerical Method" and also as part of "Conclusion No. 1." It also appears in "Step No. 9" of the Illustrative Example where it is stated that the computed permanent set "s" is 0.20311 in. per blow.

Jonas has written a thoughtful discussion which raises an important question, namely: should R_u be 200,000 lb as given in the paper, or should R_u be 400,000 lb or 405,000 lb as suggested in the discussion.

The discussion states: "It can be shown that in the Illustrative Example given by the author, equilibrium does not obtain at the end of permanent set unless Eqs. 13 and 16 are modified."

In the Illustrative Example the "end of permanent set" occurs approximately in time interval 55 when the point of the pile reaches its maximum penetration, as can readily be seen by referring to Fig. 12. At this instant F_{11} (the internal force at the point of the pile) does not have its maximum value of 405,000, as quite reasonably assumed by Jonas, but has a value of only 200,000 lb which is the same as the value of R_u (the ultimate ground resistance.) This fact can be determined by reading values from the curves of Fig. 12. Thus in time interval 55 $D'_p = 0.202$ in., $D_{12} = 0.302$ in. and $D_{11} = 0.353$ in. Subtracting D'_p from D_{12} gives 0.1 in. as the measure of the elastic ground compression. Multiplying 0.1 in. by the spring constant of the ground K'_p $(= K'_{12} = 2{,}000{,}000)$ gives the value of R_u as 200,000 lb. Subtracting D_{12} from D_{11} gives C_{11} as 0.051 in. Multiplying C_{11} by the spring constant of the point of the pile K_{11} (= 3,900,000) gives F_{11} as 200,000 lb also. Thus equilibrium is obtained.

The maximum value of F_{11} (405,000 lb) occurs not "at the end of permanent set" but in time interval 34 when the point of the pile is forcing its way through the ground with the rather high velocity of 6.4 fps. An analysis similar to that given in the preceding paragraph but involving resort to the printed computer output, shows that in time interval 34 the following values occur:

Ultimate ground resistance R_u	200,000 lb
Viscous ground resistance	192,000 lb
Accelerating force acting on W_{12}	13,000 1b
Total	405,000 lb

This total is exactly equal to the maximum internal force in the pile, F_{11}. Therefore, it may be concluded that the correct value of R_u is 200,000 lb and that no modification of Eq. 13 and 16 is required.

Eremin's discussion raises a question regarding the velocity of sound (or stress) in a pile. None of the equations used in the writer's method includes, as a term, the velocity of sound. Nevertheless, as the computation is performed, the stress wave progresses down the pile with approximately the velocity of sound, as it should. Furthermore, if side resistance is included, the

stress wave will be slowed down automatically as Eremin states that it should be. This is an important proof of the correctness of the method.

The values of 0.05 and 0.15 proposed for the damping constant J' and J are the best now (1961) available. When experimentation or other means produces more accurate values, they should be adopted.

Eremin suggests that "tip bearing stresses," "buckling stresses," and "elastic properties of soil" have an effect on the damping forces. The effects of the first and the last of these are considered in the paper and result in Eqs. 15 and 16, and Eqs. 28 and 29. After the pile enters the ground there is little tendency to buckle if the pile is reasonably straight, therefore the effect of buckling stresses has not been considered in the writer's paper.

Eremin refers to data obtained from driving piles by vibration. No mention was made of such data in the paper.

Cornfield's discussion is more than welcome. The English were pioneers in applying the wave equation to pile driving.[5] However, the fact that electronic computers were not available in 1938 when their major paper[5] was written, was a severe handicap.

The first paragraph of Cornfield's discussion contains the essence of a lot of practical pile driving experience, and is worthy of careful consideration.

A parameter investigation is suggested in connection with the writer's method. Samson of Texas A & M College is at present (1961) planning such an investigation.

Cornfield draws certain tentative conclusions, partly from wave equation data previously published[35,36] and partly from test load results. Conclusions such as these are valuable if applied within specific limits but may become inaccurate beyond these limits. The wave equation can be helpful in determining these limits.

The curves in references 35 and 36 were prepared before viscous damping was introduced into the wave equation computation. Inclusion of viscous damping produces somewhat more conservative results.

Chellis and Zaskey have presented an extensive and important discussion. The writer commends it highly. His only comments are by way of adding supplementary information.

As a means of saving space, tabulation has been found preferable to curve drawing for recording the results of a considerable number of wave equation computations.

The wave equation curves of Figs. 15 and 16 are based on the assumption that $J = J' = 0$, whereas it is recommended in the writer's paper that until more accurate values are available, J should be given the value of 0.15 and J' the value of 0.05. Consequently these curves (as noted in the discussion) yield values that are less conservative than those that would be obtained by following the writer's paper.

The programming of a computer at Texas A & M College, College Station, Texas, for wave equation computations, as mentioned in the discussion, is under Charles H. Samson, Jr, A. M. ASCE. Use of the computer and program, which contains certain refinements introduced by Samson, will be made available to anyone. The project is being sponsored by the Texas Highway Department and is under Randle B. Alexander, F. ASCE, Bridge Engineer, Austin, Texas.

In conclusion the writer wishes to thank all those who presented discussions. They have thrown light on many aspects of the problem that were either not mentioned or not fully included in the writer's paper.

Errata.—Page 38, under DIAGRAMMATIC REPRESENTATION the word "can" should read "cap"; page 44, line 14, "Eq. 24" should read "Eq. 27"; page 47, line 3, "Q one" should read "Q"; page 50, three lines from bottom, "Slide" should read "Side"; page 61, line 5, "Eq. 24" should read "Eq. 27"; page 61, line 7, "25, and 26" should read "28 and 29"; page 61, four lines from bottom, "Eq. 24" should read "Eq. 27"; and page 61, next to last line, "Eq. 24" should read "Eq. 27."

Discussion by Chellis and Zaskey.—Page 67, line 12, "impluse" should read "impulse"; page 67, line 31, "of" should read "or"; page 67, line 36, "lone" should read "long"; page 69, line 16, "effects" should read "affects"; page 69, line 39, Delete extra letter "c"; and page 74, line 18, "easy" should read "each."

GROUTING OF GRANULAR MATERIALS[a]

Discussion by R. H. Grice

R. H. GRICE,[29]—A Penetration Ratio, an approximate measure of the ease of grouting fine fissures is presented. The writer is particularly interested in how this ratio was obtained as he considers that it is a fundamental characteristic of grout mixes. Its measurement should be an essential part of a standardized procedure for use in the design and quality control of grout mixes.

A penetration test would be of particular value in the study of lubricated grouting and its relationship with dispersant treated grouts. Work on these lines would be likely to modify the groutability criteria proposed in this paper.

Test standardization is particularly important as mixing procedures, injection pressures and rates are critical in the design and handling of the highly thixotropic grouts. These are produced by the addition of swelling bentonites and of 1 % to 3 % of lignosulphonates to water-cement grouts.

---

a March, 1961, by John C. King and E. G. W. Bush (Proc. Paper 2791).

[29] Geologist, H. G. Acres & Co. Ltd., Niagara Falls, Canada.

GROUTING TO PREVENT VIBRATION OF MACHINERY FOUNDATIONS[a]

Discussion by Richard R. Schindler

RICHARD R. SCHINDLER,[12] M. ASCE.—Gnaedinger demonstrates the elimination of foundation vibrations by injecting chemical grout to alter the elastic properties of the soil and the natural frequencies of vibration of the foundation-soil system. Such an approach may be of interest also to the structural engineer concerned with the prevention of damage due to seismic disturbances or nuclear weapons energy releases. This problem differs in being one of transient motion and in the magnitudes of energies and weights involved. But the conclusions of Gnaedinger and the data of the Symposium appear pertinent. Also, the type of soils correctly associated with earthquake damage are, fortuitously and fortunately, those most suitable to grouting operations.

This discussion attempts to evaluate qualitatively the effects of grouting in relation to some of the soil mechanics problems connected with seismic oscillations. The first two are quantitatively less significant. But the third, the prevention of consolidation by grouting, could possibly contribute to forestalling earthquake damage or to reducing the need for structural provisions against differential settlement.

Intensity of Ground Motion in Relation to Soil Properties.—The change in energy of seismic waves passing from one medium to another is still a matter of considerable study. But B. Gutenberg[13] cites extensive data indicating that the intensities perceived by instruments situated on rock are less than those recorded by instruments on alluvium. (This applies primarily to later waves, the initial shock being usually recorded with relatively little difference.) He notes that, "Ground effects may produce appreciable differences in duration and amount of shaking even at localities only a fraction of a mile apart."

Seismic waves passing from a stratum of rock to one of alluvium are known to double in intensity, as shown theoretically and substantiated with field measurements by G. W. Housner,[14] M. ASCE. It is not inconceivable that passing from alluvium to rock the intensity would decrease. But the degree of similarity between a grouted soil and bedrock needs to be determined.

The effect of grouting on the intensity of seismic oscillations should be considered negligible until soundly established. Yet it is likely to be beneficial rather than detrimental.

---

a April 1961, by J. P. Gnaedinger (Proc. Paper 2793).

12 Paul J. Tolen, Structural Engr., Los Angeles, Calif.

13 "Effects of Ground on Earthquake Motion," by B. Gutenberg, Bulletin, Seismological Soc. of America, Vol. 47, No. 3, July, 1957.

14 "Geotechnical Problems of Destructive Earthquakes," by G. W. Housner, Geotechnique, Vol. 4, No. 4, December, 1954.

Soil-Superstructure Interaction.—A building on a grouted foundation, with increased elasticity will vibrate with a shorter frequency than on the original soil. This affects the stress conditions in the structure adversely. The accompanying smaller rocking displacements tend to aid the stress conditions, but, simultaneously, may reduce desirable damping effects. Energy dissipation by stress waves produced in the ground by oscillating buildings has not been evaluated conclusively.

Analyzing the effect of foundation conditions over a wide range in their interaction with five, ten and fifteen story buildings, Merritt and Housner[15] conclude that rocking motion is not a significant factor for most ordinary structures, frequencies being altered by less than 10% over a range of all foundation conditions to be anticipated in practice. The extraordinary structures are only those which are both narrow and on soft soil.

The effect of grouting on the soil-superstructure interaction, which is so important for elimination of vibration, appears, consequently, not to be significant for shock attenuation.

Consolidation.—Studies of earthquake damage have demonstrated that buildings on alluvium or soft ground are usually more susceptible to failures than buildings on rock or hard ground. Such studies also indicate that the cause of damage is not only the intensity of the shock per se, but also the differential settlement effected by ground consolidation.

Although many earthquake damage reports come to this conclusion (Mexico 1957, Japan 1948, Tehachapi 1952, and others), a particularly striking example is given by V. A. Murphy:[16] The town of Napier, New Zealand, is located partly on an 85 ft deep alluvium and partly on a 100 ft high limestone hill. During a 1931 earthquake the buildings located on the hill experienced no serious foundation failures and only light damage to the structures. The buildings on the alluvium were subjected to settlement which caused serious foundation failures and damage to the superstructures. The lesser damage on the hill could well be due to the lesser shock intensity transmitted by rock. However, emphasis is given the observation that the failures on the alluvium are, judging by their nature, attributable to foundation settlement rather than to building motion.

That densification by grouting, in effect analogous to compaction, decreases the settlement potential of a soil is almost self-evident, and is illustrated by Bruce E. Clark,[17] Aff. ASCE.

Where unfavorable soil conditions obtain, reduction in differential settlement resulting from consolidation induced by seismic vibrations and building motion may be achieved by grouting the soil. The engineer has to balance the factors pertaining to the grouting operation with those connected with making structural provisions against the differential settlement.

The three aspects presented indicate that in aseismic design grouting may find another field of application. But the solution of soil mechanics problems connected with either steady state or transient motion are still being studied

---

15 "Effect of Foundation Compliance on Earthquake Stresses in Multistory Buildings," by Merritt and Housner, Bulletin, Seismological Soc. of America, Vol. 44, No. 4, October, 1954.

16 "The Effect of Ground Characteristics on the Aseismic Design of Structures," by V. A. Murphy, Proceedings, 2nd World Conf. on Earthquake Engrg., Japan, 1960.

17 "Symposium on Grouting: Grouting at Ft. Campbell Theatre," by Bruce E. Clark, Proceedings, ASCE, Vol. 87, No. SM 2, April, 1961.

by many investigators.[18,19,20] A systematic approach based on Quinlan's elastic Theory of Soil Mechanics[21] appears quite promising. It could lead to the technique sought by Gnaedinger for the prediction of natural frequencies in vibrating foundation-soil systems. By an extension this approach could perhaps also be made applicable to the determination of natural frequencies of impulsively disturbed foundation-superstructure systems, sought by engineers confronted with earthequake or nuclear weapons hazards. Even without a rigorous solution, the experience with and research on grouting published in this Symposium demonstrates its value in eliminating vibration of machinery foundations and its potential value in aseismic design.

18 "Bibliography of Effects of Soil Conditions on Earthquake Damage," by C. M. Duke, Earthquake Engrg. Research Inst., 1958.

19 "Symposium on Dynamic Testing of Soils," Amer. Soc. for Testing Materials, 1953.

20 "Proceedings of the Second World Conference on Earthquake Engineering," Science Council of Japan, 1960.

21 "The Elastic Theory of Soil Dynamics," by P. M. Quinlan, Symposium on Dynamic Testing of Soils, Amer. Soc. for Testing Materials, 1953.

UNCERTAINTIES IN EARTH DAM DESIGN[a]

Discussion by B. V. Ranganatham

B. V. RANGANATHAM.[7] —This paper is of particular interest to the writer who had the opportunity to examine the stability of earth dams built in India several centuries ago.[8] The added interest is from the fact that there have been some catastrophic failures of some recently built earth dams and one example is briefly discussed in the following.

The recently completed Panshet earth dam which was expected to augment the drinking water supply of the Poona City, has died a premature death, 760 ft breach in its 3,000 ft length, before it could serve the city's population. The rainfall in the catchment area of the Mutha river is somewhere around 200 in. and the earlier expressed doubts (expressed in 1957 before starting of construction) whether high earth dams in this region which is particularly deficient in suitable earth for the core as well as the casing, would be safe in heavy rainfall, came true. The floods caused by the breach in the Panshet dam meant the natural death, 100 ft top to bottom breach, of the Khadakvasala masonry dam which is 12 miles downstream and which had served well for several decades. The breaches in the dams were responsible for the sudden upsurge of water in the Mutha rendering about 60,000 people homeless with loss of life placed around 200. This only explains the one other uncertainity—danger from overtopping during monsoon—which is inherent in earth-dam design. One of the logical developments in earth-dam construction of special significance to such regions will be towards self-spillway rockfill type.[9]

The final sections adopted for the embankment of Terminus Dam and New Hogan are no doubt among the best possible solutions. The writer, however, would like to refer to two factors, viz. the conservative nature of estimating mechanical properties of soil and the very low values of safety factors allowed in the design, which perhaps have a balancing affect on one another to have produced the satisfactory solutions.

It is reported that cohesion has been neglected on the basis that it is not considered to be a unique property of the soil. . . .and that the minimum value of ϕ from the unconsolidated-undrained tests has been arbitrarily selected as 11°. It is to be pointed out that this much avowed conservation is unrealistic, if not contrary to reality. The $C' = 0$ hypothesis in long term satability analysis[10]

---

[a] June 1961, by John M. Bird (Proc. Paper 2832).

[7] Dept. of Building Science, Univ. of Liverpool, United Kingdom.

[8] "Stability of Earth Dams Built in the Past in India in the Light of Modern Developments in Soil Mechanics," by B. V. Ranganatham, Transactions, C.B.I.P., India Research Congress, Hyderabad, 1959.

[9] "Flow of Water Through Rockfill and its Application to the Design of Dams," by J. K. Wilkins, Proceedings, 2nd Australian-New Zealand Conference, S. M. and F. E., 1956.

[10] "Effective Stress Method of Stability Analysis to Determine the Cohesion Intercept Operation at Long Term Failures," by D. J. Henkel, Proceedings, 4th Internatl. Conf., S. M. and F. E., Vol. II, 1957.

is an emperical one derived from observations of slope failures in overconsolidated fissured clays with load release (as in cuttings) and with access of adequate free water. The value of ϕ' used with this hypothesis is that determined from consolidated-drained tests. In addition, an earth dam, besides being far from the conditions warranted for the validity of the preceding hypothesis, grows stronger with time owing to (1) dissipation of any excess construction pore pressures (thereby there is a gain in strength, if any) and (2) the increase in chemical and structural bond perhaps with the deposition of fine sediments from the seeping flood water.

It is also reported that the design value of the angle of internal friction for the rockfill has been reduced to 40° as a measure of safety against the development of potential sliding planes in the rock shells which could result through placement of thin continuous layers of the mica-like particles. This approach seems to be purely a speculative concept unrelated to any experimental evidence or field observation. The writer would like to suggest the investigation of shearing strength of saturated meta-sandstone with flat mica-like grains by conducting field shear tests[11] with the aid of square steel frames with an area of about 1.0 sq m or more and a height of about 0.3 m.

With regard to the consideration of field methods to minimize nonuniformities, a minor observation will be made of the successful blending of materials in a recently constructed earth dam, by simultaneous supply from more than one borrow area at a predetermined proportion. The borrow areas were demarcated dependent on the uniformity (statistical) of grading of the materials. In addition spot checks were kept continually during the progress of construction. Thus, in the writer's opinion, the extensive survey of grading of borrow materials now reported in the paper may be usefully followed up with obtaining the actual grading of the compacted fill in the impervious core of the New Hogan Dam at least for a limited reach. Such data can serve as useful guidance for future designers.

---

11 "Field Tests on Soils and Rocks," by A. Dvorak and P. Peter, Proceedings, 5th Internatl. Conf., S. M. and F. E., Vol. I, 1961.

PROCEEDINGS PAPERS

The technical papers published in the past year are identified by number below. Technical-division sponsorship is indicated by an abbreviation at the end of each Paper Number, the symbols referring to: Air Transport (AT), City Planning (CP), Construction (CO), Engineering Mechanics (EM), Highway (HW), Hydraulics (HY), Irrigation and Drainage (IR), Pipeline (PL), Power (PO), Sanitary Engineering (SA), Soil Mechanics and Foundations (SM), Structural (ST), Surveying and Mapping (SU); and Waterways and Harbors (WW), divisions. Papers sponsored by the Department of Conditions of Practice are identified by the symbols (PP). For titles and order coupons, refer to the appropriate issue of "Civil Engineering." Beginning with Volume 82 (January 1956) papers were published in Journals of the various Technical Divisions. To locate papers in the Journals, the symbols after the paper number are followed by a numeral designating the issue of a particular Journal in which the paper appeared. For example, Paper 2703 is identified as 2703(ST1) which indicates that the paper is contained in the first issue of the Journal of the Structural Division during 1961.

VOLUME 86 (1960)

OCTOBER: 2615(EM5), 2616(EM5), 2617(ST10), 2618(SM5), 2619(EM5), 2620(EM5), 2621(ST10), 2622(EM5), 2623(SM5), 2624(EM5), 2625(SM5), 2626(SM5), 2627(EM5), 2628(EM5), 2629(ST10), 2630(ST10), 2631(PO5)[c], 2632(EM5)[c], 2633(ST10), 2634(ST10), 2635(ST10)[c], 2636(SM5)[c].

NOVEMBER: 2637(ST11), 2638(ST11), 2639(CO3), 2640(ST11), 2641(SA6), 2642(WW4), 2643(ST11), 2644(HY9), 2645(ST11), 2646(HY9), 2647(WW4), 2648(WW4), 2649(WW4), 2650(ST11), 2651(CO3), 2652(HY9), 2653(HY9), 2654(ST11), 2655(HY9), 2656(HY9), 2657(SA6), 2658(WW4), 2659(WW4)[c], 2660(SA6), 2661(CO3), 2662(CO3), 2663(SA6), 2664(CO3)[c], 2665(HY9)[c], 2666(SA6)[c], 2667(ST11)[c].

DECEMBER: 2668(ST12), 2669(IR4), 2670(SM6), 2671(IR4), 2672(IR4), 2673(IR4), 2674(ST12), 2675(EM6), 2676(IR4), 2677(HW4), 2678(ST12), 2679(EM6), 2680(ST12), 2681(SM6), 2682(IR4), 2683(SM6), 2684(SM6), 2685(IR4), 2686(EM6), 2687(EM6), 2688(EM6), 2689(EM6), 2690(EM6), 2691(EM6)[c], 2692(ST12), 2693(ST12), 2694(HW4)[c], 2695(IR4)[c], 2696(SM6)[c], 2697(ST12)[c].

VOLUME 87 (1961)

JANUARY: 2698(PP1), 2699(PP1), 2700(HY1), 2701(SA1), 2702(SU1), 2703(ST1), 2704(ST1), 2705(SU1), 2706(HY1), 2707(HY1), 2708(HY1), 2709(PO1), 2710(HY1), 2711(HY1), 2712(ST1), 2713(HY1), 2714(PO1), 2715(ST1), 2716(HY1), 2717(SA1), 2718(SA1), 2719(SU1)[c], 2720(SA1)[c], 2721(ST1), 2722(PP1)[c], 2723(PO1)[c], 2724(HY1)[c], 2725(ST1)[c].

FEBRUARY: 2726(WW1), 2727(EM1), 2728(EM1), 2729(WW1), 2730(WW1), 2731(EM1), 2732(SM1), 2733(WW1), 2734(SM1), 2735(EM1), 2736(EM1), 2737(PL1), 2738(PL1), 2739(PL1), 2740(PL1), 2741(EM1), 2742(ST2), 2743(EM1), 2744(WW1), 2745(WW1), 2746(SM1), 2747(WW1), 2748(EM1), 2749(WW1), 2750(WW1)[c], 2751(EM1)[c], 2752(SM1)[c], 2753(PL1)[c], 2754(ST2)[c], 2755(PL1).

MARCH: 2756(HY2), 2757(IR1), 2758(AT1), 2759(CO1), 2760(HY2), 2761(IR1), 2762(IR1), 2763(HY2), 2764(ST3), 2765(HY2), 2766(HW1), 2767(SA2), 2768(CO1), 2769(IR1), 2770(HY2), 2771(SA2), 2772(HY2), 2773(CO1), 2774(AT1), 2775(IR1), 2776(HY2), 2777(HY2), 2778(SA2), 2779(ST3), 2780(HY2), 2781(HY2)[c], 2782(HW1)[c], 2783(SA2)[c], 2784(CO1), 2785(CO1)[c], 2786(IR1)[c], 2787(ST3)[c], 2788(AT1)[c], 2789(HW1).

APRIL: 2790(EM2), 2791(SM2), 2792(SM2), 2793(SM2), 2794(SM2), 2795(SM2), 2796(SM2), 2797(SM2), 2798(EM2), 2799(EM2), 2800(EM2), 2801(EM2), 2802(ST4), 2803(EM2)[c], 2804(SM2)[c], 2805(ST4)[c].

MAY: 2806(SA3), 2807(WW2), 2808(HY3), 2809(WW2), 2810(HY3), 2811(WW2), 2812(HY3), 2813(WW2), 2814(HY3), 2815(WW2), 2816(HY3), 2817(HY3), 2818(SA3), 2819(WW2), 2820(SA3), 2821(WW2), 2822(WW2)[c], 2823(HY3), 2824(SA3), 2825(HY3), 2826(SA3)[c], 2827(HY3)[c].

JUNE: 2828(SM3), 2829(EM3), 2830(EM3), 2831(IR2), 2832(SM3), 2833(HW2), 2834(IR2), 2835(EM3), 2836(IR2), 2837(IR2), 2838(SM3), 2839(SM3)[c], 2840(IR2)[c], 2841(HW2)[c], 2842(EM3)[c], 2843(ST5), 2844(ST5), 2845(ST5), 2846(ST5)[c].

JULY: 2847(PO2), 2848(SU2), 2849(HY4), 2850(PO2), 2851(HY4), 2852(PO2), 2853(SU2), 2854(HY4), 2855(PO2), 2856(PO2), 2857(PO2), 2858(SA4), 2859(SU2), 2860(SA4), 2861(PO2), 2862(SA4), 2863(HY4), 2864(HY4), 2865(HY4), 2866(HY4), 2867(HY4), 2868(PO2)[c], 2869(SA4)[c], 2870(SU2)[c], 2871(HY4), 2872(HY4)[c], 2873(SU2), 2874(SA4).

AUGUST: 2875(WW3), 2876(WW3), 2877(WW3), 2878(SM4), 2879(ST6), 2880(EM4), 2881(SM4), 2882(EM4), 2883(WW3), 2884(EM4), 2885(SM4), 2886(WW3), 2887(EM4), 2888(WW3), 2889(AT2), 2890(AT2), 2891(AT2), 2892(AT2), 2893(AT2), 2894(AT2), 2895(AT2), 2896(AT2), 2897(AT2), 2898(AT2), 2899(AT2), 2900(AT2), 2901(AT2), 2902(SM4), 2903(ST6), 2904(ST6), 2905(SM4), 2906(ST6), 2907(EM4), 2908(ST6), 2909(EM4), 2910(ST6), 2911(EM4), 2912(SM4), 2913(ST6), 2914(WW3)[c], 2915(ST6)[c], 2916(EM4)[c], 2917(SM4)[c].

SEPTEMBER: 2918(SA5)[c], 2919(HW3)[c], 2920(HY5)[c], 2921(SA5), 2922(PL2), 2923(IR3), 2924(HY5), 2925(HY5), 2926(CP1), 2927(HY5), 2928(IR3), 2929(IR3), 2930(HY5), 2931(CP1), 2932(PL2), 2933(HY5), 2934(HY5), 2935(HY5), 2936(HY5), 2937(HW3), 2938(CP1), 2939(PL2), 2940(SA5), 2941(SA5), 2942(SA5), 2943(HY5), 2944(PL2)[c], 2945(CP1)[c], 2946(IR3), 2947(HW3), 2948(IR3), 2949(IR3)[c].

OCTOBER: 2950(PP2), 2951(PP2), 2952(PP2), 2953(ST7), 2954(SM5), 2955(ST7), 2956(ST7), 2957(ST7), 2958(ST7), 2959(SM5), 2960(EM5), 2961(EM5), 2962(ST7), 2963(ST7), 2964(EM5), 2965(SM5), 2966(SM5), 2967(ST7), 2968(ST7), 2969(ST7), 2970(ST7), 2971(SM5), 2972(SM5)[c], 2973(EM5)[c], 2974(ST7)[c], 2975(PP2).

c. Discussion of several papers, grouped by divisions.

AMERICAN SOCIETY OF CIVIL ENGINEERS

OFFICERS FOR 1961

PRESIDENT

GLENN W. HOLCOMB

VICE-PRESIDENTS

Term expires October 1961:
CHARLES B. MOLINEAUX
LAWRENCE A. ELSENER

Term expires October 1962:
DONALD H. MATTERN
WILLIAM J. HEDLEY

DIRECTORS

Term expires October 1961:
THOMAS J. FRATAR
EARL F. O'BRIEN
DANIEL B. VENTRES
CHARLES W. BRITZIUS
WAYNE G. O'HARRA
FRED H. RHODES, JR.
N. T. VEATCH

Term expires October 1962:
ELMER K. TIMBY
SAMUEL S. BAXTER
THOMAS M. NILES
TRENT R. DAMES
WOODROW W. BAKER
BERNHARD DORNBLATT

Term expires October 1963:
ROGER H. GILMAN
HENRY W. BUCK
EARLE T. ANDREWS
C. MERRILL BARBER
JOHN D. WATSON
HARMER E. DAVIS

PAST PRESIDENTS

Members of the Board

FRANCIS S. FRIEL
FRANK A. MARSTON

EXECUTIVE SECRETARY
WILLIAM H. WISELY

TREASURER
E. LAWRENCE CHANDLER

ASSISTANT SECRETARY
DON P. REYNOLDS

ASSISTANT TREASURER
LOUIS R. HOWSON

PROCEEDINGS OF THE SOCIETY

HAROLD T. LARSEN
Manager of Technical Publications

PAUL A. PARISI
Editor of Technical Publications

MARVIN L. SCHECHTER
Associate Editor of Technical Publications

IRVIN J. SCHWARTZ
Assistant Editor of Technical Publications

COMMITTEE ON PUBLICATIONS

THOMAS M. NILES, *Chairman*

WAYNE G. O'HARRA, *Vice-Chairman*

BERNHARD DORNBLATT
HENRY W. BUCK
JOHN D. WATSON
HARMER E. DAVIS